

NASA Contractor Report 3678

NASA
CR
3678
c.1

Flight in Low-Level Wind Shear

Walter Frost

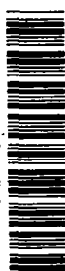
CONTRACT NAS8-33458
MARCH 1983



LOAN COPY - R
AFWL TECHNICAL
KIRTLAND AFB

0062416

TECH LIBRARY KAFB, NM





NASA Contractor Report 3678

Flight in Low-Level Wind Shear

Walter Frost
FWG Associates, Inc.
Tullahoma, Tennessee

Prepared for
George C. Marshall Space Flight Center
under Contract NAS8-33458



National Aeronautics
and Space Administration

Scientific and Technical
Information Branch

1983



TABLE OF CONTENTS

SECTION	PAGE
1.0 INTRODUCTION	1
2.0 WIND SHEAR MODELS	3
2.1 Needs for Improved Wind Shear Data	3
2.2 Current Wind Shear Models	3
2.3 Scales of Wind Shear	14
2.4 Conclusions Relative to Wind Shear Models	18
3.0 AIRCRAFT PERFORMANCE IN WIND SHEAR	19
3.1 Basic Considerations	19
3.2 Equations of Motion with Three-Degrees-of-Freedom	20
3.3 Effects of Wind Shear Terms	22
3.4 Qualitative Analysis	25
3.5 Mathematical Analysis	32
4.0 FLIGHT IN STRONG WIND SHEAR ENVIRONMENTS	39
4.1 Fixed Control Models	39
4.2 Automatic Control Systems	42
4.3 Pilot Models	43
4.4 Comparison of Computer Simulation with Manned Flight Simulator Studies	47
4.4.1 Description of Study	47
4.4.2 Idealized Wind Speed Profiles	47
4.4.3 Flight Path Deterioration Parameters	51
4.4.4 Description of Test Plan	53

SECTION	PAGE
4.4.5 Results of Flight Path Deterioration Parameters (FPDP)	58
5.0 DETECTION AND WARNING SYSTEMS	63
5.1 Airborne Aids for Coping with Low-Level Wind Shear	63
5.1.1 FAA Flight Tests for Airborne Aids	63
5.1.1.1 Modified Flight Director	63
5.1.1.2 Acceleration Margin	64
5.1.1.3 Modified Go-Around Guidance	65
5.1.2 Safe Flight Instrument	67
5.1.3 Bliss's Aircraft Control System for Wind Shear	70
5.1.4 Advantages and Disadvantages of Airborne Systems	72
5.2 Ground-Based Wind Shear Detection and Warning Systems	74
5.2.1 Low-Level Wind Shear Alert Systems (LLWSAS)	74
5.2.2 Pressure Jump System	75
5.2.3 Acoustic Doppler System	75
5.2.4 Laser Systems	75
5.2.5 Pulse Microwave Doppler Radar	75
5.3 Current Status of Low-Level Wind Shear Detection and Warning Systems	79
6.0 CONCLUSIONS	82
REFERENCES	86
APPENDIX A: GENERAL EQUATIONS OF UNSTEADY MOTION	94
APPENDIX B: NOMENCLATURE	104

LIST OF ILLUSTRATIONS

FIGURE	TITLE	PAGE
2.1	Typical Thunderstorm Cross Section (schematic) [22]	5
2.2	Squall Line Thunderstorm Outflow (schematic) [22]	6
2.3	Grid System Superimposed on Typical Thunderstorm Wind Speed Contour Maps	8
2.4	Desert or High-Plains Type Thunderstorm [22]	9
2.5	The Path of Eastern 66 on June 24, 1975, in the Vertical Plane Including the Glide Slope of Runway 22-L at JFK [26] .	10
2.6	A Vertical Cross Section Through the May 29, 1978, Micro- burst Showing Isotachs of Horizontal Wind Speeds [25] . . .	12
2.7	Wind Speed Along a Typical Flight Path Through a Thunderstorm	13
2.8	Turbulence Power Spectra for Thunderstorm Conditions [34] .	17
3.1	Head Wind Shearing to Tail Wind or Calm [48]	26
3.2	Tail Wind Shearing to Head Wind or Calm [48]	27
3.3	Flaps 30 Constant Speed Climb Capability [51]	30
4.1	Flight Paths of DC-8-Type Aircraft Landing with Fixed Controls at a -2.7° Glide Slope	40
4.2	Comparison of Different Types of Aircraft Landing with Fixed Controls in Thunderstorm Cases 9 and 11 at a -2.7° Glide Slope	40
4.3	Comparison of Indicated Airspeed of DC-8-Type and B-747- Type Aircraft Landing with Fixed Controls in Thunderstorm Case 9	41
4.4	Comparison of DC-8-Type Aircraft Landing with Fixed Controls in Thunderstorm Case 9, Considering Individual Wind Components Separately and Combined	43

FIGURE	TITLE	PAGE
4.5	Flight Path Comparison of DC-8-Type Aircraft Landing with (1) Fixed Controls, (2) Automatic Controls, and (3) Automatic Controls with Turbulence Included, in Several Different Thunderstorm Cases	44
4.6	Rate of Change of Thrust Required of DC-8-Type Aircraft Landing with an Automatic Control System in Thunderstorm Cases 9 and 11	45
4.7	Wind Models Used to Simulate a Thunderstorm Downburst Cell .	48
4.8	Mean Wind Profiles with Horizontal Distance at 200 m (660 ft), 300 m (985 ft), and 400 m (1315 ft) Height Above Ground	49
4.9	Wind Spectra Indicating Frequencies Associated with Thunderstorm Wind Shear [15]	50
4.10	Comparison of Computed and Manned Simulator Flight Path Trajectories Through a Longitudinal Sine Wave of ω_{ph} Frequency	55
4.11	Comparison of Computed and Manned Simulator Flight Path Trajectories Through a Longitudinal Sine Wave of 20.6 m/s (40 kts) Amplitude	55
4.12	Comparison of Computed and Manned Simulator Flight Path Trajectories Through a Vertical 1 - Cosine Wave Amplitude of ω_{ph} Frequency	56
4.13	Comparison of Computed and Manned Simulator Flight Path Trajectories Through a Vertical 1 - Cosine Wave of 15.45 m/s (30 kts) Amplitude	56
4.14	Comparison of Computed and Manned Simulator Flight Path Trajectories Through a Combination Longitudinal S-Shaped and Vertical 1 - Cosine Wave of 20.6 m/s (40 kts) Amplitude	57
4.15	Airspeed Deviation Parameters for Longitudinal Sine Wave Winds	59
4.16	Airspeed Deviation Parameters for Longitudinal S-Shaped Wave Winds	61
5.1	Go-Around Advisory Augmentation Algorithm [19]	66
5.2	System Block Diagram of Safe Flight Instrument Corporation's Wind Shear Computer [76]	69

FIGURE	TITLE	PAGE
5.3	Comparison of Aircraft (solid line) Longitudinal Wind and Lagrangian Doppler Velocity (dashed line) as a Function of Time, for May 16, 1979, as Part of SESAME 1979 [79] . . .	77
5.4	Conceptual Illustration of the Doppler-Based Wind Shear Detection and Warning System	78

LIST OF TABLES

TABLE	TITLE	PAGE
3.1	Typical Values of V_E , D/m , and L/m of Different Aircraft Types	25
4.1	Phugoid Period and Horizontal Wavelength	41
4.2	Flight Deterioration Parameters Used in Comparing Computed Versus Manned Flight Simulator Control Performance in Idealized Thunderstorm Wind Shear	52
4.3	Test Plan for Simulator and Computer Runs	54

EXECUTIVE SUMMARY

The results of studies of wind shear hazards to aircraft operation carried out under NASA Marshall Space Flight Center contract for the period 1979 through 1981 are summarized in this report. The results of the study are integrated with other reported information in the literature and with cooperative programs carried out with NASA Ames Research Center and United Airlines Flight Training Center.

The report first reviews existing wind shear profiles currently used in computer and manned flight simulator studies. The governing equations of motion for an aircraft are then derived incorporating the variable wind effects. Quantitative discussions of the effects of wind shear on aircraft performance are presented. These are followed by a review of mathematical solutions to both the linear and the nonlinear form of the governing equations. Solutions with and without control laws are presented.

The application of detailed analysis to developing a warning and detection system based on a Doppler radar measuring wind speeds along the flight path is given. These real-time wind speed profiles are fed into a microcomputer, and utilizing the governing equations of aircraft motion, a flight path deterioration parameter representing a measure of the severity of the wind shear is predicted. A number of flight path deterioration parameters are defined and evaluated. Comparison of computer-predicted flight paths with those measured in a manned flight simulator for flight through hypothetical sinusoidal wind shears and 1 - cosine downdrafts is made. The fidelity of the computer program calculations with the measured manned flight simulator aircraft response is described. Also a correlation of the magnitude of the flight path deterioration parameters with aircraft controllability along the flight path for varying magnitudes of sinusoidal wind speed amplitudes and frequency oscillations is given.

The report ends with a review of some proposed airborne and ground-based wind shear hazard warning and detection systems. The advantages and disadvantages of both types of systems are discussed.

The conclusions of the review are that existing wind shear models used in computer and manned flight simulator studies are not realistic. All existing mathematical models of wind shear are spatially two-dimensional and based on highly smoothed and limited data; none include time dependence. Moreover, the small-scale microburst-type wind shear is not contained in any of the models. Complete data sets from which very good wind shear models can be developed are now available through the NASA Gust Gradient and NCAR JAWS field programs, but these need to be analyzed.

Order of magnitude analysis of the equations of motion for an aircraft illustrates that low values of horizontal wind shear are much more hazardous than larger values of vertical wind shear. The FAA AC-20-57A Advisory Circular, relative to the certification of automatic control systems, calls for 8 kts/100 ft but does not specify that the value be measured along the flight path. The value implies 8 kts/100 ft of altitude. It is believed that realistic three-dimensional time-dependent wind shear models should be used for certification.

Argument exists as to the correct flight procedure to employ when caught in severe wind shear. The main controversy is relative to the optimum speed to fly during an encounter with a head wind shearing to a tail wind. Controversy as to whether to fly at stick-shaker speed or minimum drag speed exists. The Aline Pilots Association (ALPA) Airworthiness and Performance Committee recommends flying at minimum drag speed and thus maintaining some excess kinetic energy to flair the aircraft at the last instant if impact cannot be avoided.

Initial calculations of flight through wind shear showed conflicting results depending on whether the wind speed profile varied linearly in the vertical or logarithmically. This disagreement can be traced to the initial or trimmed condition used in the analysis.

Computer simulation of aircraft flying through several mathematical thunderstorm models developed from gust front data measured with a 500-m (1500 ft) tower at NOAA/NSSL, Norman, Oklahoma, clearly illustrates that the amplitude of the phugoid oscillation of the aircraft is highly amplified. Small perturbation stability analysis clearly supports this observation. Because the wind shear in thunderstorms creates a force function having essentially the same frequency of the aircraft phugoid, it is believed that the phugoid mode normally considered benign can become hazardous when flying through a thunderstorm. Careful evaluation of flight training simulators to assure valid reproduction of the aircraft phugoid characteristics should be made when using simulators to train flight crews or evaluate airborne systems.

Flight path deterioration parameters computed from wind speeds measured with the Doppler radar looking along the flight path show good promise as an effective index of hazard level for use in wind shear warning and detection systems. Comparison of flight path deterioration parameters evaluated through computer simulation with those measured through manned flight simulators (i.e., with man in the loop) show generally consistent results. Additional work is required, however, to establish a meaningful magnitude of the parameter and a scale of wind shear severity.

Airborne wind shear warning and detection systems have been evaluated and have proven effective in manned flight simulator studies. The airborne aids, however, have been tested primarily for approach flight conditions using the standard wind shear models which are not believed to represent realistic nor the most severe conditions. The basic principle of the airborne aid is to maintain ground speed thus storing energy for conditions when the head wind shears to a tail wind. This system, of course, has limited use during takeoff at essentially maximum thrust. Additionally, the airborne system has the disadvantage that one must be in the wind shear before it provides any warning. Finally, the need for a very accurate ground speed measurement, not normally available on board the aircraft, is required for these systems.

The low-level wind shear alert system, LLWSAS, which is a ground-based warning and detection device and which has been installed at 58 major airports as of October 1982, must be considered only an interim solution. Current studies have clearly indicated that the scales of extreme wind shear are sufficiently small such that they can go undetected by most LLWSAS arrangements. Additionally, these are a surface measurement and do not provide warning when wind shear occurs along the flight path but outside the airport perimeter. Finally, arguments have been made that they give too many false alarms resulting in their warning being ignored in many cases.

The optimum warning system appears to be a dual Doppler radar which has been demonstrated without reservation to be capable of monitoring all necessary scales of wind shear. The cost of installing Doppler radar at every major airport may be prohibitive.

It has not yet been resolved as to whether monitoring the component of wind along the flight path, which all current ground-based and airborne detection systems do, is adequate. The vertical component of the wind may be a very significant parameter which must also be monitored. This, of course, can be measured using two Doppler radars; however, the cost of installation is compound. Further study as to whether the effect of the downdraft on airplane performance can be ascertained by monitoring only the longitudinal wind speed component and as to meaningful magnitudes of the downdraft velocity close to the ground is needed.

1.0 INTRODUCTION

With the advent of the digital flight data recorder, low-level wind shear has been recognized as a severe flight hazard [1]. Investigations of at least 25 commercial airline accidents and at least 5 U.S. Air Force (USAF) mishaps [2,3] have clearly proven that wind shear, resulting in a sudden change in either the speed or direction of the wind, can produce dynamic effects on aircraft which cause them to deviate significantly from the pilot's intended flight path producing impact with the ground or frightening near-misses. Both the International Civil Aviation Organization (ICAO) and the Federal Aviation Administration (FAA) now recognize wind shear as a potential hazard to the safety of aircraft operations, especially in the critical landing and takeoff phases of flight. Prior to this recognition, the role wind shear played in aircraft accidents may often have been attributed to pilot error.

It is not surprising that the temporary loss of control or structural failure due to unusual and extreme wind variations has gone undetected for many years. Practically all textbooks (see as examples References 4 through 8) and education programs on aircraft flight dynamics consider only constant or zero winds both in the development of the governing equations and in the analyses of aircraft motion in the atmosphere. It should be noted that although numerous studies relative to the influence of individual gusts or random turbulence on flight performance of aircraft (see for example References 9 through 13) have been conducted, these are generally associated with the high-frequency atmospheric fluctuations. Thus, only aircraft performance relative to changes in wind on time and spatial scales, which are small in comparison with the scales associated with severe wind shear (see for example References 14 and 15), have been studied. Moreover, only recently is wind shear of this scale being measured in the detail necessary to analyze its effect on the motion of aircraft [16,17].

Still, however, insufficient meteorological data are available to construct three-component, three-dimensional spatial, and time-dependent models of wind shear for aircraft design, operational procedures development, and simulation studies. Models of wind fields associated with thunderstorms and other sources of extreme wind shear are urgently needed to develop and verify existing detection and warning systems, to upgrade manned flight simulators for training purposes, and to establish structural and control design criteria.

The purpose of this report is to document and compile information on aircraft procedures and safety during operation in a wind shear environment. Much of the information was developed and assembled under NASA-supported or jointly-supported programs.

The report first describes existing wind shear models and indicates where additional data are needed. Next it summarizes some of the effects on aircraft performance due to spatial and temporal variation in the wind. The dynamic equations of motion are developed and additional terms, which occur due to the variable wind effects, are described. Some simple calculations are made to illustrate the influence of these additional terms on typical approach and takeoff through wind shear. A review is then given of previous studies of the effect of wind shear on aircraft performance. In these studies, a number of restrictive assumptions, such as linearity of the wind shear profile, variation only in horizontal winds, or three-degrees-of-freedom motion are made. Results of analyses of more extreme wind shear conditions, such as have been associated with aircraft accidents, are then reviewed. Finally, recent studies relative to the development of detection and warning systems are described.

2.0 WIND SHEAR MODELS

2.1 Needs for Improved Wind Shear Data

The need for additional wind shear data is manifest in manned flight simulator studies, structural and control design analyses, and detection and warning systems development.

The FAA [18] proposes to permit expanding training, checking, and certification of flight crew members in advanced flight training simulators. Under the advanced simulation plan, the simulators will have the capability to be programmed to represent a full range of aircraft flight conditions, as well as specific aircraft accidents in abnormal environmental conditions. In this way, flight crews can experience a far-ranging set of flight environments and malfunctions, which will assist the crew in making proper judgments when abnormal situations occur in flight.

Phase II of the FAA proposed simulator upgrade program includes the requirement for representative crosswind and three-dimensional wind shear dynamics based on aircraft-related data. In another FAA report [19], seven candidate standard wind shear profiles for systems qualifications are reported. These models--although fast becoming standards--are not truly three-dimensional wind shear. They were constructed from data measured with instrumented towers, from reconstruction of winds from accident flight data records, and from meteorological math models.

2.2 Current Wind Shear Models

The proposed seven candidate standard wind models were selected from 21 models investigated with computer and manned flight simulator studies [19]. They consist of one mathematical model, three tower measurements, and three accident reconstructions.

The mathematical model is considered a low-severity wind shear condition and represents neutral atmospheric conditions. The three tower measurements, one from Cedar Hill tower data [20] and two from the 500-m tower at the National Severe Storms Laboratory (NSSL), Norman, Oklahoma [17], are considered to be of low to moderate severity. The tower data from Cedar Hill are considered to represent a nighttime stable boundary layer, whereas the data from NSSL represents thunderstorm conditions. The three accident reconstructions are the Logan International Airport, Boston, 1973, Iberian DC-10 Airline accident; the Kennedy International Airport, New York, 1975, Eastern B-727 Airline accident; and the Philadelphia International Airport, Philadelphia, 1976, Allegany DC-9 Airline accident. The latter two accidents are considered to represent high-severity thunderstorm models, whereas the former is considered to represent winds associated with a warm front of moderate severity.

Although Reference 19 concludes that a collection of realistic three-dimensional wind models of three levels of severity have been established, variation of the wind field in a lateral direction from the flight path and with time is not included. Thus, during a simulation with these wind models an aircraft moving sideways to the wind field would experience uniform winds in that direction, which is a highly unlikely situation.

Recently, there has been growing evidence that a small-scale but severe low-level thunderstorm wind, now referred to as a "microburst," occurs with surprising frequency, and cannot only adversely affect airplanes but can produce major damage to property on the ground [21]. The precise nature of these small-scale events is not clear, but aircraft accident investigations and surface damage surveys indicate their horizontal extent is typically less than 5 km (3.2 mi) in length and 1 to 5 min in duration. Unfortunately, most previous thunderstorm investigations have not concentrated on such a small scale but rather on the larger scale (5 to 25 km), which is more closely related to gust fronts, tornado cyclones, and overall storm structure. Because the proposed standard wind shear profiles are highly idealized and/or heavily

smoothed, it is believed that they do not include the detailed kinematic structure of these events.

To understand the nature of thunderstorm wind shear (probably the most hazardous wind shear condition) and the limitations of the current models, a description of the thunderstorm is necessary. Figure 2.1 is a simplified cross section of a thunderstorm. General airflow and precipitation features are indicated. Of particular interest are the occurrences of downdrafts and outflow regions, which account for rapidly varying winds, or wind shear, in the low levels. Substantial insight into the larger scale nature of extended thunderstorm outflow has been given by Goff [17], Frost and Camp [23], and Goff [24] in several examinations of gust fronts. An expanded view of the outflow or gust front region of Figure 2.1 is given in Figure 2.2. Goff et al. [22] based his gust front description on measurements of winds during the passage of thunderstorms by a 500-m (1500 ft) tower.

Frost et al. [14] utilized the data from Goff [17] to construct tabulated thunderstorm wind fields for use with computer "lookup" routines. The data set from Goff [17] consists of longitudinal, W_x , lateral, W_y , and vertical, W_z , wind speed components in a vertical plane. Data from 20 thunderstorms were measured during the months of May through June over the period of 1971 through 1973 with the WKY-TV/NSSL 500-m meteorological tower, Norman, Oklahoma. Time histories of the wind speeds were converted to horizontal spatial distributions using Taylor's hypothesis (i.e., $x = \bar{W}t$). Ten-second averaged values of wind

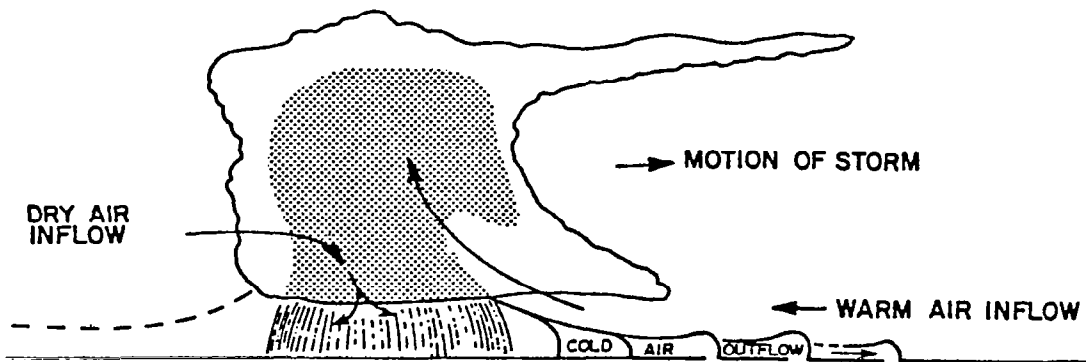


Figure 2.1 Typical thunderstorm cross section (schematic) [22].

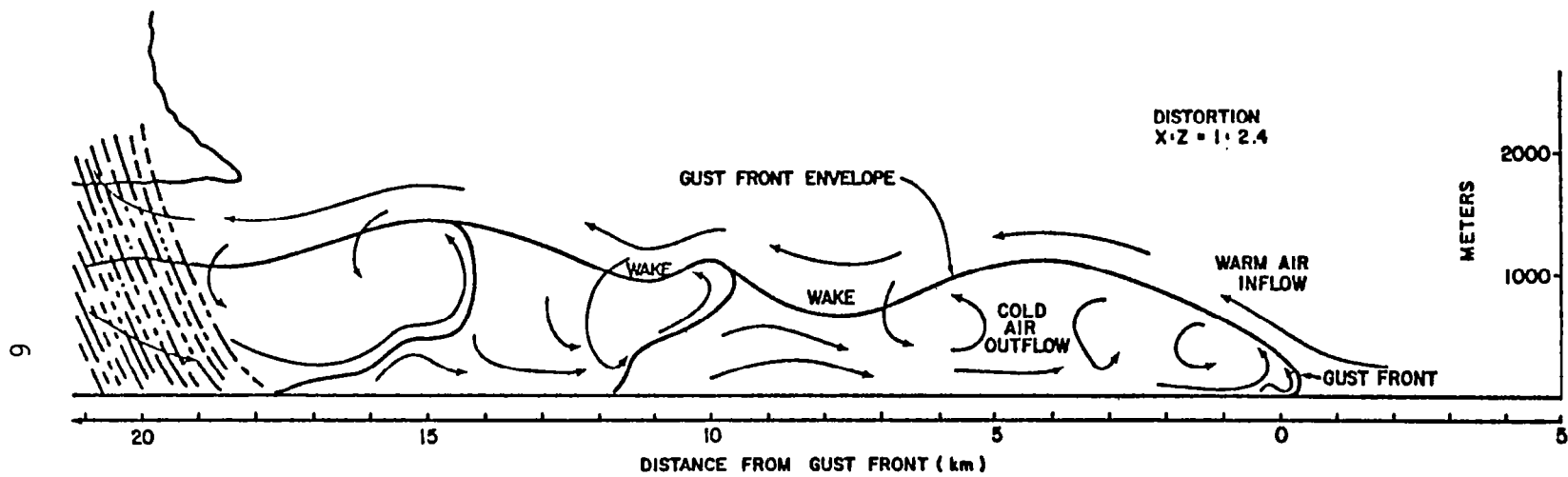


Figure 2.2 Squall line thunderstorm outflow (schematic) [22].

speed components are provided in the form of isotach maps for W_x , W_y , and W_z , respectively. These data were interpolated onto a 41 x 11 point grid system, as illustrated for the horizontal wind component in Figure 2.3, and stored as discrete values on magnetic tape. It should be noted, however, as shown by the insert on Figure 2.3, that the data represent only a vertical plane through that part of the storm which passes the tower. Tabulated values for all 20 thunderstorm wind speeds are given in Frost, et al. [16]. The thunderstorm tower data discussed in Foy [19] are similarly tabulated.

Many thunderstorms may not contain well-defined gust fronts (regions of outflow extending over many kilometers) as defined by Goff. However, essentially all thunderstorms contain downdraft air, which usually impacts and spreads out over the surface. Figure 2.4 shows a schematic view of a high-plains or desert thunderstorm where dry, cold air tends to produce significant downdrafts. Although extensive evidence is lacking, in some cases, the downdraft and immediate outflow associated with it at the surface can be quite intense and can occur on a rather small scale.

Fujita and Wakimoto [25] and Fujita and Caracena [26] have performed several analyses on a phenomenon they have termed microburst, to indicate a coupled small but intense downdraft and outflow, which occurs in thunderstorms which, in most cases, may be of very low rainfall rate/radar reflectivity. One such analysis depicts a microburst occurring along the flight path of Eastern Airlines Flight 66, which crashed short of the runway at New York's JFK Airport in 1975. This conceptual analysis, using sparse data from the on-board flight data recorder, is presented in Figure 2.5. Keenan [27] developed one of the proposed standard wind shear models reported in Reference 19 by laying a grid system on Figure 2.5. By sketching in flow lines using the numbers determined from the flight data recorder and employing conservation of mass, a spatial model of the wind field from the Eastern 66 accident was reconstructed. In this case, both the lateral variation of the wind field as well as the lateral velocity component itself are unknown. Thus, during a simulation, the aircraft experiences no realistic lateral wind component, and if displaced laterally, it "sees" no

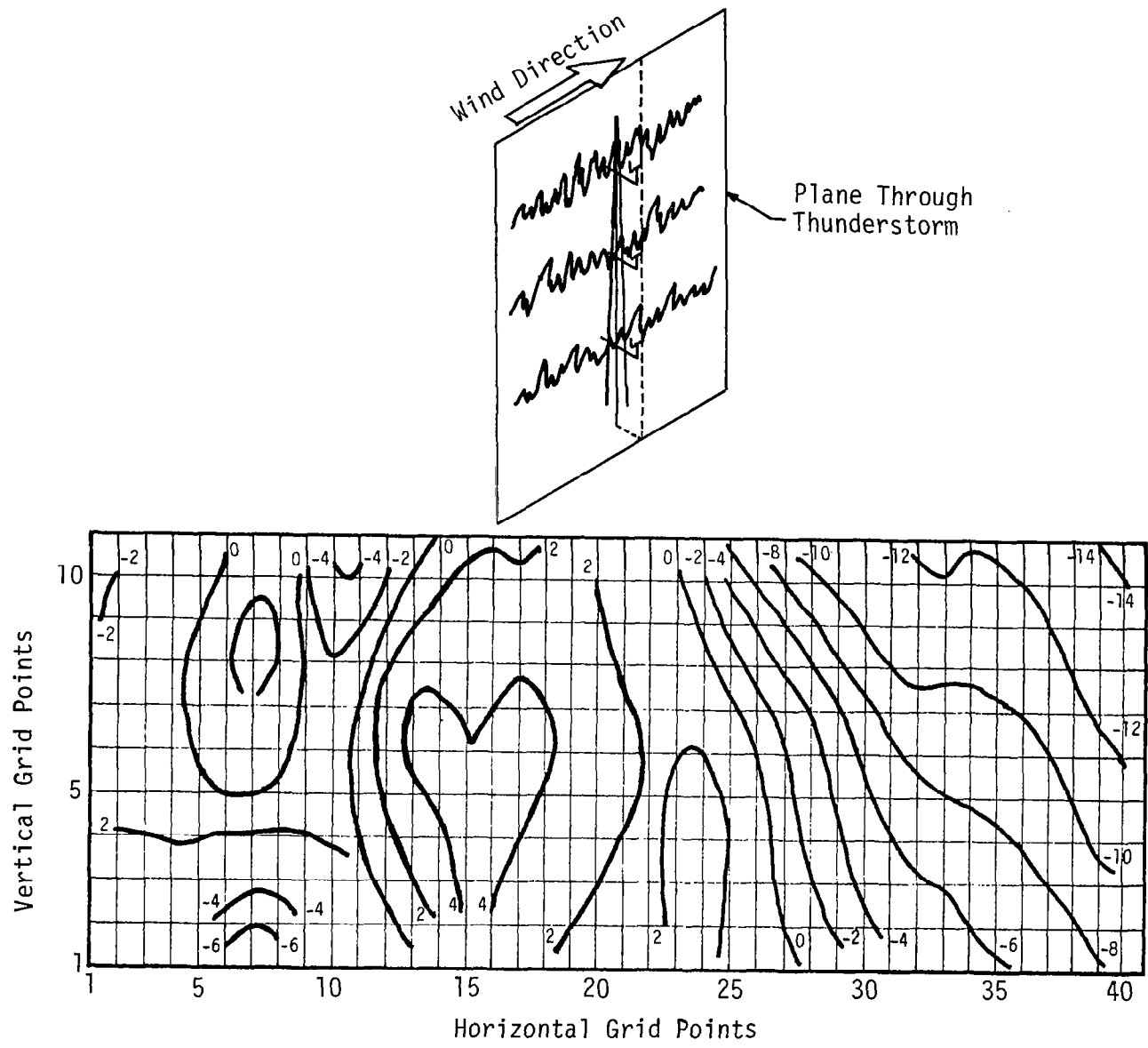


Figure 2.3 Grid system superimposed on a typical thunderstorm wind speed contour map.

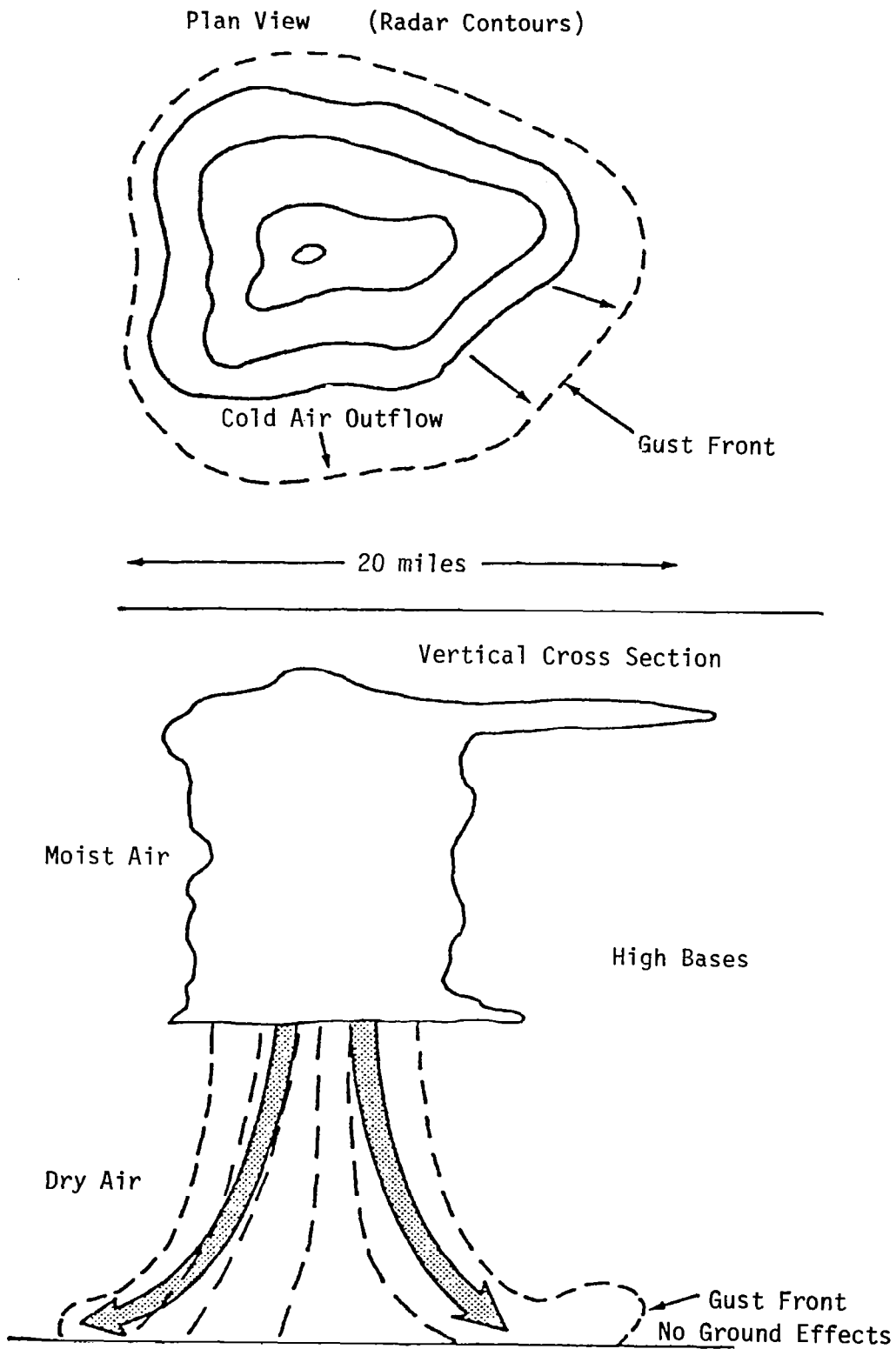


Figure 2.4 Desert or high-plains type thunderstorm [22].

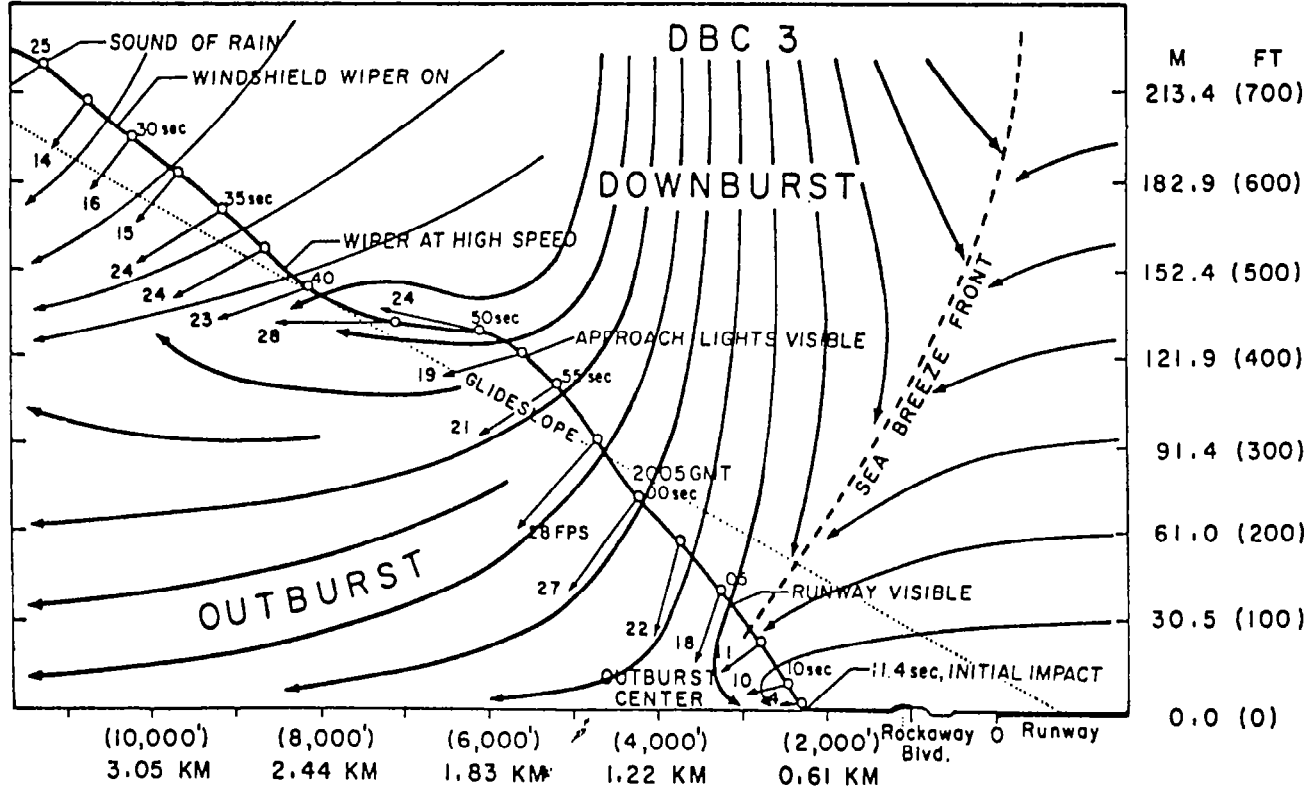


Figure 2.5 The path of Eastern 66 on June 24, 1975, in the vertical plane including the glide slope of runway 22-L at JFK [26].

variation in the wind. Insufficient data are available to fully determine how strong the wind shear in the lateral direction can be and therefore how significantly it can influence an aircraft during approach and takeoff.

Fujita [28] attempted a detailed examination of microbursts in Project NIMROD (Northern Illinois Meteorological Research on Downbursts). On May 29, 1978, an interesting observation of an intense microburst, which occurred near a National Center for Atmospheric Research (NCAR) Doppler radar installation at Yorkville, Illinois, was made. Figure 2.6 (taken from Fujita and Wakimoto [25]) shows analyzed Doppler velocity fields for this event. The maximum horizontal wind measured was 31 m s^{-1} (60 kts), at an altitude less than 200 m and probably as low as 20 to 60 m (66 to 196 ft) above the radar. Such an intense microburst occurring so low to the surface would be extremely hazardous should an aircraft encounter it during takeoff or approach. Other downburst events are reported in Fujita and Wakimoto [25].

Two 3° glide slopes are drawn on Figure 2.6. The approximate wind speeds along paths #1 and #2 are compared with values reconstructed from the Eastern 66 accident (from Foy [19]) and from the tower data, Thunderstorm #9 (Case H, Goff [17]) in Figure 2.7. In general, the longitudinal wind speed profile is similar but the magnitude is larger for the microburst. The very high vertical wind speed proposed by Foy [19] is not apparent in either the microburst or the gust front. In fact, no other apparent sources of wind shear data show such a strong downdraft. This high value is undoubtedly due to assuming only two-dimensional conservation of mass when reconstructing the wind field from Figure 2.5.

Frost et al. [14] investigated the magnitude of vertical downdrafts. The smoothed data from the 500-m (1500 ft) tower gave downdraft values no greater than 3 m/s. Actual values of downdraft as high as 15.5 m/s (not those reconstructed by Foy [19]) were reported in Fujita and Caracena [26]. These values, however, are undoubtedly averaged over much shorter periods of time than 10 seconds for which the data presented by Goff are averaged. Reference 26 gives no information on the

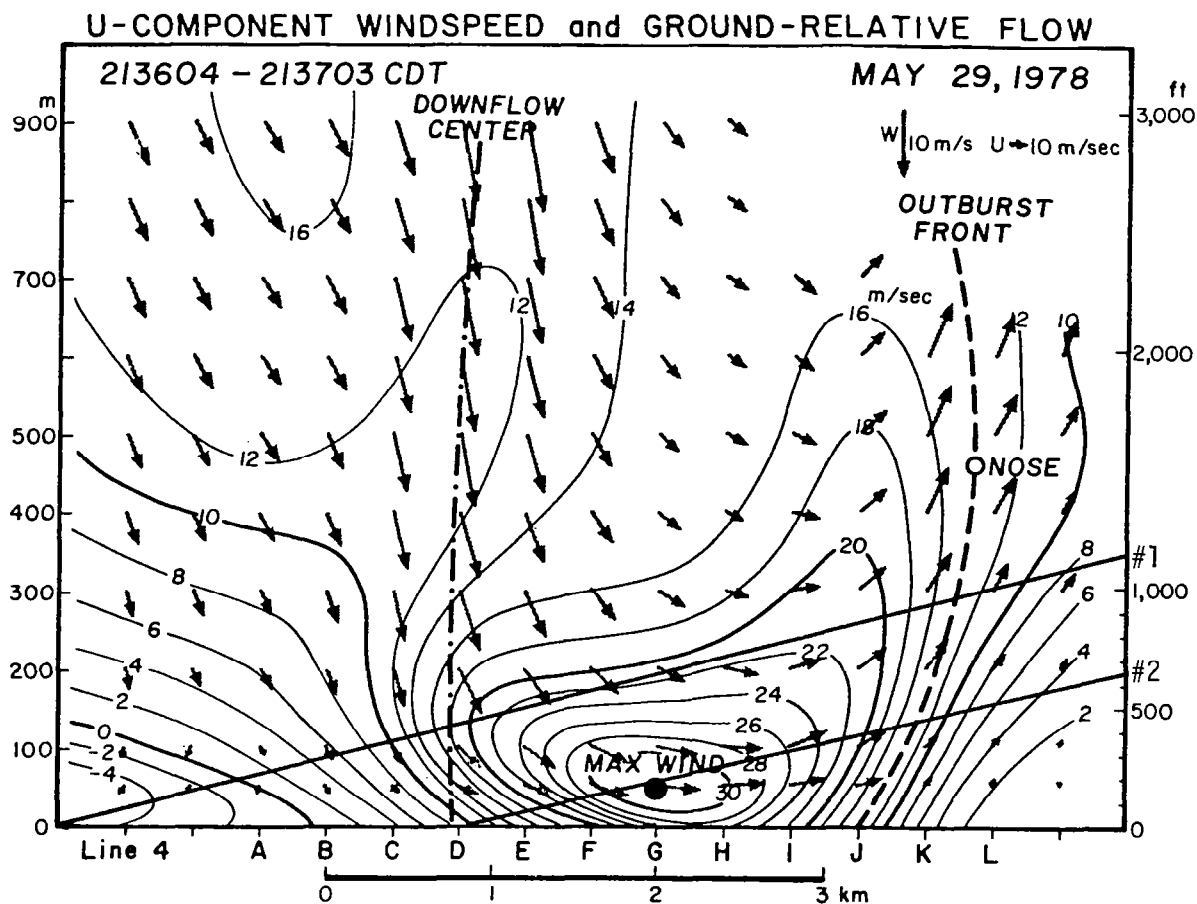


Figure 2.6 A vertical cross section through the May 29, 1978, microburst showing isotachs of horizontal wind speeds. The height of the maximum wind is estimated to be 50 m or lower. Arrows are ground-relative velocities in the plane which is stretched vertically [25]. (The flight path lines #1 and #2 are superimposed by the present author.)

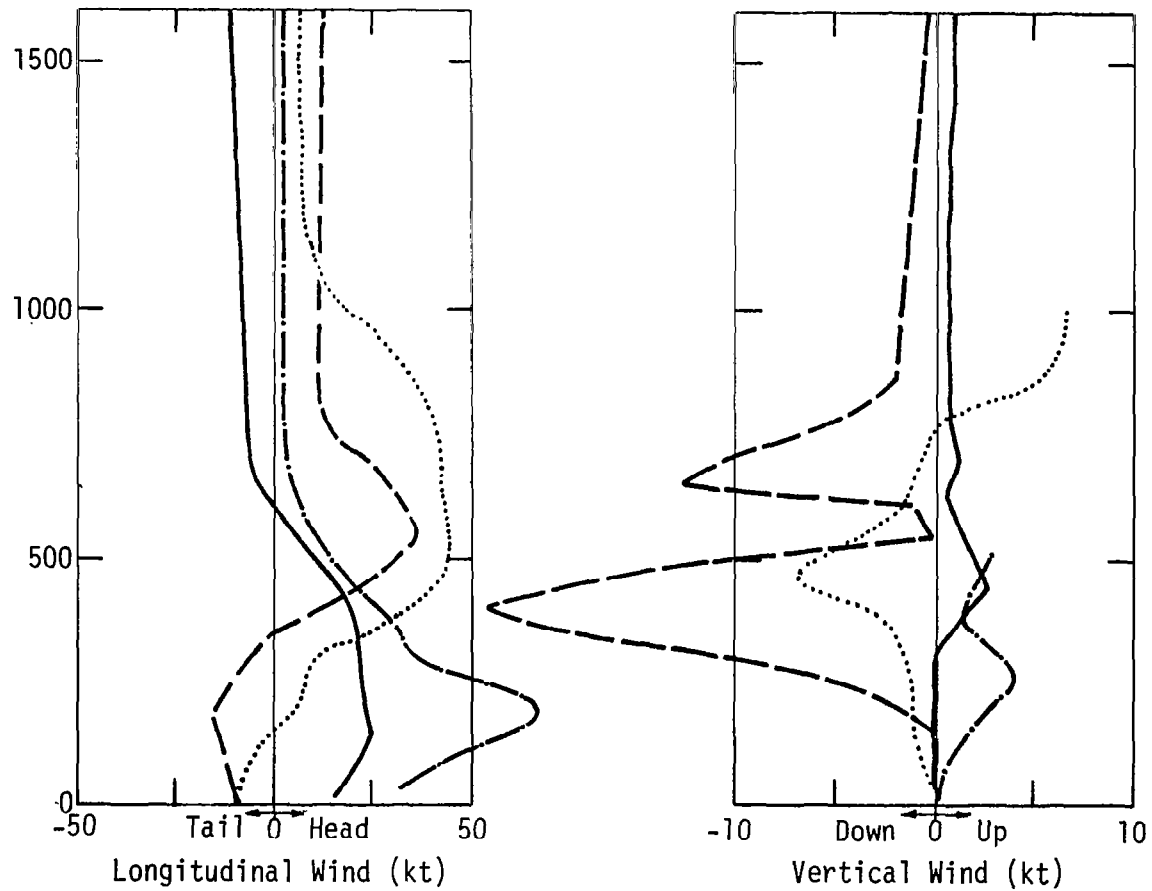


Figure 2.7 Wind speed along a typical flight path through a thunderstorm.
 Path #1 (Figure 2.6) ; Path #2 (Figure 2.6) -.-.-.- ;
 Eastern 66 [19] — — — ; Case H Thunderstorm [19].

averaging time utilized in arriving at the quoted value of 15.5 m/s. It is apparent, however, that the thunderstorm wind field developed by Keenan [27] and reported in Foy [19] contain much more extreme downdrafts than those measured by Goff [17]. Thus, there are conflicting data and opinions as to the maximum magnitude of the downdraft that can occur in a thunderstorm. Although it is expected that the 10-sec averaged data of Goff will have lower values than the peak downdraft wind speed reported by Fujita and Caracena, the discrepancies in the values cannot be completely attributed to averaging time.

Alexander [29] gives a statistical summary of vertical wind speed data recorded with NASA's 150-m (500 ft) ground wind tower facility, Kennedy Space Center, Florida. One year of continuous around-the-clock vertical wind speed measurements were processed to determine the intensity, frequency, time of occurrence, etc. of the daily maximum vertical gust. Both updrafts and downdrafts were studied. These values represent 0.1-sec averages, and the maximum vertical downdraft recorded was 9.3 m/s (18.1 kts), although data recorded during Hurricane Agnes did contain an extreme downdraft in excess of 11.9 m/s (23.1 kts).

Sinclair [30] indicates downdrafts at an altitude of 100 m (300 ft) for an Oklahoma thunderstorm may be considerable in excess of 15.5 m/s (30 kts). Sinclair has measured downdrafts as high as 28 m/s based on a 1/25-sec averaging period. Finally, the numerical models of Williamson et al. [31] do not predict wind speed downdrafts greater than 10 m/s (19.4 kts). Thus, it is evident that research is needed to resolve the magnitude of the maximum downdrafts that can occur in a thunderstorm and the heights at which they occur.

2.3 Scales of Wind Shear

A critical aspect of shear is the length and time scales over which the wind is measured. In the atmosphere, with particular reference to aircraft problems, four scale regimes can be defined [32]:

1. The small or turbulent scale which may extend to scales as large as a few hundred meters,

2. The cloud scale which may range from 0.01 to 10 km (0.006 to 6.2 mi),
3. The overall thunderstorm which may range from 10 km (6.2 mi) to perhaps 50 km (31 mi), and
4. The large or synoptic scale which ranges from 50 to 10,000 km (31 to 6214 mi).

Winds on the storm or larger scales occur over such a long period, with respect to an aircraft's motion, that they are easily accommodated by the pilot and are of no concern other than how they might affect scheduled arrivals, fuel economy, etc. The turbulent scale accounts for bumpiness during aircraft flight, and is serious only when the "bumps" are intense, possibly resulting in structural damage to the aircraft or aircraft failure, excessive pilot work load, and passenger discomfort or injury. The scale distinction between turbulence and wind shear, however, is primarily a matter of interpretation.

There is, however, substantial evidence that wind shears occurring on a scale of 1 to 10 km can create serious difficulties to aircraft, particularly in the landing or takeoff mode. The wind shear models discussed in the previous section incorporate scales of this magnitude. However, the high-frequency or high-wave number disturbances (i.e., turbulence) have been filtered out by the measurement technique or the extrapolation method inherent in the model. The wind speed components from the tower data are averaged over a 10-sec period. Thus, frequencies higher than 0.1 Hz are not contained within the measurement. For radar data, the wind speeds measured are the average value for a volume element typically 150 m long and of variable radial dimension. Finally, it is not clear what time or length scales are associated with wind speeds reconstructed from accident investigations; however, extrapolation of the flight data recorder values to a two-dimensional grid smooths the data immeasurably.

To include the high-frequency components of thunderstorm wind variation (i.e., turbulence) current wind shear models generally superimpose simulated turbulence on the quasi-steady winds. The purpose of the turbulence is to insure a realistic pilot work load. The turbulence

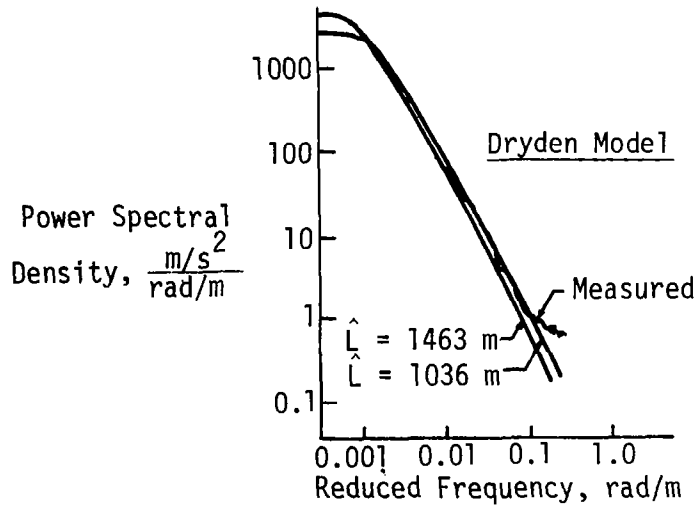
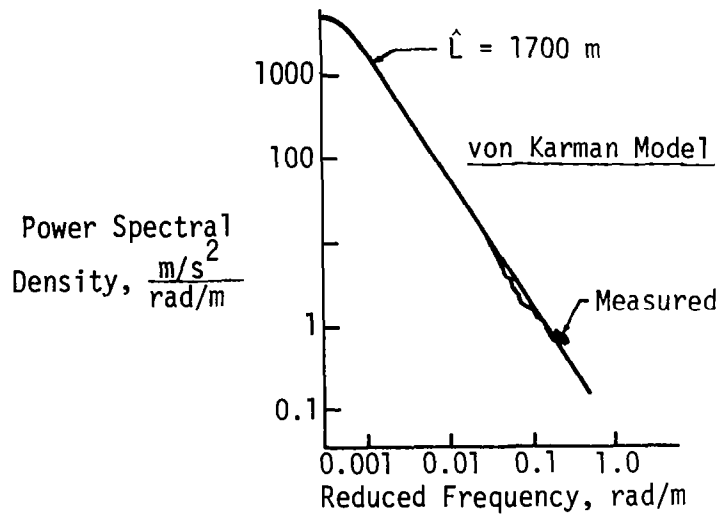
simulation reported in Foy [19] is based on a Dryden spectrum with the intensity and length scale of each of the three velocity components programmed as a function of altitude. Unfortunately, the values of intensity and length scale utilized as input to these simulation models are not fully known for the thunderstorm or other severe wind shear environments.

Measurements of the power spectral density function for turbulence in thunderstorms is reported as early as 1962 by Steiner and Rhyne [33]. Their data were measured over an approximate range of reduced spatial frequency of 0.004 to 0.4 rad/m. The theoretical von Karman spectrum follows the data in this frequency range very well as demonstrated by Houbolt et al. [34], see Figure 2.8a taken from this reference. The Dryden spectrum, on the other hand, does not compare as well with the data. All reported data were measured in the altitude range of 12 to 8 km and thus are probably not representative of the low-level approach and takeoff environment.

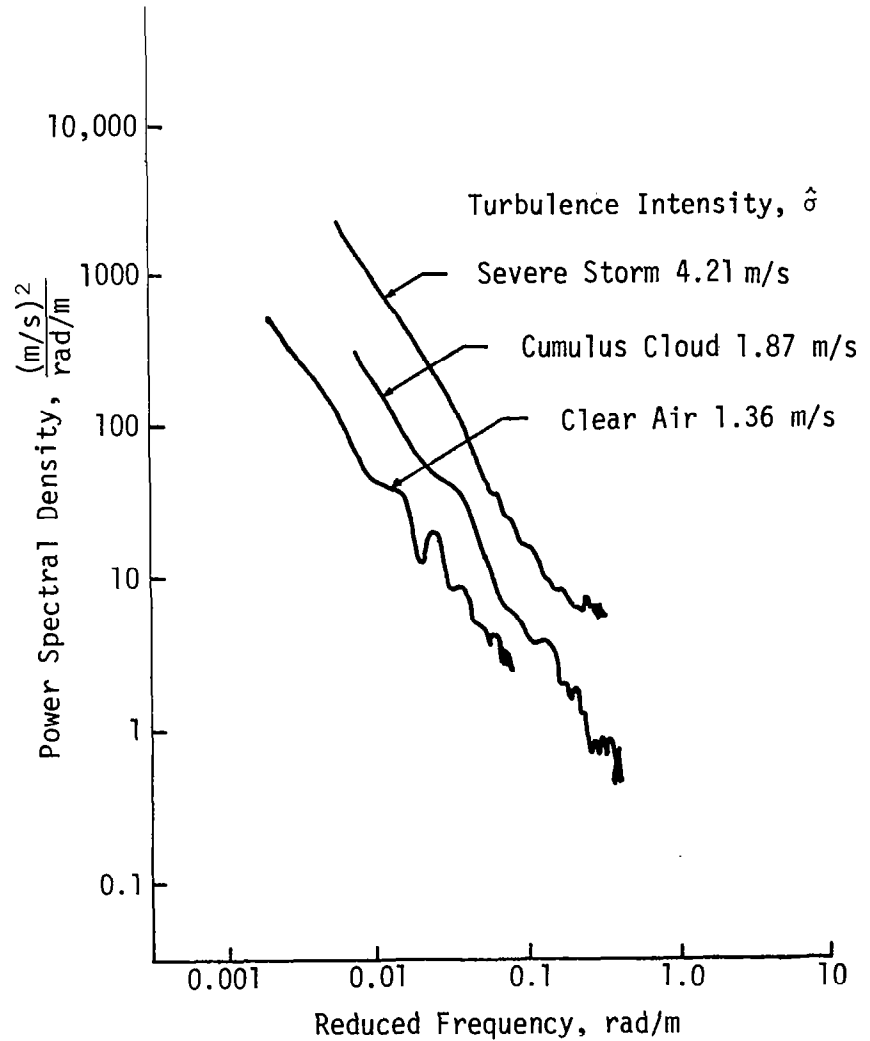
Houbolt et al. [34] gives a comparison of the power spectral density function of severe storms with that of cumulus clouds and clear air turbulence as shown in Figure 2.8b. One can see from Figure 2.8 that the turbulence spectra for severe storms behave very similar to that of cumulus clouds and clear air turbulence with the only major difference being higher amplitudes of the power spectrum, which indicates higher turbulence intensity.

Houbolt et al. [34] recommends for evaluation of the Dryden spectrum a value of $\hat{L} = 1036$ m (3400 ft) and values of $\hat{\sigma}$ of 10.2 to 4.75 m/s (33.5 to 15.6 ft/s) for the vertical fluctuation and of 9.82 to 5.63 m/s (32.2 to 18.5 ft/s) for the lateral fluctuations. Again, these data are measured at very high altitudes and probably do not include effects due to the presence of the ground. The ground is expected, however, to have a strong effect on the turbulence length scale and intensities. No actual data for \hat{L} and $\hat{\sigma}$ below 500 m (4500 ft) nor how they vary with height in thunderstorm conditions is presently available.

It should be noted that no turbulence information relative to the distribution of gust across an airfoil is available. These gusts



(a) Measured and fitted spectra for thunderstorm. \hat{L} is integral length scale.



(b) Typical power spectra of vertical component of turbulence measured in clear air, cumulus cloud, and thunderstorm.

Figure 2.8 Turbulence power spectra for thunderstorm conditions [34].

can significantly influence the rolling motion of the aircraft and cause control upset to the point where corrective action may cause structural damage to the aircraft. A detailed discussion of turbulence modeling for thunderstorm wind shear is provided in Frost et al. [14].

2.4 Conclusions Relative to Wind Shear Models

It is apparent that further data on wind shear is needed before standard models can be adopted for system qualification. Experiments are, however, in progress on gathering three-dimensional data for all three wind velocity components (Fujita et al. [32]) and for measuring the length scale and intensity of turbulence as well as distribution of turbulence across the airfoils during approach and takeoff in and near thunderstorms (Camp et al. [35]). Until these data are available and processed into the appropriate format for use in computer simulation and manned-flight simulator programming, the existing models are all that are available for use in qualitative analyses of aircraft performance in severe wind shear conditions. Their limitations, however, must be borne in mind. The following section describes the influence of wind shear on aircraft performance based on our existing knowledge of prevailing wind fields as described in the foregoing as well as on hypothetical models developed to isolate certain physical characteristics of wind shear.

3.0 AIRCRAFT PERFORMANCE IN WIND SHEAR

3.1 Basic Considerations

To investigate the effects of wind shear on aircraft performance, we must first examine the equations of motion of an aircraft in a variable wind field. The general form of the dynamic equations are, therefore, summarized in Appendix A. In the derivation of these equations, the earth is assumed to be a stationary plane in inertial space. This assumption is well justified for takeoff and landing problems, which are the main considerations in this study. Also, the airplane is treated as a rigid body having a plane of symmetry. This assumption implies that the motions of the atmosphere are of sufficiently large scale that they act uniformly over the airplane at any given moment. As noted earlier, little work has been done on the effects of wind shear distributed over the aircraft. This topic is addressed by Houbolt [36]. The spatial distribution of wind over aircraft has, however, been diagnosed as a significant factor in several recent aircraft accidents. For example, the National Transportation Safety Board (NTSB) reports that on February 24, 1980, a Beechcraft Bonanza BE-35 aircraft crashed near Valdosta, Georgia, during an encounter with severe thunderstorms [37]. All the occupants were killed when their aircraft experienced an in-flight breakup. On August 26, 1978, two persons were killed when a Piper PA-28 aircraft experienced an in-flight breakup during an encounter with severe thunderstorms near Boulton, North Carolina.

Also, large aircraft have experienced breakup during flight near or through thunderstorms [38]. A C-141 jet military cargo transport lost a wing when it broke up in flight over England. Although it is unlikely that the wing failure was caused by weather-induced stresses alone, reconstruction of the thunderstorm suggests very sharp downdraft gradients were encountered (wind speeds in excess of 51 m/s (100 kts) were suspected).

Thus, it is apparent that strong wind gradients can pose a hazard to the structural integrity of an aircraft, as well as to its flying qualities. However, knowledge of the magnitudes of these wind shears in three dimensions is not yet available, and no analysis has been carried out to date on how such severe gradients would influence the lateral, roll, and yaw motions of the aircraft on approach and takeoff. To date, computer analyses and flight simulator studies are based on two-dimensional models of wind shear. Therefore in the following discussion, the major emphasis is placed on three-degrees-of-freedom analyses. As mentioned, studies are under way to measure the three-dimensionality of wind shear [32] or gust gradients across airfoils [39], and the results from these studies will be used to develop meaningful three-dimensional models of severe wind shear phenomena.

As previously discussed, however, wind shear is defined in terms of relatively long-scale motions in the atmosphere. The higher frequency wind fluctuations (i.e., turbulence) may increase the pilot's work load but not necessarily affect the general flight path of the aircraft. Therefore, analyses based on the assumption that the wind fluctuation acts over the entire aircraft are expected to lead to meaningful qualitative conclusions.

3.2 Equations of Motion with Three-Degrees-of-Freedom

To reduce the governing equations to three degrees of freedom and thus simplify the discussion as to how wind shear terms enter, consider Equation A.2 in Appendix A. This equation reduces to the form:

$$m(\dot{V} + \dot{W}_{xw} + q_w W_{zw}) = T_{xw} - D - mg \sin \theta_w \quad (3.1)$$

$$m[\dot{W}_{zw} - q_w (V + W_{xw})] = T_{zw} - L + mg \cos \theta_w$$

The nomenclature is given in Appendix B. From Equation A.4a the wind components relative to the aircraft are related to those measured relative to the earth by:

$$W_{xw} = W_{xE} \cos \theta_w - W_{zE} \sin \theta_w \quad (3.2)$$

$$W_{zw} = W_{xE} \sin \theta_w + W_{zE} \cos \theta_w$$

Hence the time derivative becomes:

$$\dot{W}_{xw} = \dot{W}_{xE} \cos \theta_w - \dot{W}_{zE} \sin \theta_w - (W_{xE} \sin \theta_w + W_{zE} \cos \theta_w) \dot{\theta}_w \quad (3.3)$$

$$\dot{W}_{zw} = \dot{W}_{xE} \sin \theta_w + \dot{W}_{zE} \cos \theta_w + (W_{xE} \cos \theta_w - W_{zE} \sin \theta_w) \dot{\theta}_w$$

where $q_w = \dot{\theta}_w$. Thus, Equation 3.1 becomes

$$m\dot{V} = T_{xw} - D - mg \sin \theta_w - m(\dot{W}_{xE} \cos \theta_w - \dot{W}_{zE} \sin \theta_w) \quad (3.4)$$

$$mV\dot{\theta}_w = -T_{zw} + L - mg \cos \theta_w + m(\dot{W}_{xE} \sin \theta_w + \dot{W}_{zE} \cos \theta_w)$$

Equation 3.4 shows the direct influence of wind shear terms on the rate of change of airspeed, V , and pitch angle, θ_w . Of course, wind variations also influence the values of D and L as discussed in Appendix A. Wind shear terms, however, do not appear directly in the moment equation (Equation A.5), but wind shear does enter through the aerodynamic moment coefficients.

Equation 3.4 expresses the influence of wind shear on the rate of change of airspeed and pitch referenced to the wind axes. These are the changes which the pilot observes from his airspeed indicator and flight director. The force equations can also be written in terms of the inertial velocity as

$$m\dot{V}_E = -L \sin \delta - D \cos \delta - mg \sin \theta_E + T_{xE} \quad (3.5)$$

$$mV_E \dot{\gamma} = L \cos \delta - D \sin \delta - mg \cos \theta_E + T_{zE}$$

In this case, wind shear terms do not appear directly in the equations; however, changes in wind are reflected not only in L and D but also in δ , which is given by the expression

$$\delta = \sin^{-1}[(W_{xE} \sin \theta_E + W_{zE} \cos \theta_E)/V] \quad (3.6)$$

Regardless of whether Equation 3.4 or Equation 3.5 is used to compute the flight trajectory, the angle of attack, α , is directly influenced by wind shear through the relationship

$$\dot{\alpha}_w = q + [T_{zw} - L + mg \cos \theta_w - m(\dot{W}_{xE} \sin \theta_w + \dot{W}_{zE} \cos \theta_w)]/mV \quad (3.7)$$

This equation is obtained by rearranging Equation A.7a. Details of the derivation of Equation 3.7 are given in Reference 40.

3.3 Effects of Wind Shear Terms

The effects of wind shear can be estimated by comparing the magnitude of the terms appearing in Equation 3.4. Consider as an example an airplane having the characteristics of a B-727 descending at a sink rate of $\dot{z} = 3.75$ m/s (7.3 kts) and a ground speed of $\dot{x} = 75$ m/s (145 kts) in still air, the thrust (considered acting only along the x axis), lift, and drag per unit mass are approximately

$$T/m = 1.14 \text{ m/s}^2 (2.2 \text{ kts/s});$$

$$L/m = 9.81 \text{ m/s}^2 (19.1 \text{ kts/s});$$

$$D/m = 1.21 \text{ m/s}^2 (2.4 \text{ kts/s}).$$

The derivative of the x-component of wind velocity for a wind varying only spatially is given by

$$\dot{W}_{xE} = \dot{x}(\partial W_x / \partial x)_E + \dot{z}(\partial W_x / \partial z)_E$$

and for the z-component by

$$\dot{W}_{zE} = \dot{x}(\partial W_z / \partial x)_E + \dot{z}(\partial W_z / \partial z)_E \quad (3.8)$$

Equation 3.8 is derived from Equation 3.3 where the subscript E is now

dropped for convenience and the approximation $\cos \theta_w = 1$, $\sin \theta_w = 0$, and $\dot{\theta}_w = 0$ is made.

Now consider Equation 3.1 with the same approximations:

$$\frac{T}{m} - \frac{D}{m} = \dot{x} \frac{\partial W_x}{\partial x} + \dot{z} \frac{\partial W_x}{\partial z} \quad (3.9)$$

$$g - \frac{L}{m} = \dot{x} \frac{\partial W_z}{\partial x} + \dot{z} \frac{\partial W_z}{\partial z}$$

For the terms on the right to be comparable in magnitude to T/m and D/m , $\partial W_x / \partial x \approx 0.02 \text{ s}^{-1}$ (1 kt/100 ft) and $\partial W_x / \partial z \approx 0.32 \text{ s}^{-1}$ (19.5 kts/100 ft). In turn, for the wind shear terms in Equation 3.9 to be comparable in magnitude to L/m , then $\partial W_z / \partial x \approx 0.13 \text{ s}^{-1}$ (7.7 kts/100 ft) and $\partial W_z / \partial z \approx 2.61 \text{ s}^{-1}$ (159.1 kts/100 ft).

Consideration of this simple calculation reveals that relatively large vertical gradients in the horizontal and/or vertical wind velocity components can be tolerated because the sink rate, \dot{z} , during most approaches and takeoffs is small. Of significantly more interest is the observation from the simple calculation that relatively small values of shear in the horizontal direction result in values of the wind shear terms having the same order of magnitude as the lift and drag terms. It is obviously not the magnitude of the shear alone but the product of the horizontal velocity and the shear as well as the value of the glide slope, θ_w , which dictates the strength of the wind shear effects.

In practically all literature related to wind shear prior to 1977, magnitudes of vertical wind shear are reported. Values on the order of 0.13 to 0.16 s^{-1} (8 to 10 kts/100 ft) are considered to be severe. These values correspond relatively close to the 0.32 s^{-1} (19.5 kts/100 ft) predicted by the simple calculation. It appears, however, that considerably more attention should be given to horizontal wind shear. A value of 8 kts/100 ft is the value of wind shear to which automatic landing systems are presently certified in the United States and the United Kingdom [41,42]. No discussion is given as to whether this is a vertical or horizontal shear. The above results suggest that

certification advisories should specify the value of wind shear which applies along the flight path.

In the atmospheric boundary layer under normal conditions the major wind shear is in the vertical direction. The CAeM Extraordinary Session, 1974, as reported in Reference 41, confirmed that statistics show there is approximately a 100 percent probability that the value of 8 kts/100 ft will be exceeded on at least one landing per lifetime of the average aircraft. Reference 41 reports the following frequency for vertical wind shears of the given intensity:

0.05 s⁻¹ (3 kts/100 ft) on 50 percent of the occasions

0.08 s⁻¹ (5 kts/100 ft) on 17 percent of the occasions

0.13 s⁻¹ (8 kts/100 ft) on 2 percent of the occasions

0.16 s⁻¹ (10 kts/100 ft) on 0.4 percent of the occasions.

There is, however, very little if any information relative to the expected frequency or intensity of wind shears in the horizontal direction. This is partly due to the difficulty associated with measuring horizontal shears. Also, wind shears in the horizontal direction will be strongly influenced by terrain features, discontinuities in surface texture, and other microscale features. Fichtl et al. [43] summarized a number of surface features which can influence wind fields around airports. Frost and Camp [23] have also surveyed various meteorological phenomena which can create strong wind shear.

From results reported by Goff [17], the average value of horizontal shears measured over several levels of a 500-m (1500 ft) tower during the passage of approximately 20 thunderstorms is $\partial W_x / \partial x = 0.09 \text{ s}^{-1}$ (5.3 kts/100 ft) and $\partial W_x / \partial z = 0.04 \text{ s}^{-1}$ (2.4 kts/100 ft). These values were computed with Taylor's hypothesis, which implies that the variations in wind are frozen in the flow field as the storm passes over the tower. Hence, the values are considerably smaller than instantaneous values. It is readily apparent, however, that horizontal wind shears in thunderstorm conditions very quickly exceed the magnitude of 0.02 s^{-1} (1 kt/100 ft) estimated as significant from simple calculations.

Table 3.1 shows the lift and drag to mass ratios for three aircraft types. These values are for roughly steady flight at landing speeds in which case the lift per unit mass is very close to the value of the acceleration of gravity, g . Thrust or drag per unit mass depend upon the lift/drag ratio. If this ratio is high, then thrust is low, and the effect of the terms $\dot{x}\partial W_x/\partial x$ and $\dot{z}\partial W_x/\partial z$ --which act like horizontal forces--will be relatively large (see Equation 3.1). This is all the more true if the aircraft is travelling at high speed. The above arguments suggest commercial airliners which have lower values of D/m and higher values of V_E are more susceptible to wind shear than smaller, lighter aircraft.

3.4 Qualitative Analysis

The influence of wind shear on aircraft motion is described qualitatively in several recent articles [44-53]. Melvin [44] appears to have given one of the first descriptions of the effect of wind shear during approach; this is summarized as follows.

When a wind shear is encountered during approach, the effects are twofold and opposite in direction. One effect is dependent upon the rate of the shear while the other is dependent only upon the magnitude of the shear.

The first effect is associated with the attempt to maintain a prescribed airspeed. If an aircraft is on an approach at 62 m/s (120 kts) IAS with a 10.3 m/s (20 kt) head wind, ground speed will be 51 m/s (100 kts). If the head wind ceases, the aircraft will need to

TABLE 3.1. Typical Values of V_E , D/m , and L/m of Different Aircraft Types.

	DHC-6	B-727	Queen Air
V_E , m/s (kts)	46 (90)	72 (140)	56 (110)
D/m , N/kg	3.420	1.008	1.230
L/m , N/kg	9.807	9.807	9.807

accelerate to a ground speed of 62 m/s (120 kts) to maintain its airspeed. This can be accomplished by pushing the nose over and accepting a loss of altitude or by prompt application of thrust to accelerate the aircraft at a rate equivalent to the rate of wind shear.

The second effect is associated with the attempt to fly a prescribed glide slope. Consider an aircraft flying a 3° ILS on a stabilized approach. If the aircraft described above encounters instantaneous wind shear from a 10.3 m/s (20 kt) head wind to no wind, the airspeed will drop from 62 m/s (120 kts) to 52 m/s (100 kts), the nose will pitch down, and the aircraft will drop below the glide slope. The loss in altitude will be directly proportional to the new wind condition, assuming thrust is maintained constant (the principle of exchange of potential energy for kinetic energy). Once the energy exchange is accomplished, the aircraft has more thrust than is required to fly the glide slope under the no-wind condition. Thus, it will gradually gain on the glide slope and overfly it.

The apparent effect of a decreasing head wind is illustrated in Figure 3.1. The effect is different depending upon where the shear occurs relative to the ground, the rate of shear, and the magnitude of shear. If the wind shear occurs very close to the ground, the aircraft will hit short. On the other hand, if the shear occurs some distance from the ground, the aircraft will tend to overfly the touchdown zone.

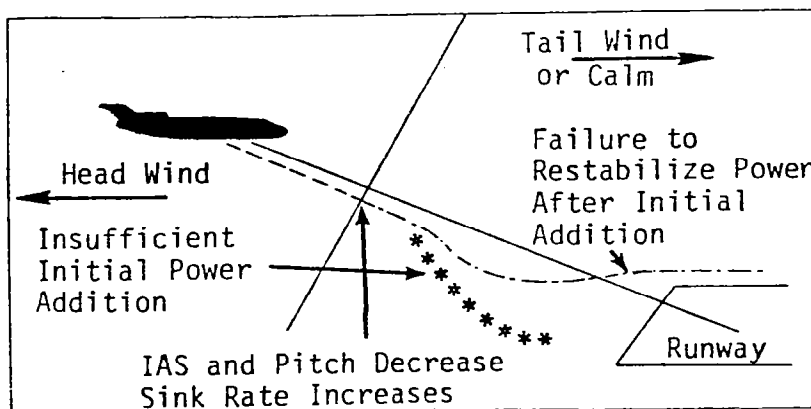


Figure 3.1 Head wind shearing to tail wind or calm [48].

As Melvin points out, however, no pilot should attempt to maintain glide slope with a constant thrust setting [47]. In the high head wind before encountering the shear, the pilot will be using a larger thrust setting than is required to fly the glide path in a no-wind condition. When the wind begins to decrease, the aircraft will tend to lose air-speed and fall below the glide slope. The pilot, in recognizing this, will add thrust to return to the glide path. (Theoretically, the amount of thrust required to equal that required to accelerate the aircraft mass at the same rate the wind is shearing.) Once the aircraft is back on the glide slope, the pilot will need to gradually reduce thrust to account for the lessening head wind. When the wind shear ceases, the aircraft no longer needs to accelerate and a thrust reduction should be applied to prevent overflying the glide slope.

Figure 3.2 illustrates the condition of a tail wind which rapidly decreases to a calm or head wind. Initially, the IAS and pitch will increase and the aircraft will overfly the glide slope. To compensate for this, a thrust reduction is required initially to reduce the aircraft's high ground speed, followed by a gradual thrust increase. When the wind ceases altogether or changes to a head wind, a large thrust addition is required to restabilize power after the initial reduction and to prevent loss of ground speed.

Once again, the effect of the tail wind shearing to a calm or head wind is dependent upon the altitude at which the shear occurs. If the

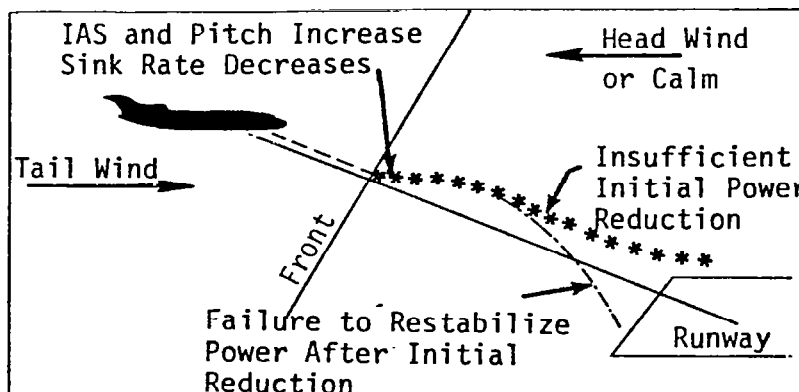


Figure 3.2 Tail wind shearing to head wind or calm [48].

shear occurs close to the ground and the thrust is not reduced quickly enough, the approach will be high and fast with the danger of overshooting. If, on the other hand, the shear occurs well above the ground, the aircraft will first rise above the glide slope and, if the thrust is held relatively constant, sink back below the glide slope, landing short.

Higgins and Patterson [51] have also looked qualitatively at flying procedures in hazardous wind shear. They used static performance curves to provide pilots with some ideas relative to handling shears. They point out that if implemented, these ideas would aid in avoiding catastrophe if the pilot's aircraft was inadvertently caught in a combination of severe downdraft and/or severe wind shear that resulted in high rates of descent and/or severe loss of airspeed, especially within approximately 122 m (400 ft) of the ground. They also discuss the following points:

- Basic performance conditions
- Airplane energy management concepts
- Maneuvering margins
- Angle of attack consideration
- Attitude considerations
- Performance effects of acceleration along the flight path
- Performance effects during flap retraction.

The key points of some operational techniques they recommend relative to hazards of landing, approach, and takeoff in wind shear environments are:

- When forced to fly at speeds near stick-shaker because of wind shears, good climb performance and maneuver margins still exist. Rapidly accelerating the aircraft away from stick-shaker could result in a significant loss of altitude.
- High attitudes are required at stick-shaker speeds and go-around thrust to attain the maximum climb capability of the aircraft.

- Rapidly accelerating to maintain V_{REF} or V_2 airspeeds during a wind shear will severely reduce climb capabilities. Conversely, decelerating to stick-shaker speeds can provide added climb capability to compensate for large downdrafts.

The recommendations are based on performance analyses from charts which are valid for stabilized 1-g flight conditions at constant indicated airspeeds for the airplane weight given in the report. The authors point out that if pilots make use of any of the specific attitudes from these charts as a guide for operation of a B-727, the attitudes should be treated only as initial targets. Flight in severe wind shear is a dynamic, constantly changing situations and confirmation that any given attitude is adequate for any given situation comes from instrument readings which show that the aircraft is responding in a satisfactory and desirable manner.

ALPA's Airworthiness and Performance Committee (see Steenblik [52]), on the other hand, is concerned that many airline flight training departments continue to train pilots to promptly trade airspeed for altitude by pitching up until the airspeed decays enough to activate the stick-shaker (last recommendaton by Boeing article). The committee argues that pilots should attempt to achieve minimum drag speed (best angle of climb speed) during wind shear encounters.

When performance is critically limited by wind shear effects, the ALPA committee recommends that pilots fly near the minimum drag point for best climb angle performance until ground impact is eminent, then exchange all available energy to flair the aircraft and soften the impact or to sustain flight in ground effects until clear of the shear.

A distinction must be made between excess thrust over drag capability, which contributes to long-term flight path performance and energy trades (kinetic for potential and vice versa). A turbojet aircraft attains its maximum climb angle performance at approximately its minimum drag speed. There is a small range below the exact minimum drag speed for which drag does not increase significantly, but drag does increase rapidly as speed is lowered, rapidly reducing climb angle performance.

It is unreasonable to think that any pilot would deliberately fly up the back side of a drag curve (see Figure 3.3) when performance is limited by wind shear. However, this does not mean that a pilot, upon realizing that impact with the ground or an obstacle is eminent, would not pull the aircraft up and sacrifice airspeed to avoid or reduce impact. The best climb performance occurs when the aircraft is most energy efficient and that is at the minimum drag point. Aircraft performance limited by wind shear cannot be increased by flying up the back side of the drag curve.

Steenblik [52] concludes that in the 1975 Continental Airlines' takeoff accident in Denver, there was no way the aircraft could accelerate inertially fast enough to overcome the effects of the shear and avoid ground contact. Steenblik [52] believes that it would have been impossible for the pilot to have flown out of the shear conditions by just increasing the pitch. The ALPA committee goes on to point out that

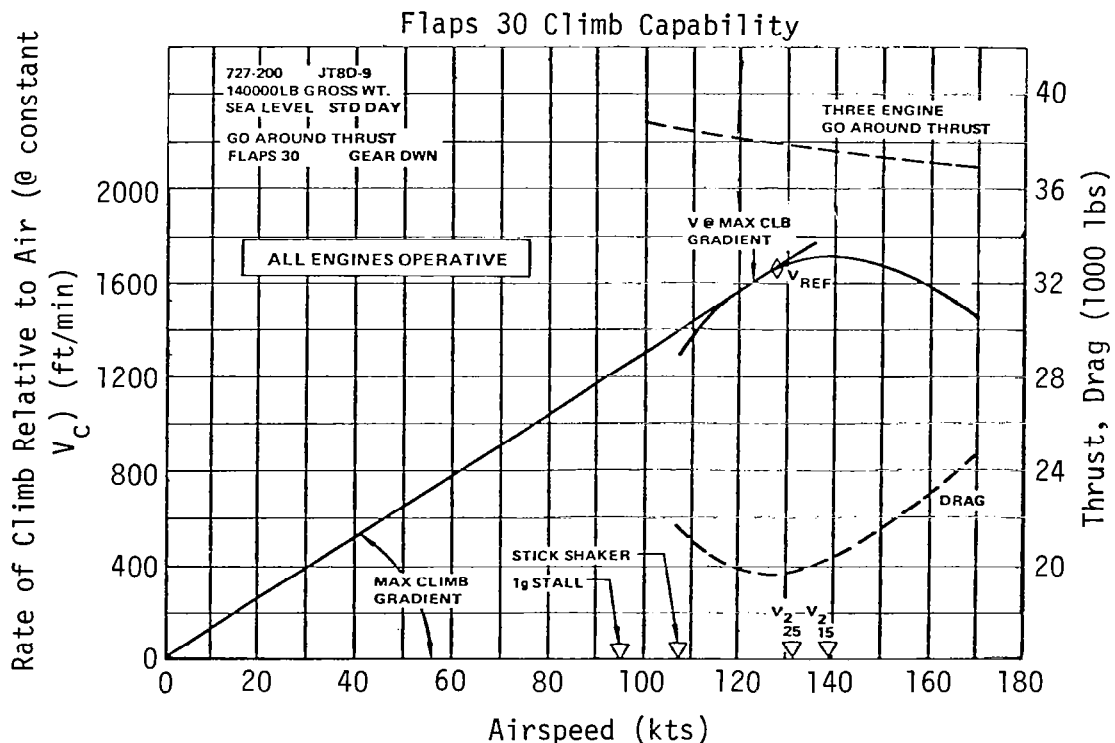


Figure 3.3 Flaps 30 constant speed climb capability [51].

there appears to be some confusion relative to the all-engine climb capability of an aircraft at the stick-shaker speed. Considering that the climb capability might be approximately 1200 ft/min for a representative aircraft, many fail to recognize that the all-engine climb capability is probably double that amount at the minimum drag point. Deliberately trading all available energy down to the stick-shaker speed while increasing drag to the point of drastically reducing climb capability is, in the committee's belief, an unsafe practice.

If an aircraft is operated at the minimum drag point (or in the fairly flat portion of the drag curve), it will achieve its best performance; then if energy is traded as the aircraft enters ground effects, the trade could result in a successful go-around, but at least would result in minimizing ground impact. If the initial climb moves the aircraft well up the back side of the drag curve, however, there will be reduced capability for a sustained climb and energy available as a last resort will be very limited.

The importance of carrying extra speed for landing cannot be overemphasized; such an energy trade can give much faster results than improved performance from an increase in thrust. An energy trade, however, is a one-shot affair; only a thrust increase can make a long-term contribution to a new flight path. Pilots should not be reluctant to trade energy down to the minimum drag point--after that point, energy to be traded should be reserved to use when ground impact is eminent.

Excess energy to trade down to the minimum drag point is important, as is the early recognition of the effects of wind shear and the rapid application of maximum thrust. Bliss [53], however, concludes that the airspeed/ground speed concept is essential for wind shear protection. He believes that without the correct ground speed value, a wind shear warning system cannot solve the problem adequately, and no amount of training can be of any use for a severe wind shear situation. This, he claims, is true for either a manual or coupled approach. The acceleration margin device, in Bliss's opinion, also becomes useless on a non-precision approach.

A pilot's conception of speed is traditionally oriented solely with reference to indicated airspeed (IAS). The conventional performance charts (those used by Higgins and Patterson [51]) are therefore referenced to indicate airspeed values which Bliss believes are valid only in static air, but worthless in a wind shear. In every case where the control of an airplane is placed in a hazardous condition due to wind shear, it is specifically the result of either an excessively high or excessively low ground speed value at an attitude low enough to compromise or preclude recovery.

To establish the magnitude of the effects described above, analytical models with varying degrees of sophistication have been developed. The author is unaware of any models, however, which include all six degrees of motion with any realistic three-dimensional model of severe wind shear. Thus, only results for three-degrees-of-freedom and two-dimensional wind fields are discussed in the following section.

3.5 Mathematical Analysis

Etkin [54], in 1946, appears to be one of the first to analyze flight in wind shear. Using a system of linearized equations, he investigated the performance of a light airplane gliding at 27 m/s (52 kts) through wind shears of $\partial W_x / \partial z = 0.04, 0.03, \text{ and } 0.002 \text{ s}^{-1}$ (2.6, 1.7, and 0.9 kts/100 ft). He predicted that the aircraft would overshoot the desired touchdown point by roughly 792, 549, and 274 m (2600; 1800, and 900 ft), respectively. These results are based on the assumption of an approach at constant relative velocity, V , and constant pitch angle, γ . The results of Etkin's study for the magnitude of overshoot, Δx , can be expressed as

$$\Delta x = \Gamma z_i^2 / 2V_e \sin \gamma_e \quad (3.10)$$

where $\Gamma = \partial W_x / \partial z$ and $\Delta x = x_{\text{shear}} - x_{\text{steady wind}}$ is the length of overshoot.

Etkin concludes that the distortion of the flight path during both glide and climb is greatest when the rate of descent is small and when the wind velocity is large relative to airplane speed. Thus, the

aircraft most affected would be machines with low wing loading and flat glides. Fast machines with steep glides would be less disturbed. This result appears to be in variance with the conclusions reached above. It is shown later that flight path calculations using a linear wind shear in the vertical direction give seemingly contradictory results to the same computation using a logarithmic wind speed profile, which is more realistic of the atmospheric boundary layers.

Gera [55], using a similar system of equations as Etkin, assessed the influence of wind shear on the longitudinal motion of airplanes. He also assumes completely horizontal wind with linear variation in speed with altitude and arrives at almost the identical conclusions as Etkin.

Gera shows that the deviation from the touchdown point in wind shear as contrasted with steady winds is expressed by the relationship

$$\Delta x = \frac{\sigma}{\sin \Delta \gamma_w} \left[z_i + \frac{g}{2V_e^2} \left(\frac{\sin \Delta \gamma_w}{\sin \gamma_e} - 2 \right) z_i \right] \quad (3.11)$$

where σ is a nondimensional wind shear parameter defined by

$$\sigma = V_e (\partial W_x / \partial z) / g \quad (3.12)$$

This expression gives the amount of overshoot and undershoot at ground level relative to the flight path and steady wind. Gera concludes that in a head wind decreasing with altitude there is an undershoot ($\Delta x < 0$) as long as the inequality

$$z_i < \frac{2V_e^2}{g \left(2 - \frac{\sin \Delta \gamma_w}{\sin \gamma_e} \right)} \quad (3.13)$$

is true. If the height lost during the descent through the shear layer exceeds the right-hand side of the inequality, an overshoot will occur. It is important to note, however, that for moderate values of wind shear there is always an initial undershoot regardless of the thickness of the shear layer. This result is in agreement with the qualitative discussion given earlier.

In Gera's analysis for the above result, the undershoot was calculated for the case in which the airspeed, angle of attack, and throttle setting were the same in both steady wind and wind shear. It was found that these conditions were possible if the airplane in wind shear assumed a pitch attitude different from the steady wind value. For the case where the airspeed, angle of attack, and pitch angle are the same for both the conditions of steady wind and wind shear (possible, at least in theory, by having different control deflections and throttle settings under the two conditions), Equation 3.11 reduces to Equation 3.10. The value of Δx in this situation for normal glide is always positive, and hence an overshoot always occurs. The reference conditions for Gera's analysis are zero external moment and constant airspeed, angle of attack, and pitch angle. Etkin began his analysis with an arbitrary initial value of angle of attack. This value became constant, however, in a very short period of time; so essentially, the analysis was for constant angle of attack (which in this case is also constant pitch angle) and constant airspeed.

Gera [55] also investigates the effect of linear wind shear on longitudinal stability. For the assumption of constant airspeed, constant angle of attack, and pitch angle, the effect of wind shear on the short-period motion and the phugoid damping was negligible, but the phugoid frequency and damping ratio were found to vary considerably with wind shear. The time for the phugoid to damp to half amplitude increases in a climb and decreases in a dive, as expected. Positive shear (head wind changing to a tail wind, which is typically the situation associated with flying through a downburst) is shown to amplify these effects. He also notes that wind shear affects the phugoid mode even in level flight.

Etkin [4] analyzes the longitudinal stability of a typical STOL airplane for linear vertical wind shears from $-3.4 \times 10^{-5} \text{ s}^{-1}$ (-0.002 kts/100 ft) (the head wind case) to $3.4 \times 10^{-5} \text{ s}^{-1}$ (0.002 kts/100 ft) (the tail wind case). These are very low wind shear values. He found, however, the effects on both the phugoid and pitching mode to be very large. A strong head wind decreases both the frequency and damping of

the phugoid, and a strong tail wind changes the real pair of matching roots into a complex pair representing a pitching oscillation of long-period and heavy damping.

Sherman [56] also used a linearized system of equations to carry out a stability analysis of wind shear effects on a large jet transport. In the case of the phugoid mode, positive wind shear (a shear that changes head wind to tail wind) caused the phugoid to remain periodic and stable, although the time to damp to half amplitude decreased as the shear gradient increased. A negative shear (a shear that changes tail wind to head wind) caused the phugoid to become unstable for values of the shear parameter, σ , greater than unity (i.e., $\sigma > 1$).

The general conclusions from the above are that wind shear has a pronounced effect on the phugoid modes of aircraft stability but little or no effect on the short-period modes. The paper by Moorhouse [57] lends further support for this argument.

The assumption of linear wind shear discussed in the preceding results does not present a realistic simulation of the atmospheric boundary layer wind profiles. Typical wind speed profiles found in the atmospheric boundary layer under moderate climatological conditions are best represented by a logarithmic profile [58,59]

$$W_{x_E} = \frac{u^*}{\kappa} [\ln(z_E/z_0) + \psi(z_E/L)] \quad (3.14)$$

The function $\psi(z_E/L)$ (note L is the Monin-Obukhov length scale) takes different forms depending on the characteristics of the atmospheric boundary layer, i.e.,

Neutral Boundary Layer:

$$\psi(z_E/L) = 0 \quad (3.15)$$

Unstable Boundary Layer:

$$\psi(z_E/L) = \int_{z_0/L}^{z_E/L} z_E/L [1 - (1 - 18z_E/L)^{-1/4}] dz_E/L \quad (3.16)$$

Stable Boundary Layer:

$$\psi(z_E/L) = 5.2z_E/L \quad (3.17)$$

These forms of wind profiles do not lend themselves to linearized models.

Luers and Reeves [60] attack this problem by utilizing a nonlinear system of equations similar to Equation 3.5. The landing of seven commercial/military-type aircraft was computer simulated starting from an initial altitude of 90 m (300 ft). Deviations in touchdown point in excess of 910 m (3000 ft) resulting from variation of the horizontal wind during the final 90 m (300 ft) of descent with no pilot or auto-pilot feedback were computed. Vertical wind shear associated with a range of values of surface roughness, z_0 , and stability, L , were considered.

Their analysis, however, neglected the wind shear terms in the rate-of-change-of-angle-of-attack relationship given by Equation 3.7. With these terms included, it is found [61] that the results of Luers and Reeves overpredict the magnitude of the touchdown deviations by roughly 60 percent. The trends of their results are correct, however, even though the magnitude of deviation from the desired touchdown point is too high.

Interestingly, the results of the flight path analysis utilizing the nonlinear system of equations and the logarithmic wind shear profiles resulted in the aircraft undershooting the runway when landing in a head wind and overshooting the runway when landing in a tail wind. This result is in direct contrast to the results reported by Etkin [54] and Gera [55] for linear wind shear profiles. Undershooting the touchdown point was also reported by Frost and Reddy [62] and by Denaro [63].

Denaro [63], analyzing aircraft flare, explains this apparent contradiction in the effect of wind shear by a combination of two factors. First, a logarithmic wind shear has a higher rate of change of wind magnitude at the lower altitudes than does a comparable linear shear. (Note the wind shear for a logarithmic profile goes as $1/z_E$ and

becomes very large near the ground.) An aircraft at flare altitude is likely to experience large wind gradients and therefore large airspeed changes. In a logarithmic head wind shear, the aircraft is significantly below the normal speed for which the flare control is designed. Second, because the onset of shear is gradual, the throttles do not respond as much initially as they do in the linear shear case. Consequently, when the aircraft reaches flare altitude in a logarithmic head wind shear, it does not have greatly advanced throttles as in the linear head wind shear case. Therefore, throttle freeze and retard at this point have a significant effect on reducing airspeed even further. The aircraft starts flare at a rather low sink rate, but response is poor and the sink rate is not well arrested. With the higher sink rate in the latter stages of flare, the aircraft lands both hard and short.

Frost and Reddy [62] and Luers and Reeves [60], however, found short landings even without a control system being involved. In this case the difference between the results for a linear profile and a logarithmic velocity profile are a consequence of the initial trim conditions used to start the computation. For a fixed control system, the aircraft is trimmed at the value of wind shear existing at the initial altitude from which the calculation begins. With a logarithmic velocity profile at sufficiently high altitudes, the wind shear is very low. As the aircraft approaches the ground, the wind shear for a logarithmic velocity profile increases rapidly whereas the linear wind shear remains constant. However, the thrust and elevator setting have been set for the lower magnitude wind shear. Inspection of Equation 3.4 illustrates that for fixed thrust and possible decreasing values of drag and lift due to reduced wind speed (note that L and D are functions of angle of attack and the rate of angle of attack as well as other transient variables [40]), the increasing wind shear term strongly influences the sink rate of the aircraft. Frost and Reddy [62] had no difficulty removing this fast sink rate when an automatic control system was incorporated into the computer analysis.

The preceding analyses have investigated only shear of the horizontal wind. Under more severe wind shear conditions, particularly

thunderstorms, major fronts, and flow fields around buildings or other surface terrain features, the vertical wind component can be extreme. References 40, 62, 64, 65, 66, and 67 report investigations with the vertical wind speed component included in the equations of motion. The impetus to investigate flight with severe variations in both vertical and horizontal wind speeds was generated by the Eastern 66 accident in a severe thunderstorm at JFK International Airport on June 24, 1975. This accident created immense concern relative to flight through thunderstorms. Frost et al. [16] and Foy [19] developed mathematical models of wind fields associated with strong environmental shears. Frost and Crosby [40] and Turkel and Frost [64], utilizing these models in the form of computer table lookup routines, investigated the flight of various types of aircraft through thunderstorms and other strong wind shear conditions. The following sections describe these results along with results from other studies reported in the open literature.

4.0 FLIGHT IN STRONG WIND SHEAR ENVIRONMENTS

4.1 Fixed Control Models

Initial numerical studies of flight in thunderstorm-type wind shear were carried out under the assumption of fixed controls. Figure 4.1 shows the computed descent of a DC-8-type aircraft through 11 different thunderstorms. In nearly all of these approaches an oscillation near the phugoid frequency of the aircraft is strongly amplified. This directly supports the conclusions of the stability analyses relative to the phugoid mode described earlier.

McCarthy and Blick [66] independently analyzed flight in thunderstorms. Using a linearized model and a superposition technique, they investigated the flight behavior of a B-727-type aircraft in a thunderstorm, using wind data that had been obtained from in-flight measurements near thunderstorms. They also found amplified flight path oscillations at frequencies near the phugoid frequency of the aircraft.

Frost and Crosby [40] applied their models to a number of aircraft types. The flight paths computed for two of the more severe thunderstorms are shown in Figure 4.2. In nearly all cases, the aircraft demonstrated high-amplitude oscillations at frequencies near the phugoid frequency. Table 4.1 shows the computed phugoid period and horizontal wavelength versus those predicted by simple theory. For the commercial-type aircraft, the frequency of the oscillations observed in the thunderstorm flight paths are very close to those predicted for the phugoid oscillations from simple theory. For the smaller DHC-6-type aircraft, the oscillations occurred at a somewhat higher frequency than the classical phugoid frequency. Correspondingly, the smaller aircraft showed less sensitivity to the thunderstorm wind fields. These results suggest that thunderstorm wind fields have characteristic scales of wind shear which can create hazardous oscillations in the flight paths of commercial-type aircraft. Severe oscillations in airspeed were also

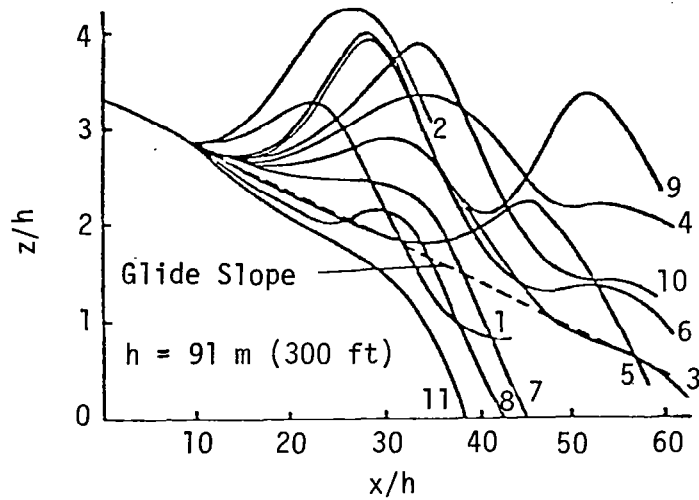


Figure 4.1 Flight paths of DC-8-type aircraft landing with fixed controls at a -2.7° glide slope (numbers on curves designate different thunderstorm cases).

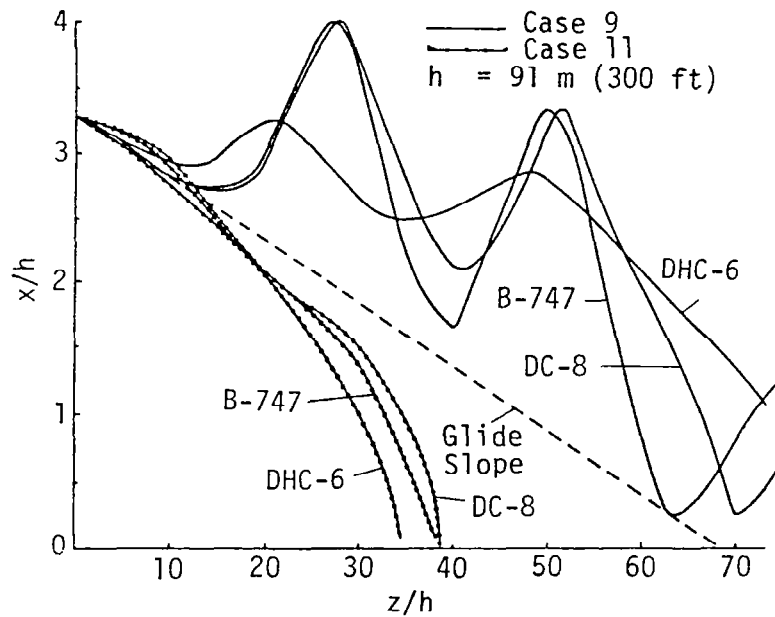


Figure 4.2 Comparison of different types of aircraft landing with fixed controls in thunderstorm cases 9 and 11 at a -2.7° glide slope.

TABLE 4.1. Phugoid Period and Horizontal Wavelength.

Aircraft Type	V m s ⁻¹	T (sec)		λ (m)		λ̂ = λ/h	
		Com-puted	Pre-dicted	Com-puted	Pre-dicted	Com-puted	Pre-dicted
DC-8	70	29.9	31.7	2,180	2,203	23.84	24.09
B-747	66	28.8	30.0	2,067	2,085	22.60	22.80
DHC-6	46	27.1	20.7	2,405	1,016	26.3	11.11

$$T = \sqrt{2\pi}V/g; \lambda = VT$$

computed, Figure 4.3. McCarthy et al. [67,68] computed almost identical results with their model.

Augmentation of the phugoid mode during flight through severe wind shear suggests an accident-causing factor. McCarthy et al. [68] states that longitudinal wind gusts providing energy at the phugoid frequency may result in airspeed oscillation of a nature that would be difficult to control and, in fact, may lead to stalls and otherwise disastrous results.

Most pilots are adamant that because of the low frequency of the phugoid oscillations, they can be controlled without difficulty.

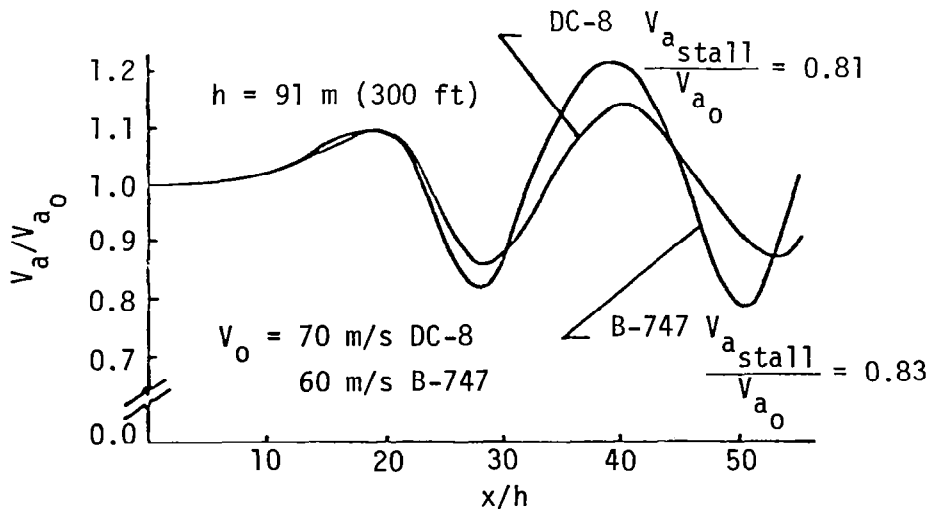


Figure 4.3 Comparison of indicated airspeed of DC-8-type and B-747-type aircraft landing with fixed controls in thunderstorm case 9.

However, during approach through a thunderstorm with other distractions such as poor visibility, runway slipperiness, etc., the effects of the phugoid oscillations can be insidious, and before the pilot realizes the presence of the oscillations, he may have reached a situation that is uncontrollable. In actual fact, this effect of first rising and then falling below the glide slope is exactly that described qualitatively by Melvin [44,45].

Additionally, nearly all conclusions relative to the phugoid oscillations by pilots and aerodynamicists alike are not based on the concept or experience of a forcing function (i.e., variable wind speed) driving the system at its critical frequency. In fact, most training is based on steady winds. In turn, there is some question as to how well phugoid oscillations are reproduced in a manned flight simulator. Thus, it is believed that the effect of forcing the aircraft at its phugoid frequency can be hazardous and should not be taken glibly.

In many of the thunderstorm analyses carried out [26,69], the concept of a downburst, or extreme downdraft in the heart of the thunderstorm cell, is suggested as the significant wind component contributing to loss of flight control. Thus, the vertical wind is considered the prime factor creating hazardous conditions. Nearly all of the previous arguments, however, suggest that the horizontal wind component is equally important in creating flight hazards. To test the individual effects of the wind speed components, the computer program was run first with only the longitudinal wind component and then second with only the vertical wind component. Figure 4.4 shows the separate effects of the two wind components for a DC-8-type aircraft landing with fixed controls in a typical thunderstorm outflow. It is apparent that in the absence of the longitudinal wind component, the influence of the wind on the aircraft flight path, is considerably reduced. McCarthy et al. [68] arrived at identical results.

4.2 Automatic Control Systems

The preceding results show that serious departures from the glide slope occur during simulated landing of aircraft with fixed controls in

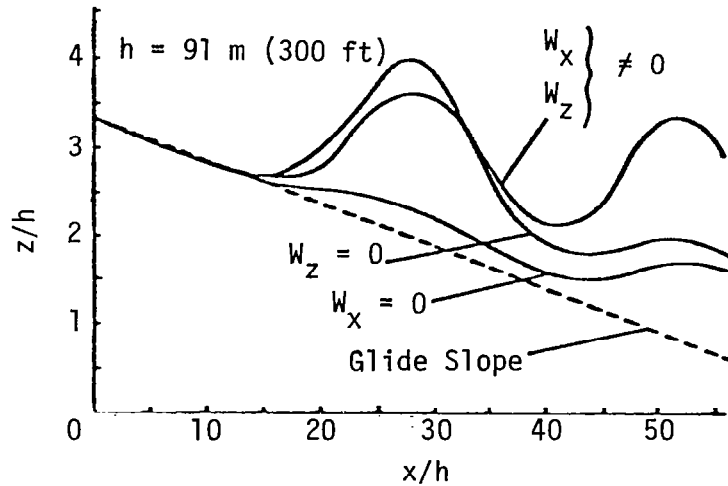


Figure 4.4 Comparison of DC-8-type aircraft landing with fixed controls in thunderstorm case 9, considering individual wind components separately and combined.

thunderstorm gust fronts. Since the assumption of fixed controls is not realistic, Frost and Crosby [40] investigated automatically controlled flight. The automatic control systems using variable gains almost completely eliminate the severe perturbations from the flight path for the thunderstorm models considered in the study, Figure 4.5. However, the large control inputs and small response times required for the automatic control system to track the glide path in the thunderstorm cases may be difficult to achieve in operational hardware.

Figure 4.6 shows the thrust control necessary to maintain the glide path during approach through a thunderstorm. The thunderstorm studied resulted in a tail wind shearing to a head wind. The insert in Figure 4.6 shows the correspondence between Melvin's [44] qualitative description of thrust requirement and that predicted by the computer simulation.

4.3 Pilot Models

The automatic control computer model [40,62] was then expanded to incorporate a simulation of a human pilot into the computed response of the aircraft in wind shear [64].

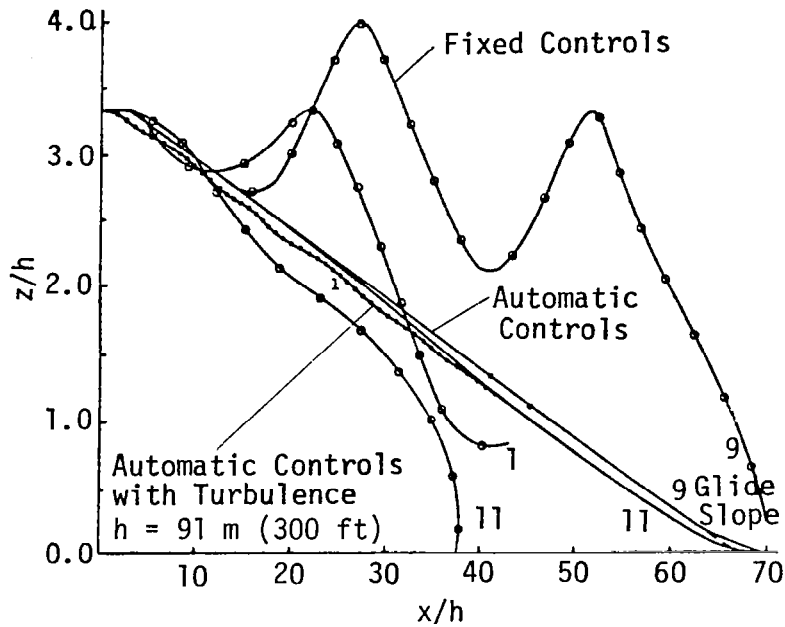


Figure 4.5 Flight path comparison of DC-8-type aircraft landing with (1) fixed controls, (2) automatic controls, and (3) automatic controls with turbulence included, in several different thunderstorm cases.

Human pilot transfer function data were taken during compensatory tracking simulator experiments by Adams and Bergeron [70]. They tested six pilots (ages 30 through 47) and two test engineers in a flight simulator equipped with an oscilloscope and control stick. The subjects' static gains, lead and lag time constants throughout the runs were measured and variations between the subjects for given controlled dynamics (degree of vehicle controllability) were examined.

For the eight pilots the values of the transfer functions using a response time step of 0.01 second ranged between 0.254 and 0.905. For the reported study of Turkel and Frost [64], a parametric study of pilot performance ratings between zero and one was considered more useful than using any specific pilot rating from the data of Adams and Bergeron [70]. The pilot model was incorporated into the control loop of Frost and Reddy [62]. Since the pilot does not move the servos to correct the plane's deviations as efficiently as the autopilot and, in effect, always lags the autopilot, the pilot's control signal inputs were

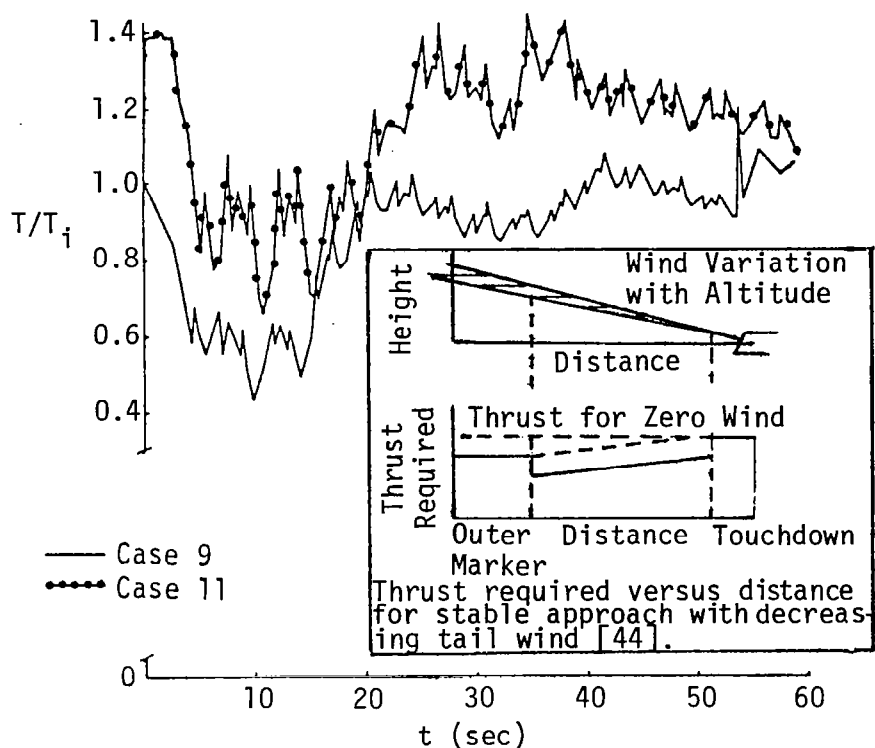


Figure 4.6 Rate of change of thrust required of DC-8-type aircraft landing with an automatic control system in thunderstorm cases 9 and 11.

reduced by a "perfection percentage," where 0 percent corresponds to zero inputs (fixed stick), 100 percent corresponds to "perfect" autopilot control, and a rating of 50 percent can be said to be average. This was accomplished in the program by multiplying the control signals by the "perfection percentage." The pilot constantly attempts to return the aircraft to the desired state but this occurs at a slower response rate than the "near-perfect" automatic control system.

Fixed-stick, autopilot, and manned performance were compared for a B-727-type medium-sized commercial transport and for a Queen Air small commuter-type aircraft flown through a glide slope longitudinal wind profile detected by Doppler radar [71]. The wave-form wind disturbance was shown to excite the phugoid oscillations of both aircraft when they were flown in the fixed-stick mode, but presented no control problems for manned aircraft.

To investigate the significance of wind shear with a frequency equal to the phugoid, a fictitious quarter-sinusoidal wind field was modeled. A simulation was made for fixed-stick, autopilot-controlled, and manned aircraft with characteristics of a B-727 through this profile for a 6 m/s (12 kt) amplitude head-wind-to-tail-wind phugoid-frequency shear wave. This case revealed phugoid oscillations but clearly showed that this shear wave was not a serious problem for a manned vehicle.

However, in a stronger disturbance--10 m/s (19 kt) head-wind-to-tail-wind phugoid-frequency shear wave--significant deviation from the glide slope was noted for the autopilot, the 50-percent-rated pilot, and the 25-percent-rated pilot flight simulations, although no hazardous situations occurred. The low performance 5-percent-rated pilot initially lost control of the aircraft and dropped farthest below the glide slope. However, thrust was eventually increased to bring the aircraft back to the glide slope.

In flight simulations through a full 14 m/s (27 kt) phugoidal-frequency sine wave, comparisons were made between autopilot control and control by pilots of varying skill. The autopiloted aircraft executed the best approach, while the high-skilled pilot descended below the glide slope but was eventually able to bring the aircraft back onto the glide path. However, the low-skilled pilot could not maintain adequate control and landed short.

Classifying pilot response by means of a performance rating encompasses the many intangibles encountered in pilot modeling which are too complex to simulate. These intangibles include pilot personality, training, knowledge, and warning of the encountered wind shear, as well as the element of surprise. Hence, a pilot with a low performance rating (for example, 0.03, which corresponds to a minimal control input) may be classified as poorly trained, slow-to-react, unknowledgable, or uninformed of the eminent wind shear. The report concludes that more work is clearly needed on pilot modeling, specifically to determine pilot response to the wind shear environment. However, for purposes of the study, the proposed pilot's "perfection percentage" gave useful results.

4.4 Comparison of Computer Simulation with Manned Flight Simulator Studies

4.4.1 Description of Study

Frost et al. [72] and McCarthy and Norviel [73] compared computer simulation with manned-flight simulator studies. The aim of this work was:

1. To utilize the three-degrees-of-freedom aircraft trajectory computer program to examine aircraft/pilot response through wind shears including longitudinal sine waves, S-shaped waves, 1 - cosine vertical winds, and combinations at various frequencies and amplitudes as approximations to the winds encountered in a thunderstorm downburst cell.
2. To determine if the control system algorithm and aircraft trajectory program combination gives an accurate representation of the behavior of the real pilot by comparing the computed results with those measured in a manned flight simulator when subjected to the same input wind field models.

The aircraft computer program was a three-degrees-of-freedom (horizontal, vertical, and pitch) program. This program and the pilot/control system models are described in detail in Turkel et al. [74]. For comparison purposes, quantitative flight path deterioration parameters were defined. These parameters were investigated to determine the degree to which they serve as a measure of hazardous flight conditions existing on approach through sinusoidally varying winds. The sinusoidal winds are an idealization of winds associated with flight through thunderstorm cells.

4.4.2 Idealized Wind Speed Profiles

The wind speed profiles selected for study are shown in Figure 4.7. They are based on the observation that an aircraft flying through a downburst would first encounter an increasing head wind with the wind changing to zero and resulting in an increasing and then decreasing tail wind. Depending upon the wind storm, this may either have a full sine wave effect or a S-shaped or half-sine-wave effect. In turn, the aircraft would encounter an increasing downdraft reaching a maximum at the

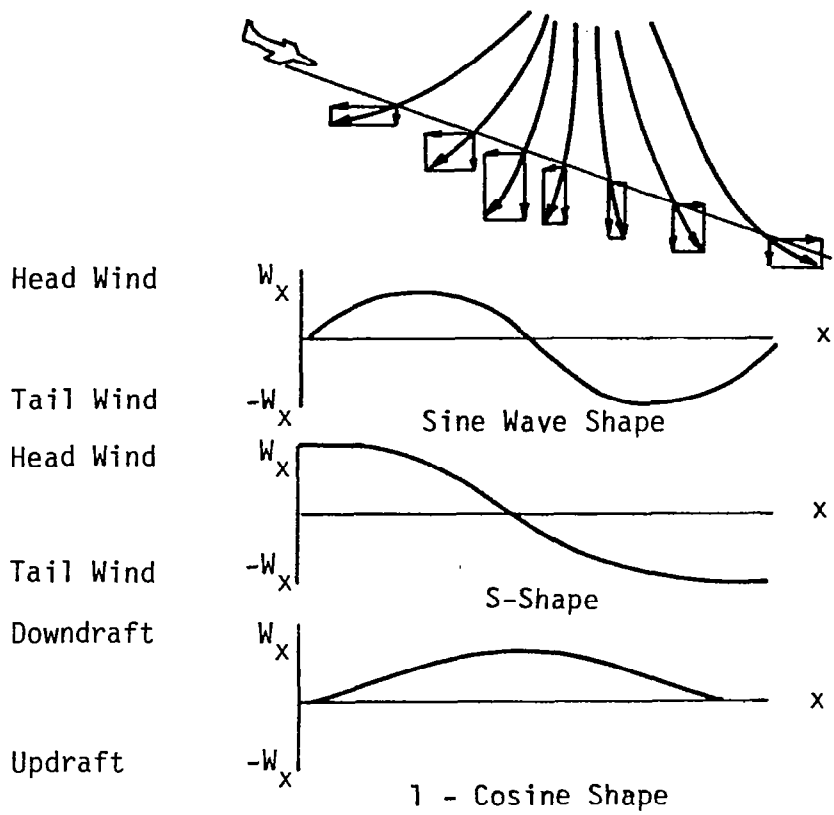
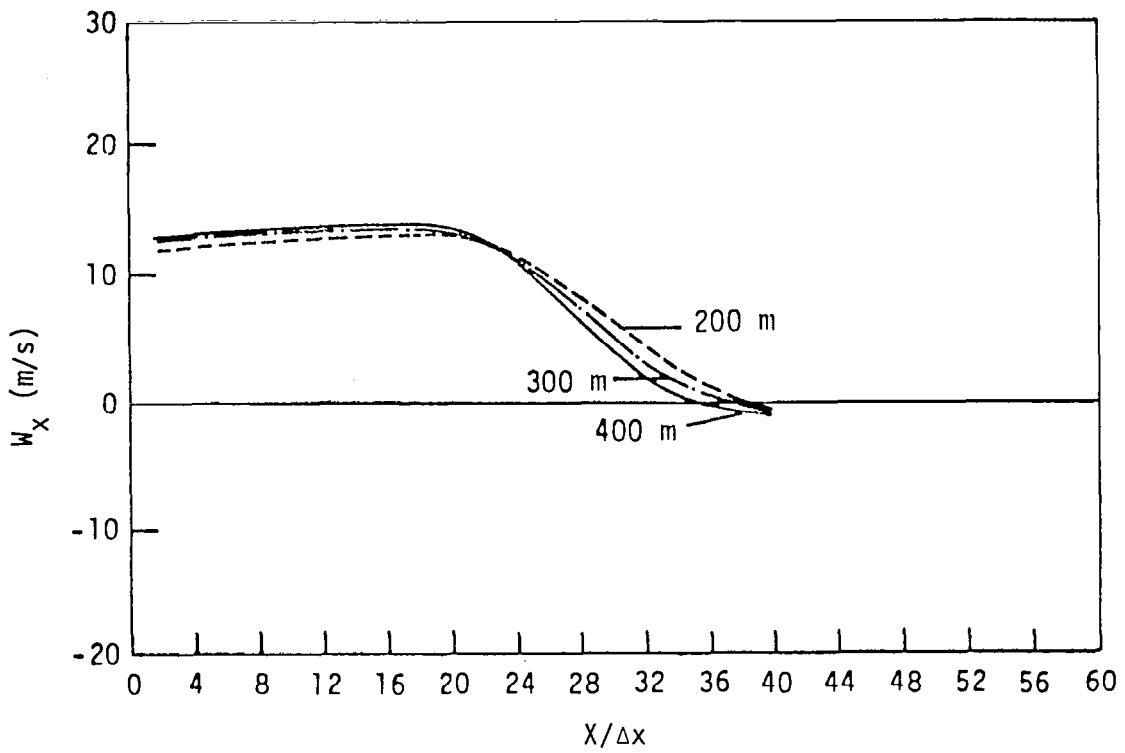


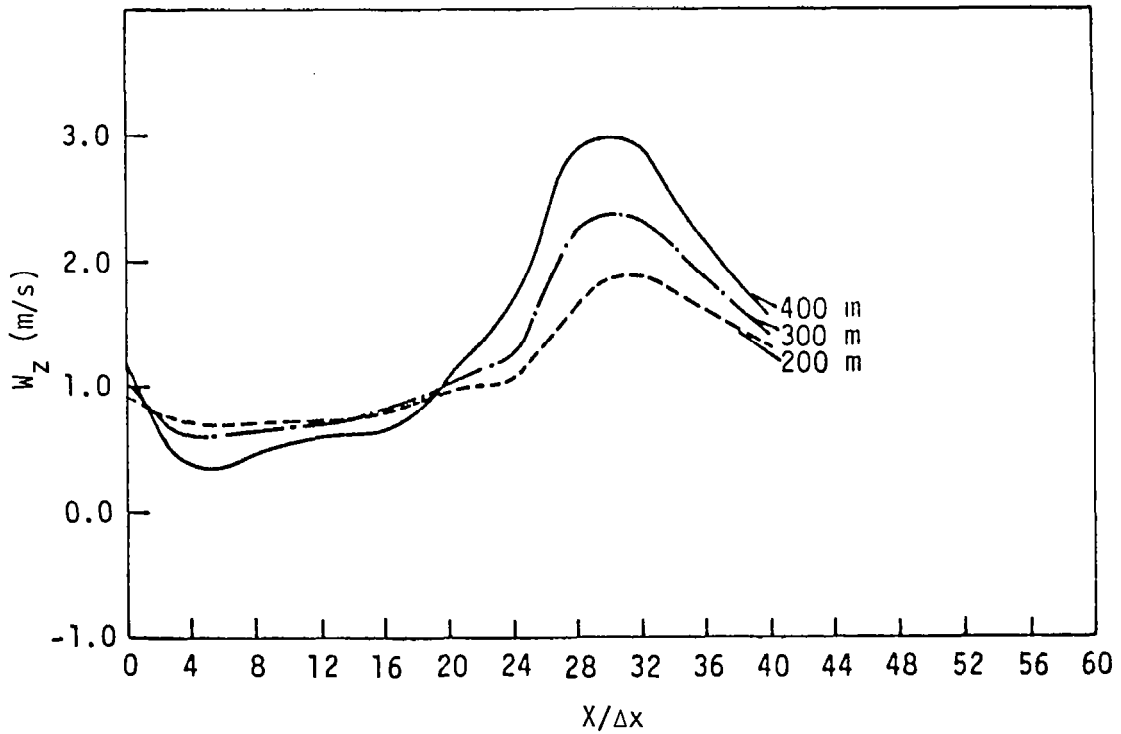
Figure 4.7 Wind models used to simulate a thunderstorm downburst cell.

center of the downburst and then decreasing again to zero at the far side of the outflow. Evidence of this type of wind field has been determined by a number of studies (see Section 2.2). Figure 4.8 shows the average wind speed for 20 thunderstorm cases along a 3° glide slope at three different elevations. Note that the horizontal wind shear clearly illustrates an S-shaped sinusoid while the vertical wind demonstrates a similar profile to the 1 - cosine shape shown in Figure 4.7.

Goff [15] examined the periodic nature of thunderstorm data. He computed the wind shear energy spectrum for the longitudinal wind component and the vertical wind component. Figure 4.9 shows that the energy for thunderstorm wind shears is contained in a frequency range that encompasses the typical phugoid frequency of most aircraft. The scale across the top of the figure indicates that the peak in the energy spectrum occurs somewhere near 100 to 50 seconds with respect to the

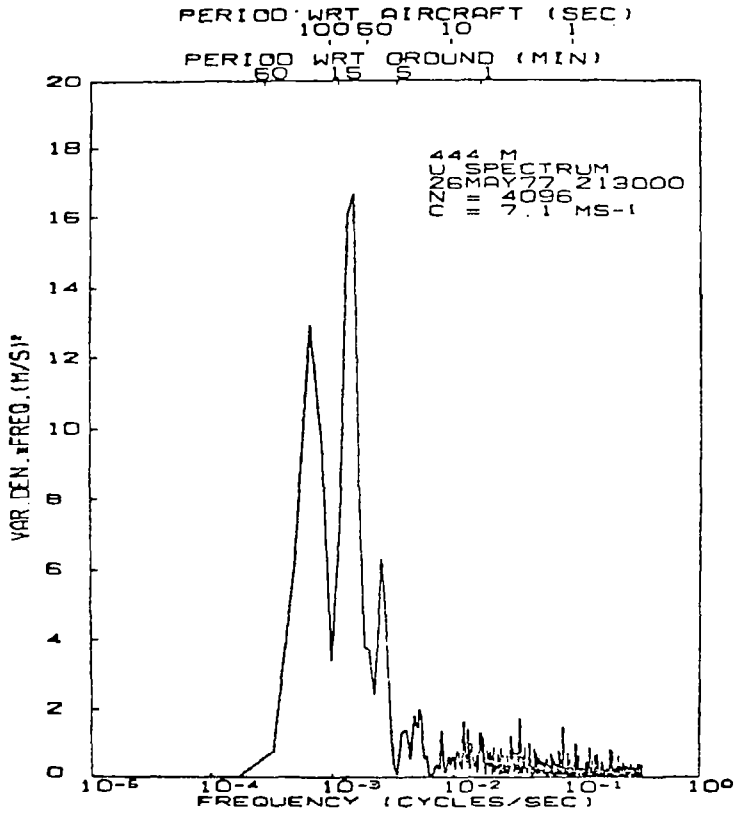


a) Longitudinal winds

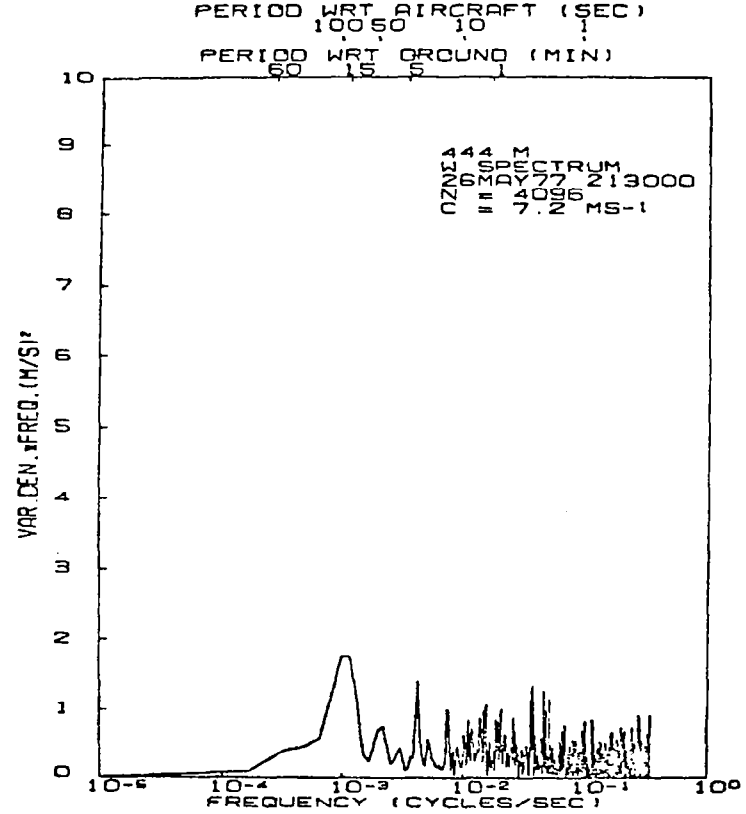


b) Vertical winds

Figure 4.8 Mean wind profiles with horizontal distance at 200 m (660 ft), 300 m (985 ft), and 400 m (1315 ft) height above ground.



a) W_x spectrum (longitudinal component)



b) W_y spectrum (vertical component)

Figure 4.9 Wind spectra indicating frequencies associated with thunderstorm wind shear (n = number of observations in the time series and c = the mean tower wind speed) [15].

aircraft's motion. This is equally true of the vertical spectrum, although note that the vertical spectrum contains very little energy when compared to the longitudinal component. Finally, qualitative inspection of Figure 2.6, page 12, clearly shows that the aircraft, when passing through a microburst, depending on the location of the flight path, will initially encounter increasing head winds, which then decrease and finally reverse direction to become a tail wind (see for example flight path #1 on Figure 2.7, page 13). Thus, the theoretical curves characterize the thunderstorm winds.

To test the hypothesis that a varying wind having a frequency near that of the aircraft phugoid frequency could indeed cause the high amplitude and loss of control illustrated by some of the analytical models earlier, a number of computer runs and flight simulator tests were conducted. The frequencies of the sinusoids were 1, 1-1/2, and 2 times the phugoid frequency of the aircraft type under study.

4.4.3 Flight Path Deterioration Parameters

In order to assess the potential severity of a wind shear hazard existing along a flight path, a quantitative parameter is needed to describe the response of the aircraft/pilot system. Variations of a parameter, referred to as a flight path deterioration parameter (FPDP), was therefore defined.

Table 4.2 gives expressions for the FPDP proposed for flight path and airspeed deviations. These are based on the following logic. Normalized altitude, HP/HG , was chosen as a flight path deviation parameter where HP is the height of the aircraft above the ground and HG is the height of the glide slope above the ground. The airspeed deviation parameter chosen is simply the deviation of airspeed from the reference value. However, in both flight path and airspeed parameters the positive deviations are examined separately from the negative deviations to avoid the cancellation errors. Also, the root mean square value of the velocity and height departure from the reference value was studied.

TABLE 4.2. Flight Deterioration Parameters Used in Comparing Computed Versus Manned Flight Simulator Control Performance in Idealized Thunderstorm Wind Shear.

$$1. \quad \Delta H = \frac{1}{T_L} \int_0^{T_L} (HP - HG)^2 dt$$

where T_L is the total landing time, HP is aircraft altitude, and HG is glide slope height.

$$2a. \quad GS+ = \frac{1}{T_n} \int_0^{T_n} \frac{HP}{HG} dt$$

where HP/HG above or on glide slope ≥ 1 and T_n is the time above or on glide slope. T_n/T_L is percentage of time above or on glide slope.

$$2b. \quad GS- = \frac{1}{T_m} \int_0^{T_m} \frac{HP}{HG} dt$$

where HP/HG below glide slope < 1 and T_m is the time below glide slope. T_m/T_L is percentage of time below glide slope.

$$3. \quad \Delta U = \frac{1}{T_L} \int_0^{T_L} (V_a - V_{a_0})^2 dt$$

where V_a is airspeed and V_{a_0} is reference airspeed.

$$4a. \quad V+ = \frac{1}{T_i} \int_0^{T_i} (V_a - V_{a_0}) dt$$

for $V_a - V_{a_0} \geq 0$ where T_i is the time airspeed is equal to or greater than reference airspeed. T_i/T_L is percentage of time above or equal to reference airspeed.

$$4b. \quad V- = \frac{1}{T_k} \int_0^{T_k} (V_a - V_{a_0}) dt$$

for $V_a - V_{a_0} < 0$ where T_k is the time airspeed is below reference airspeed. T_k/T_L is percentage of time below reference airspeed.

4.4.4 Description of Test Plan

In an effort to determine if the aircraft trajectory model simulates a real aircraft/pilot system, the results of the trajectory program were compared with a series of runs that were carried out in the B-727 simulator at the NASA Ames Research Center (NASA/Ames). The simulated aircraft were flown through the three different wave-form wind models characteristic of the thunderstorm downburst cell environment. The simulator runs were designed to test aircraft/pilot response to longitudinal and vertical wind waves of varying amplitudes and frequencies. The test plan used is given in Table 4.3. Twenty-seven computer runs and 19 manned flight simulator approaches were made. The computer and simulator test results are summarized below. Complete details of these runs are given in Turkel et al. [74].

Also, a series of manned flight simulations were conducted on a B-727 simulator at the United Airlines (UAL) Flight Training Center in Denver. All approaches were flown by a UAL simulator test pilot. Twelve B-727 ILS approaches were flown for a theoretical microburst single sine wave wind shear input. The head wind was first encountered at 430 m (1400 ft) AGL. The simulator phugoid frequency was 0.025 Hz or a period of 40 seconds. Wave amplitudes of 5, 10, 15, 20, 25, and 30 m/s (10, 19, 29, 39, 49, and 58 kts) were flown. Eight of the 12 approaches were flown at the 40-second period, while the remaining were flown at 10-, 20-, 80-, and 160-second periods each.

Flight path trajectories measured in the NASA/Ames flight simulator are compared with values computed with the computer model in Figures 4.10 through 4.14. Figure 4.10 compares computed and manned simulator flight path trajectories through a longitudinal sine wave of phugoid frequency and varying amplitude, i.e., 5.15, 10.3, and 15.45 m/s (10, 20, and 30 kts). Figure 4.11 shows the same comparison for a longitudinal sine wave of 20.6 m/s (40 kts) amplitude and varying frequency, i.e., ω_{ph} , $1/2 \omega_{ph}$, and $2 \omega_{ph}$. Similar comparison of computed versus manned flight simulator trajectories are given in Figures 4.12 and 4.13 for a 1 - cosine downdraft wind shear. Figure 4.14 compares trajectories for a combination of longitudinal S-shaped and 1 - cosine downdraft winds.

TABLE 4.3. Test Plan for Simulator and Computer Runs.

	Amplitude	Frequency
Aircraft trimmed for: 3.0° glide slope 70.0 m/s airspeed 63,958 kg (140,000 lbs) gear down, flaps 30°		
S-shape head wind to tail wind shear wave	5.15 m/s (10 kts)	ω_{ph} (=38 sec)
	10.30 m/s (20 kts)	ω_{ph} (=38 sec)
	15.45 m/s (30 kts)	ω_{ph} (=38 sec)
	15.45 m/s	$2\omega_{ph}$ (=19 sec)
	15.45 m/s	$1/2 \omega_{ph}$ (=76 sec)
Full sine wave head wind to tail wind shear	5.15 m/s	ω_{ph}
	10.30 m/s	ω_{ph}
	15.45 m/s	ω_{ph}
	20.60 m/s	ω_{ph}
	20.60 m/s	$2 \omega_{ph}$
	20.60 m/s	$1/2 \omega_{ph}$
1 - cosine down draft	5.15 m/s (17 ft/s)	ω_{ph}
	10.30 m/s (34 ft/s)	ω_{ph}
	15.45 m/s (51 ft/s)	ω_{ph}
	15.45 m/s (51 ft/s)	$2 \omega_{ph}$
	15.45 m/s (51 ft/s)	$1/2 \omega_{ph}$
Combinations:		
{ S-shape, 0-5.15 m/s tail wind shear at ω_{ph} 1 - cosine, 5.15 m/s (17 ft/s) downburst at ω_{ph}		
{ S-shape, 0-10.3 m/s tail wind shear at ω_{ph} 1 - cosine, 10.3 m/s (34 ft/s) downburst at ω_{ph}		
{ S-shape, 0-20.6 m/s tail wind shear at ω_{ph} 1 - cosine, 20.6 m/s (68 ft/s) downburst at ω_{ph}		
{ S-shape, 0-20.6 m/s tail wind shear at $2 \omega_{ph}$ 1 - cosine, 20.6 m/s (68 ft/s) downburst at $2 \omega_{ph}$		

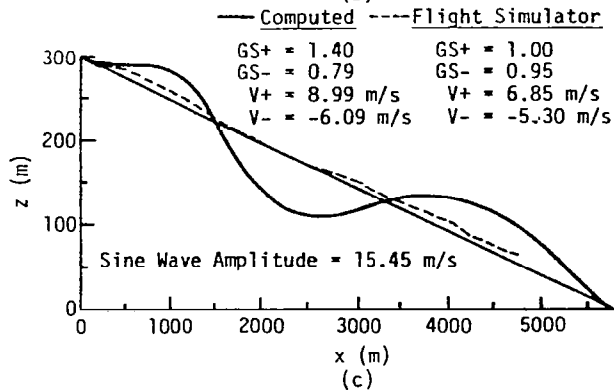
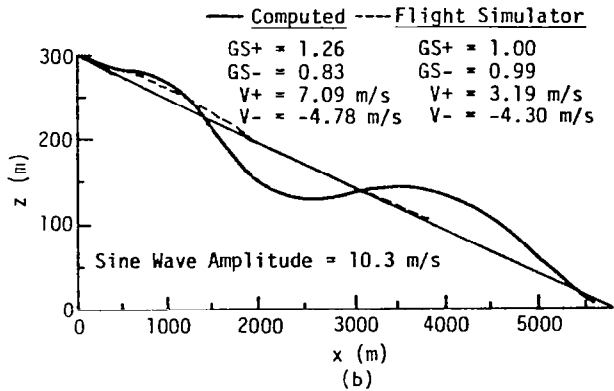
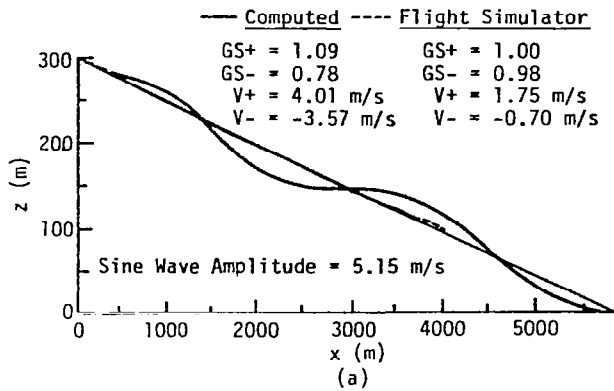


Figure 4.10 Comparison of computed and manned simulator flight path trajectories through a longitudinal sine wave of ω_{ph} frequency.

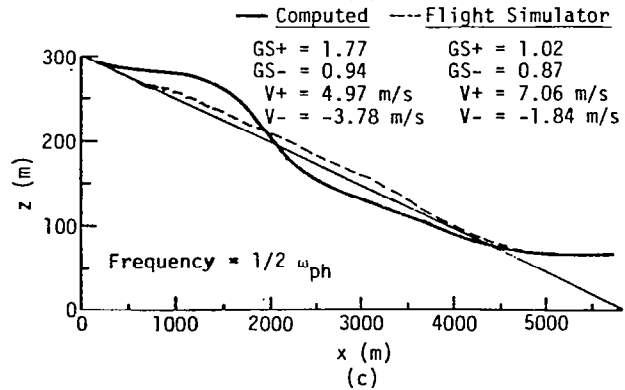
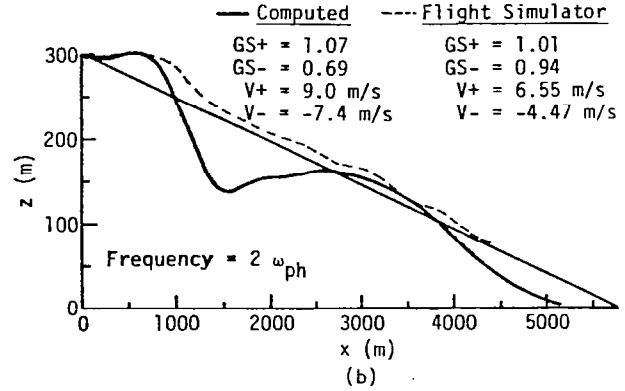
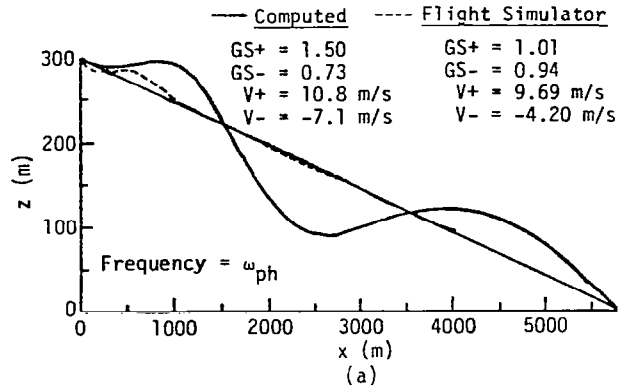


Figure 4.11 Comparison of computed and manned simulator flight path trajectories through a longitudinal sine wave of 20.6 m/s (40 kts) amplitude.

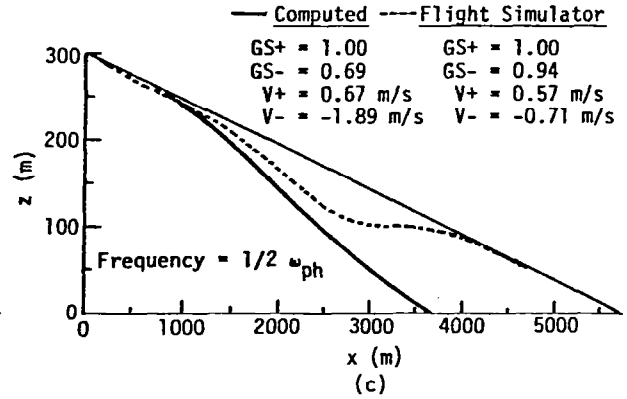
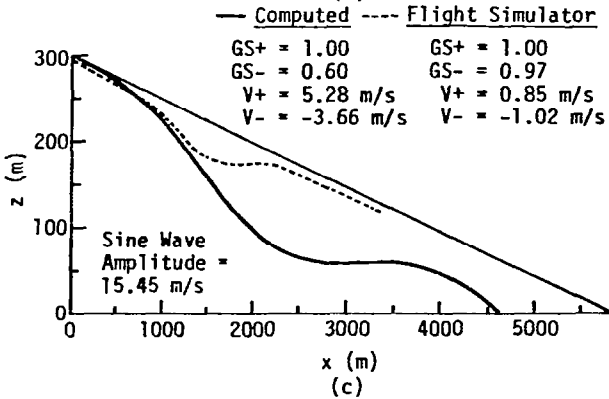
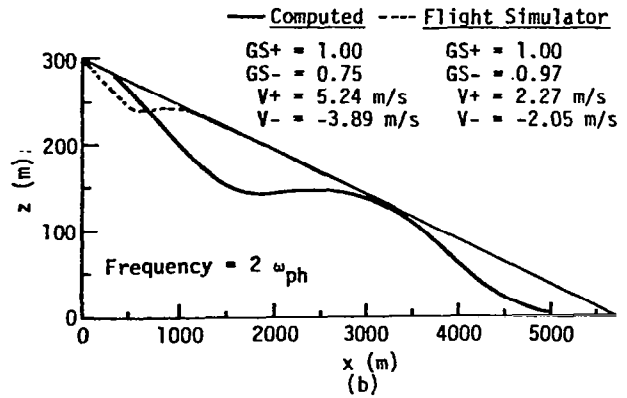
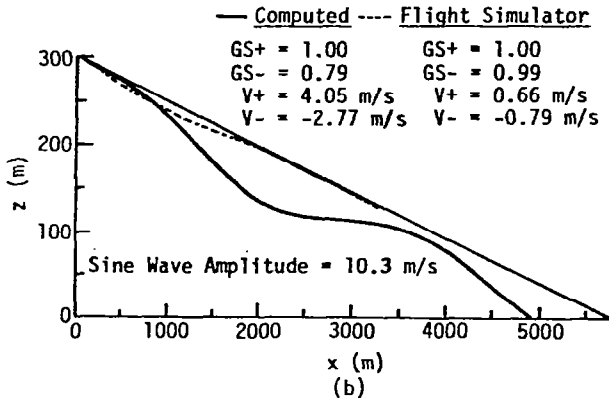
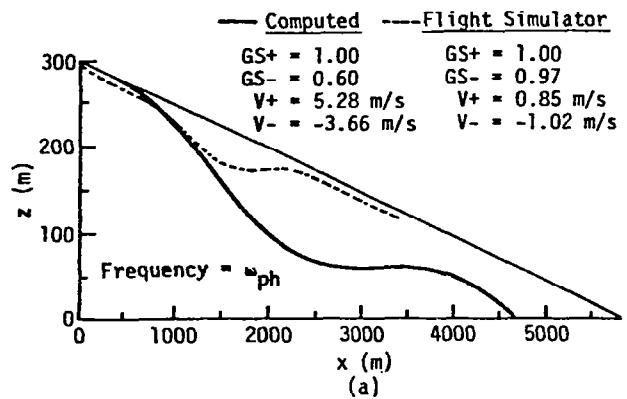
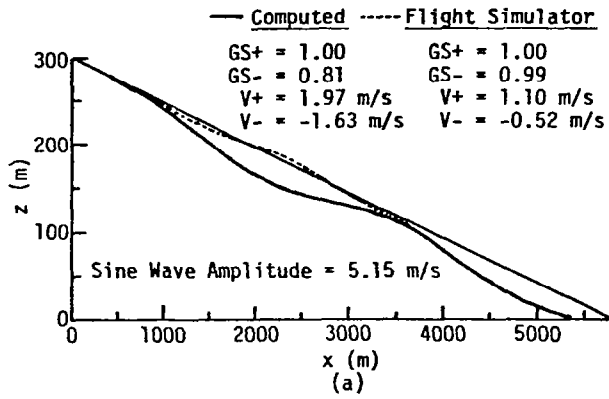


Figure 4.12 Comparison of computed and manned simulator flight path trajectories through a vertical 1 - cosine wave amplitude of ω_{ph} frequency.

Figure 4.13 Comparison of computed and manned simulator flight path trajectories through a vertical 1 - cosine wave of 15.45 m/s (30 kts) amplitude.

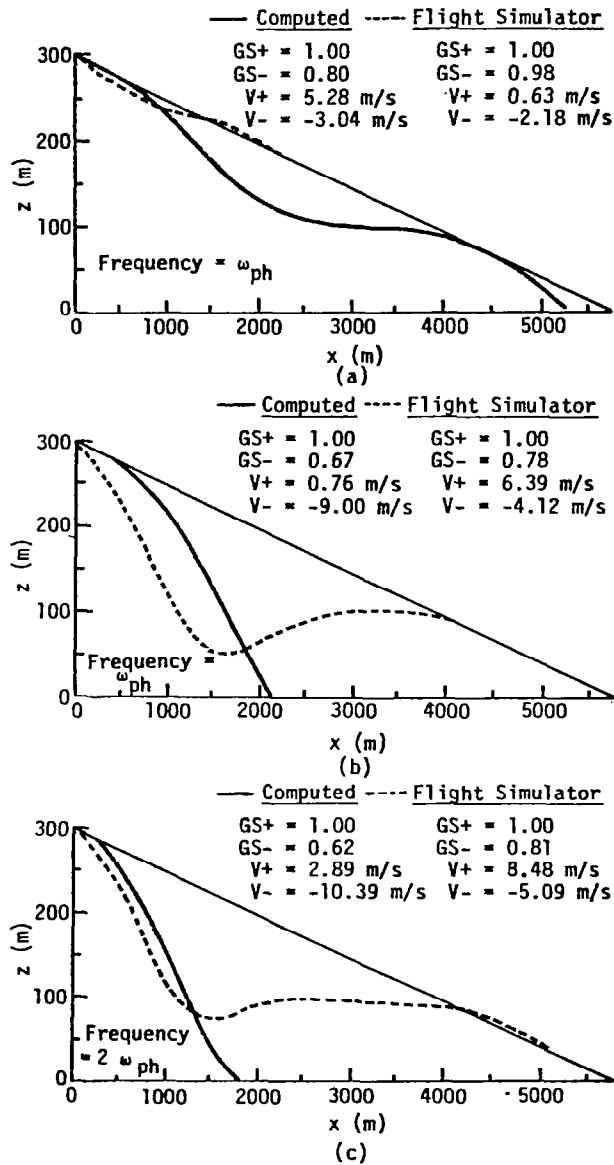


Figure 4.14 Comparison of computed and manned simulator flight path trajectories through a combination longitudinal S-shaped and vertical 1 - cosine wave of 20.6 m/s (40 kts) amplitude.

All cases shown in Figures 4.10 through 4.14 were run for a modeled B-727 aircraft trimmed (flaps 30°) for a 3° flight path angle with an approach airspeed of 70 m/s (136 kts) and an angle of attack of 6.2°. All wind profiles are encountered at $x = 0$. The flight path deterioration parameters pertaining to each case are given on the respective flight path trajectory plot.

The computer model control system utilized thrust to control airspeed and elevator deflection to control flight path angle. It should be noted that fixed gains are used in the formulation of this model to represent an initial effort to model pilot control response to wind shear profiles and to simulate engine response characteristics. A discussion of the individual flight paths is given in Turkel et al. [74] and Frost et al. [72].

In terms of aircraft/pilot response, the computer model compares well with the simulator for the full sine waves, S-shaped waves, downbursts, and combinations. However, some discrepancies exist with regard to the degree of flight path and airspeed control between the computer model and the test pilot. Although the control logic for the model pilot is similar to the control strategy of the test pilot, the test pilot flew consistently better than the model pilot. This is due to the fixed gain structure of the computer model pilot. A real pilot does not behave in the rigid manner of a fixed-gain model. In reality, a pilot acts in a variable gain decision-making process, which is probably not adequately included in the simplified models used in the study. This fixed-gain structure of the model allows for lower pilot damping of the flight path and airspeed oscillations induced by encounters with wave disturbances. The test pilot is clearly of better skill than the computer model pilot. In addition, the test pilot had the opportunity to "learn" the types of profiles he was flying during the tests.

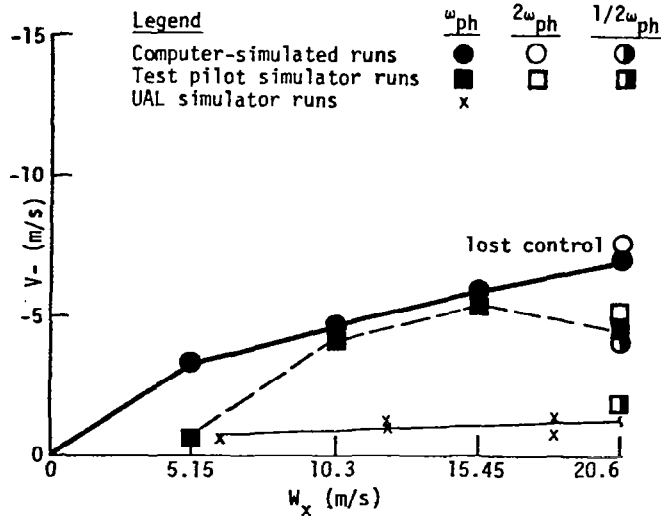
4.4.5 Results of Flight Path Deterioration Parameters (FPDP)

The airspeed deterioration parameters V^+ and V^- , calculated from the computer simulations, increase with increasing longitudinal wave

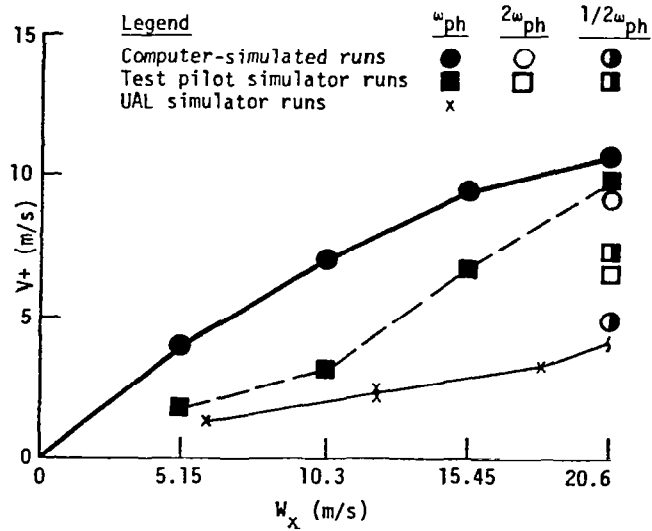
amplitude for waves at the phugoid frequency as shown in Figures 4.15 and 4.16. Also shown is a comparison with the UAL flight simulator studies. The UAL flights were carried out only with sine waves and the comparison is thus limited. The largest V- values were attained for the $2 \omega_{ph}$ waves, whereas the V+ value of the 20.6 m/s sine wave at $2 \omega_{ph}$ is not as large as that of the phugoid frequency wave. The values of V+ and V- from the computer simulations were smallest for the $1/2 \omega_{ph}$ S-shaped and sine waves. In comparison with the computer results, similar trends are noted for the airspeed deterioration parameters, with the simulator runs for the S-shaped waves, and for V+ values of the sine waves. However, in the case of the sine waves, the simulator values of V- tend to be inconsistent. This is possibly due to the pilot "learning" the profiles and "fine tuning" his control procedures. The UAL manned simulator data is consistent in trend but considerably lower. The reason for this is believed to be due to the simulated low-frequency response in the phugoid range being overly damped in the training simulator.

Control difficulty was encountered by the computer model and test pilot in flight through downbursts (particularly the $1/2 \omega_{ph}$ wave) and for the combination S-shaped longitudinal waves and $1 - \cos$ downbursts. For the downbursts, the computer and the simulator airspeed deterioration parameters (V+ and V-) were lowest for the $1/2 \omega_{ph}$ wave which, however, caused the largest deviation in flight path. This is reasonable since the long wave downburst does not have a pronounced effect on airspeed deviation but instead causes the aircraft to descend below the glide slope with the steadily descending air mass. The aircraft remains in this long wave for 76 seconds. Therefore, airspeed deterioration is probably not a meaningful warning parameter for application to downbursts. It may be noted that the glide slope deviation parameter GS- for downbursts shows very low values corresponding to large descent below the glide slope for the $1/2 \omega_{ph}$ waves.

For the combination S-shaped longitudinal waves and $1 - \cos$ downbursts, the decreasing airspeed and the descending air mass forcing the aircraft below the glide slope presented the most difficulty for the

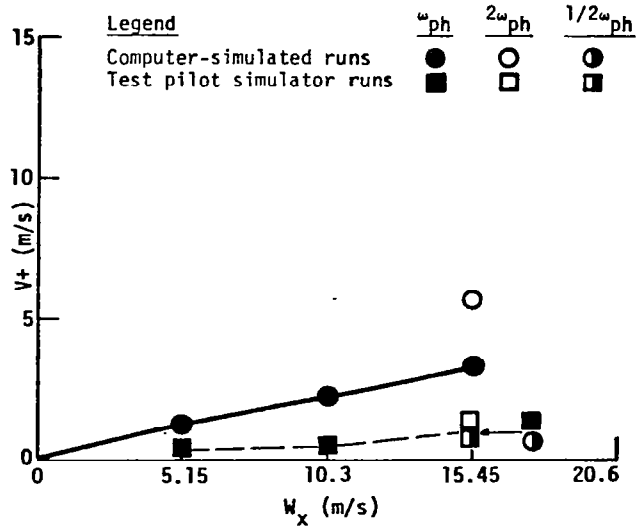


a) V_- values versus sine wave amplitude and frequency.

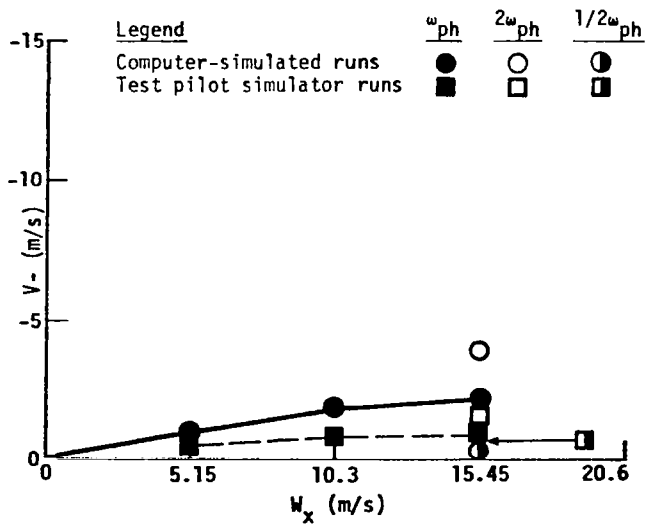


b) V_+ values versus sine wave amplitude and frequency.

Figure 4.15 Airspeed deviation parameters for longitudinal sine wave winds.



a) V_+ values versus S-shape wave amplitude and frequency.



b) V_- values versus S-shape wave amplitude and frequency.

Figure 4.16 Airspeed deviation parameters for longitudinal S-shaped wave winds.

simulated pilot and test pilot. Results show that the largest V-values for airspeed deviation correspond to the worst control cases and for the combined longitudinal and downdraft cases appears to provide a meaningful warning of hazardous wind conditions.

Thus there is not a clear indication of which FPDP is most useful or whether a combination of parameters is required. The results of the computer and simulator runs through the longitudinal S-shaped waves and sine waves indicate a need for further studies to examine the effects of large longitudinal wind gradients due to large amplitude waves at short wavelengths. A parametric analysis of a broader range of wave frequencies must be carried out to determine the bandwidth which is most hazardous to aircraft operations.

Control difficulties were noted with 1 - cosine downbursts, particularly the long duration wave at large amplitude and the strong downbursts combined with longitudinal shear. Frost et al. [72] concluded that the combination longitudinal S-shaped and vertical 1 - cosine wind profile is the most realistic profile of a downburst cell wind field in the vicinity of the ground. However, the high amplitude of the downbursts studied may not be realistic close to the ground since the vertical wind component must approach zero there. New measurements of wind shear [32,39] will help provide meaningful magnitudes of the downburst.

It is noted that because of the interrelationship of the longitudinal and vertical winds, indicated by the study, it is not clear that measurement of only the longitudinal wind component along the flight path for detection and warning of hazardous wind shear will be sufficient. This has severe ramifications since the vertical component is much more difficult to measure operationally. Proposed airborne and ground-based systems for detecting and warning of wind shear are discussed in the next section. All of these depend on measurements of only the longitudinal component.

5.0 DETECTION AND WARNING SYSTEMS

5.1 Airborne Aids for Coping with Low-Level Wind Shear

5.1.1 FAA Flight Tests for Airborne Aids

Foy [19] reports a series of piloted flight simulation studies supported by analytical and experimental analyses of airplane response to wind shear and the meteorological phenomena producing low-level shear. Approach and landing tests were run under different conditions of visibility with different levels of approach instrumentation (full ILS and localizer only), and with wide-bodied and nonwide-bodied jet transports. The manned flight simulation experiments were run with a significantly large number of experienced pilots.

A major conclusion over all the tests was that conventional (baseline) approach-management techniques, based on attempts to maintain a stabilized indicated airspeed from glide slope capture to the flare, are not effective in coping with the more severe (e.g., frontal and thunderstorm) wind shear encounters. Tests to develop improved approach management techniques considered both acceleration augmentation and the use of ground speed information. The results of these tests show that ground speed is particularly important. Although several potential solutions to the wind shear problem were indicated from the tests, the modified flight director with acceleration margin go-around indicator MFD/ Δ A system performed well enough and ranked high enough in acceptability to be recommended as a solution to the wind shear problem on approach and landing.

The MFD/ Δ A system contains the following combination of command information:

5.1.1.1 Modified Flight Director. The modified flight direction includes improved flight-director control laws that incorporate acceleration augmentation to aid in coping with wind shear on approach and

landing [75]. In comparison with the standard or baseline flight director commands, the modified steering control laws exhibit quickened response to changing wind and other transients. The modified flight director also has a modified speed command, driving the fast/slow "bug," that uses acceleration augmentation and wind shear compensation to improve speed control. For approach and landing, the pilot's speed control task is aided by supplying a speed-error indication on the fast/slow scale of the flight director. A basic assumption of the system is that a measurement of ground speed (GNS) is available in the airplane.

5.1.1.2 Acceleration Margin. Acceleration margin, ΔA , is an analog quantity designed by FAA to indicate when the airplane is getting into a hazardous situation with respect to longitudinal wind shear. Acceleration margin is computed by:

$$\Delta A = A_{\text{cap}} - [-WD]\dot{H}/H \quad (5.1)$$

$$WD = (TAS - GNS) - WX_{\text{gnd}} \quad (5.2)$$

where

A_{cap} = acceleration capability of the airplane in level flight or in approach configuration (kts/s)

WX_{gnd} = wind component at the ground and along the runway (head wind is positive) (kts)

TAS = true airspeed of the airplane (kts)

GNS = ground speed of the airplane (kts)

H = altitude of airplane center of gravity above ground; altitude is positive when measured upward (ft)

\dot{H} = rate of change of altitude with time; positive up (ft/s).

In this case, A_{cap} is a constant for the approach and will depend on the selected approach speed, the flap setting, the maximum engine thrust available, the drag, the aircraft weight, and the air density. For instance, values for the DC-10 at 158,800 kg (350,000 lbs), 50° flaps, nominal approach speed, gear down, are:

sea level, standard day, 0.86 m/s^2 (1.7 kts/s)

9000 ft, standard day, 0.51 m/s^2 (1.0 kt/s)

The term (TAS - GNS) is approximately the longitudinal wind velocity at the airplane (head wind positive), WD is thus the wind difference, or estimated wind shear, i.e., the difference in wind between the airplane's present position and ground; a decreasing head wind is a positive difference. The magnitude of H/\dot{H} is the expected time in seconds to reach the ground, and \dot{H} is negative for descent. Thus, the term $[-WD]\dot{H}/H$ is the expected acceleration demand due to longitudinal wind shear, with a decreasing head wind and a descending aircraft giving a positive demand. If the demand equals or exceeds A_{cap} , ΔA becomes zero or negative and the situation is potentially hazardous.

Tests with this system showed that the condition ΔA less than or equal to zero, if used as a criteria for advising a go-around, produced too many nuisance alarms. The algorithm was augmented with the difference, DA, between the wind change and the airspeed pad given by:

$$DA = WD - (IAS - V_{\text{app}}) \quad (5.3)$$

where

IAS = indicated airspeed (kts)

V_{app} = selected approach speed (kts)

The go-around advisory is implemented according to Figure 5.1. The switches are closed when the indicated condition is true. The effect is to inhibit the go-around advisory if either the wind difference (decreasing head wind) is less than 12.9 m/s (25 kts) or the wind difference is no more than 4.1 m/s (8 kts) greater than the airspeed pad. The particular values 4.1 and 12.9 m/s (8 and 25 kts) were chosen empirically.

5.1.1.3 Modified Go-Around Guidance. The modified go-around guidance, intended to provide a pitch steering control law for use in wind shear, is based on the following rationale:

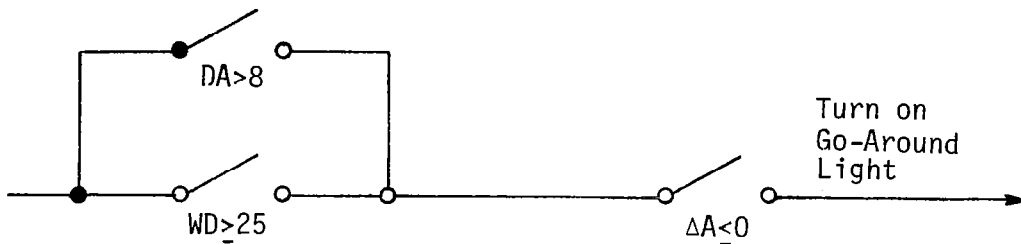


Figure 5.1 Go-around advisory augmentation algorithm [19].

- The dominating requirement during go-around is terrain avoidance and obstacle clearance. After the initial pitch-up maneuver, it is assumed that flying a nominal positive flight path angle will result in a safe go-around.
- The pitch attitude required to maintain a flight path is dependent on the prevailing wind. The steering-control law should contain compensation for this effect.
- If there is severe wind shear or some other condition such that the aircraft cannot maintain the nominal flight path angle, the aircraft will be flown at or above a minimum airspeed at a commensurate maximum pitch attitude.

Vertical speed, \dot{h} , and ground speed, GNS, inputs were used to compute flight path angle, γ . Flight path angle and angle of attack, α , were input into the computation of the pitch steering signal, Δ . This signal and the pitch rate term, $\dot{\theta}$, are the controlling terms for damping as long as the airspeed remains high. When airspeed drops to or below the stall value, a minimum function selector chooses the IAS - V_{stall} input, which results in a pitch-down command to gain airspeed. The reference flight path angle, γ_{GA} , and angle of attack, α_{GA} , were chosen empirically.

With the modified go-around method, the pilot advances the throttles to give full thrust immediately after deciding to go around. He is then not using the F/S indicator on the flight director for the thrust control. Therefore, to provide additional information, the F/S signal was modified so that the F/S displayed an approximation to angle of attack error.

The MFD/ ΔA system, which showed a significant performance improvement over baseline in the wind shear studies [19], requires instrumentation to measure certain aircraft variables and wind components that are not available in many current aircraft. Of the quantities that are usually not available or are not measured adequately, the most important is ground speed, altitude above the runway, and rate of change of altitude. Additionally, there is a firm requirement for accurate knowledge of the winds on the runway; the along-runway component is needed by algorithms such as the acceleration margin and the crosswind component to enable the pilot to anticipate his lateral control action.

Foy's tests showed importantly that there are realistic wind shear conditions that can occur on takeoff which exceed the aerodynamic lift and thrust capability of the airplane. An attempt to make a normal takeoff in such a situation, even when aided by a minimum height loss pitch-steering algorithm, cannot be handled by pilot action. The most appropriate recourse found in the study is: (1) not to attempt to takeoff at all, (2) to take off in a different direction, or (3) to prolong the takeoff roll so that rotation will lift the airplane off with 10.3 m/s (20 kts) or more of excess airspeed. Any of these actions, in practice, requires advance notice (that is, prior to starting the takeoff roll) of the wind shear condition.

5.1.2 Safe Flight Instrument

A self-monitoring wind shear warning system has also been developed by Safe Flight Instrument Corporation (Stein [76]; Greene [77]). This system is designed to sense and integrate horizontal and vertical, or downdraft, wind shear components providing the pilot of an aircraft on approach a timely warning to initiate a go-around.

The wind shear monitoring system computes the thrust required to maintain the desired glide path when a downdraft is encountered on approach. The thrust required in g's is equivalent to the angular displacement from that glide path when the actual (or potential) deviation is measured in radians. This displacement, termed downdraft drift angle (DDA), is a function of the ratio of the velocity of the descending air to the aircraft's speed;

$$DDA = W_z/V_a \quad (5.4)$$

where

DDA = downdraft drift angle

W_z = vertical wind

V_a = airspeed

The effect on the airplane's landing profile due to a change in the head wind (tail wind) component due to wind shear may be described by the rate of change of ground speed (inertial acceleration) required to maintain a constant lift condition (airspeed acceleration = 0). The magnitude of a horizontal wind shear is predicted by Greene [77] with the following formula:

$$WS_x = (V_a - \dot{x})/(H/\dot{H}) \quad (5.5)$$

where

WS_x = horizontal wind shear

V_a = airspeed

\dot{x} = ground speed

H = height or bandwidth of the shear layer

\dot{H} = vertical velocity

Figure 5.2 from Greene [77] shows the functional block diagram of Safe Flight Instrument Corporation's wind shear computer. The computer resolves the two orthogonal vectors of a wind shear encounter and provides meter output and threshold alert indication of that encounter. The two vectors are called DDA and horizontal wind shear (HWS).

HWS is derived by subtracting longitudinal acceleration from airspeed rate. Airspeed rate is obtained by taking an airspeed analog from the airspeed indicator, or air data computer, and passing it through a high-pass filter. Longitudinal acceleration is sensed by a computer integral accelerometer, the output of which has been summed with a pitch

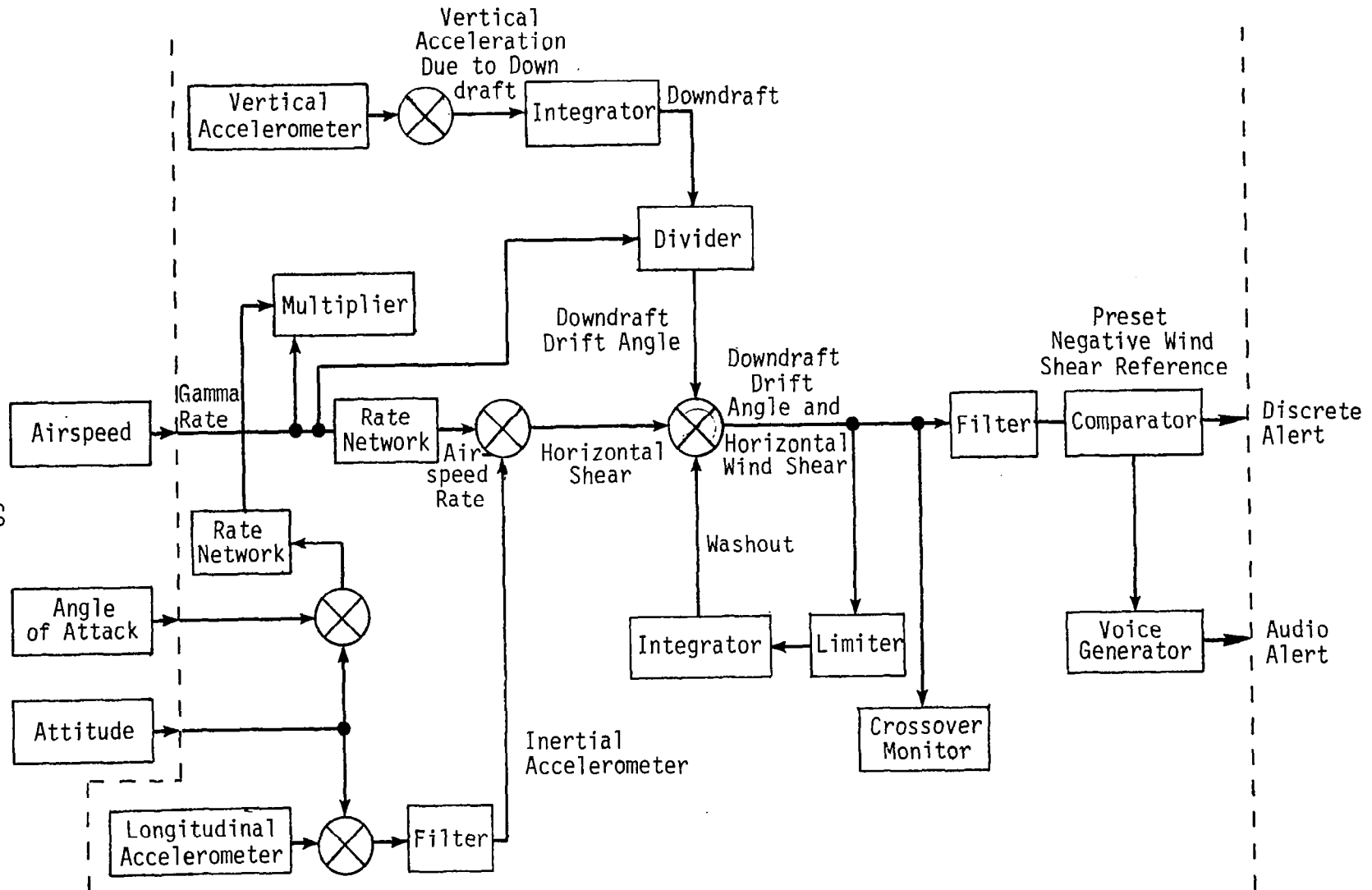


Figure 5.2 System block diagram of Safe Flight Instrument Corporation's wind shear computer [76].

attitude reference from a vertical gyro signal to correct for the acceleration component due to pitch ($g \sin \theta$). The summed acceleration and pitch signals are fed through a low-pass filter, the output of which is summed with the airspeed rate signal to comprise horizontal wind shear.

The vertical component of DDA is developed through the comparison of measured normal acceleration with calculated glide path maneuvering load. Flight path angle is determined by subtracting the pitch attitude signal from the angle of attack analog as sensed by the stall warning airflow sensor. This is then introduced into a high-pass filter and then a multiplier to which the airspeed signal has been applied. Thus the flight path angle rate, corrected for airspeed, provides the computed maneuvering load term. This term is compared in a summing junction to the output of a computer integral normal accelerometer. A failure to match is the indication of an acceleration due to downdraft. If this is the case, this acceleration when integrated, is the vertical wind velocity and is further divided by the airspeed signal to compute DDA.

The DDA and horizontal wind shear signals are combined and the summed output passes through a low-pass filter forming the output signal. This signal is fed to a comparator which provides a latched ground output signal (for a warning device) and a meter output. The warning output is set at a threshold of -0.67 m/s^2 (-3 kts/s) horizontal wind shear DDA of -0.15 rad or any combination which would total an equivalent signal level.

5.1.3 Bliss's Aircraft Control System for Wind Shear

Bliss [53] questions whether acceleration augmentation and quickening of pitch steer commands are sufficient to solve the wind shear problem. He believes that modified flight directors, as used in the FAA wind shear experiments, using the conventional IAS parameters for the approach speed, will result in the same hazardous ground speed values close to the ground and will produce the same results as exist today. According to Bliss, a flight director utilizing a totally computerized inertial vector, vertically, laterally, and longitudinally (speed vector), wherein the ground speed is integrated properly with the

indicated airspeed, is needed to resolve the wind shear problem.

Bliss states that the minimum standard instrumentation for certification is as follows:

1. An analog ground speed instrument mounted in close proximity to, or combined on the same instrument with, an analog airspeed instrument.
2. A system of three indexes:
 - a) An airspeed target index selectively adjustable by the pilot to indicate the normal minimum approach indicated airspeed value.
 - b) A first ground speed index automatically programmed to a ground speed value equal to the true airspeed value of whatever the IAS index is set on. (This then, becomes a zero wind ground speed index value.)
 - c) A second ground speed target index programmed to a ground speed value relative to the zero wind index, taking into account the surface head-wind/tail-wind component on the runway. This index is the ground speed expected approaching the threshold, and it then becomes the minimum ground speed value for that approach.
3. The use of two minimum speed values requires that they be automatically integrated to a third instrument which then becomes the primary speed instrument. The use of which eliminates the use of speed values slower than either the normal approach minimum airspeed or the normal approach minimum ground speed. (This can be a fast/slow instrument.)
4. A tail wind warning system variably programmed with altitude, which calls the pilot's attention to the excess ground speed existing on the approach when it is not possible for the aircraft to decelerate inertially to normal values before reaching the landing point.
5. An excess head wind warning (programmed much the same as the tail wind warning) of values of excess IAS variably programmed with altitude, to warn the pilot when his elevator control authority will be limited after the loss of airspeed results in normal airspeed. This warning may contain a limiter when the airplane is trimmed to a nose-up trim with the excess airspeed so that after the airspeed loss, the airplane will be in an acceptable trim condition.

6. Airports served by Part 121 carriers must be required to give surface wind information in the landing area for landing traffic, and in the vicinity of the departure end of the runway for aircraft taking off. They must also have remote wind sensors located at the highest elevation possible on any obstruction requiring unusual climb-out procedures.
7. Aircraft operating under Part 121 which are equipped with INS must have a recording on the flight data recorder of a ground speed parameter.
8. All Part 121 aircraft must have an on-board ground speed detection system capable of an accuracy of less than 2 percent error and a ground speed tracking error of less than 1.5 sec.
9. All certification of auto-land systems should be canceled until they are modified to the standards provided by this airspeed/ground speed system, including the full pilot monitoring instrumentation.
10. For the proper solution to the wind shear problem in all aircraft, a standard means for providing ground speed must be adopted. The least expensive (even light trainers may use it), may be an airborne Doppler-type system with a compatible ground-based transponder. The ground-based transponder can be located at the intersection of two or more runways for use in any appropriate direction.

5.1.4 Advantages and Disadvantages of Airborne Systems

The preceding discussion relates to airborne systems. There are several important advantages to an airborne system:

1. Each aircraft properly equipped with an airborne system carries its protection wherever it flies. Thus, a ground-based system is not required at each airport.
2. The system allows the pilot to monitor the changing longitudinal wind shear conditions in a quantitative manner, that combines shear and aircraft performance in a meaningful way.
3. Some advanced indication, even if only a few seconds, is given to the pilot, so speed banking and/or a go-around can be attempted.

The disadvantages, however, include:

1. The system requires a sophisticated ground speed measuring system for the aircraft. In the U.S. Civil Airline Fleet, essentially only the new wide-bodies transporters currently have such a capability. The larger number of smaller jets do not have such ground speed measurement capabilities. It is unclear that an acceptably accurate, inexpensive system can be developed for these aircraft, since inertial or other high-resolution navigation systems are likely required for the measurement. Finally, the requirement for ground speed measurements would be even more difficult to achieve for those aircraft in the general aviation fleet susceptible to wind shear (i.e., light-business jet transports).
2. The acceleration margin system requires an airborne wind measurement system, clearly requiring an inertial-type measurement for sufficient accuracy and resolution.
3. The system requires notice of the runway threshold wind to be given to the pilot. For microburst events and other small wind shears which can occur very rapidly, a few seconds delay in updating runway wind can seriously hamper the system's effectiveness. A telemetering of runway wind probably is needed which thus results in the requirement of equipment at each airport, and hence removing part of advantage #1 listed earlier.
4. The system makes the assumption that the longitudinal wind shear component is sufficient to determine the threat. As discussed earlier, some uncertainty remains concerning this point.
5. Perhaps the most serious limitation lies in the fact that during takeoff, wind shear so severe that a suitable acceleration margin is unavailable for aircraft survival, can be readily encountered. Also during approach an aircraft must enter a dangerous wind shear condition before having the data to make corrective action.
6. In the flight simulator testing of this system, more realistic wind shear profiles need to be tested.
7. Using the acceleration margin technique, the presence of a phugoidal instability forcing in the wind shear is not considered in A_{cap} . Thus, further, theoretical and flight simulator testing of the concept is required.

Despite the shortcomings inherent in the airborne system, it probably provides the best detection/warning capability to date for an aircraft in flight, and undoubtedly aids the pilot by providing up-front data to aid in traversing severe wind shear conditions. Although the

system may not be effective in some situations, for many others it may clearly save the aircraft.

5.2 Ground-Based Wind Shear Detection and Warning Systems

In the past few years, a number of ground-based wind shear detection/warning systems have been proposed and some tested. Notably among these is the low-level wind shear alert system (LLWSAS), the thunderstorm gust front detection systems based on combinations of wind and pressure sensors, the acoustic Doppler system, the laser system, and the pulsed microwave Doppler radar system.

5.2.1 Low-Level Wind Shear Alert Systems (LLWSAS)

The LLWSAS is an operational FAA near-term solution to the wind shear hazard. The LLWSAS detects the presence of wind shear in the vicinity of the airport at the surface. Plans to install 51 more of these units at major airports within the United States are underway. To date, 58 systems have been installed.

The system consists of an airport-centered array of six anemometers clustered at approximately 3-km (2 mi) spacing with a reference sensor located near the geographic center of the airport. The data are telemetered to a master station in the control tower and processed by a minicomputer. If the LLWSAS computer senses a vector difference of 15 kts or more between the mid-field and perimeter winds, it activates an aural alarm and a display screen in the control tower. A warning is then transmitted to the pilot by an air traffic controller.

The LLWSAS system, however, cannot guarantee protection in all cases. On August 22, 1979, an Eastern Airlines B-727 on approach to William B. Hartsfield/Atlanta International Airport dropped suddenly from 750 to 375 ft above ground level in a strong shear despite the flight crew's immediate decision to execute a missed approach. The LLWSAS on the airport remained mute. The fact that the system does not measure the wind shear at a height above the surface, where the actual aircraft problem exists, is not just a limitation; it creates the potential for false security, which does not exist.

The system, moreover, was designed to detect large horizontal wind shears that move across the airport, as seen in surface wind data. Thus, the system is suited for cold frontal passage and thunderstorm gust fronts but is not well suited to detect smaller scale phenomena such as the outflow portion of a microburst. It is equally apparent that the LLWSAS is unable to detect the downdraft associated with microbursts or other forms of vertical winds.

5.2.2 Pressure Jump System

This system is based upon the characteristic pressure jump that proceeds frontal wind shear. The system comprises a large array of pressure jump detectors distributed in a dense pattern around the airport.

Although the system has proven to be rather successful in gust front detection, false alarms resulting from turbulent wind gusts and certain technical difficulties have caused delays in implementation of the system.

5.2.3 Acoustic Doppler System

The acoustic Doppler system determines wind speed and direction by measuring frequency shift (Doppler effects) in signals reflected by the atmosphere. The system was found to be expensive and unable to operate under heavy precipitation and in zones of noise created by aircraft.

5.2.4 Laser Systems

The laser system scans directly over the sensor using a continuous wave laser. This system does not have the range required to scan the glide slope and takeoff flight path to detect wind shear. There is a possibility that this capability may be available in the future using a pulse Doppler laser technique.

5.2.5 Pulse Microwave Doppler Radar

McCarthy, et al. [78,79], Wilson et al. [80,81], Fujita and Wakimoto [25], Offi et al. [82], and Strauch [83] have all demonstrated the utility of ground-based pulsed microwave Doppler radar to measure low-level wind shear events. McCarthy et al. [78] used a NSSL Doppler radar to measure

wind data along the precision approach path to the Norman, Oklahoma, airport and verified measurements with two instrumented NCAR aircraft. Similar results are reported by Offi, et al. [82]. Comparison of Doppler-radar-measured winds with that measured by an aircraft are shown in Figure 5.3. Frost and McCarthy have proposed a detection and warning system which utilizes ground-based Doppler-measured wind data to predict aircraft performance.

The proposed operational detection and warning system operates on the following principles: The wind speed profile is measured in real time with a Doppler radar looking along the flight path. The Doppler radar takes a wind measurement in 150-m (500 ft) steps (approximately every 2 seconds of an aircraft trajectory at 72 m/s (140 kts) approach speed). The wind data can be transmitted to either the approaching aircraft or to the air traffic controller. However, more optimum is a minicomputer or microcomputer slaved to the Doppler which applies aircraft response functions to the wind profiles for specific aircraft type and simulates aircraft trajectories. The flight path deterioration parameter based on the techniques described earlier (see Section 4.0) is determined in real time. An excessive value of the parameter triggers a warning alert. Figure 5.4 conceptually illustrates the technique. Some questions which remain to be resolved prior to developing an operational system are: (1) Is the longitudinal wind speed component more significant than the vertical component? (2) What is the definition of a meaningful flight path deterioration parameter? (3) What is the most complete and computationally efficient flight trajectory computer program for real-time application to computing flight deterioration parameters?

The advantages of this concept are: (1) It quantifies the wind shear in terms of actual aircraft performance; (2) it provides a warning to an aircraft prior to the aircraft beginning the approach, as needed with the airborne systems; (3) the Doppler directly measures the wind along the glide slope and is not limited to the surface measurements; (4) it provides a numerical classification as to aircraft type (flight path deterioration parameter); (5) provides service for all sections of aviation, i.e., general aviation, corporate aviation, as well as

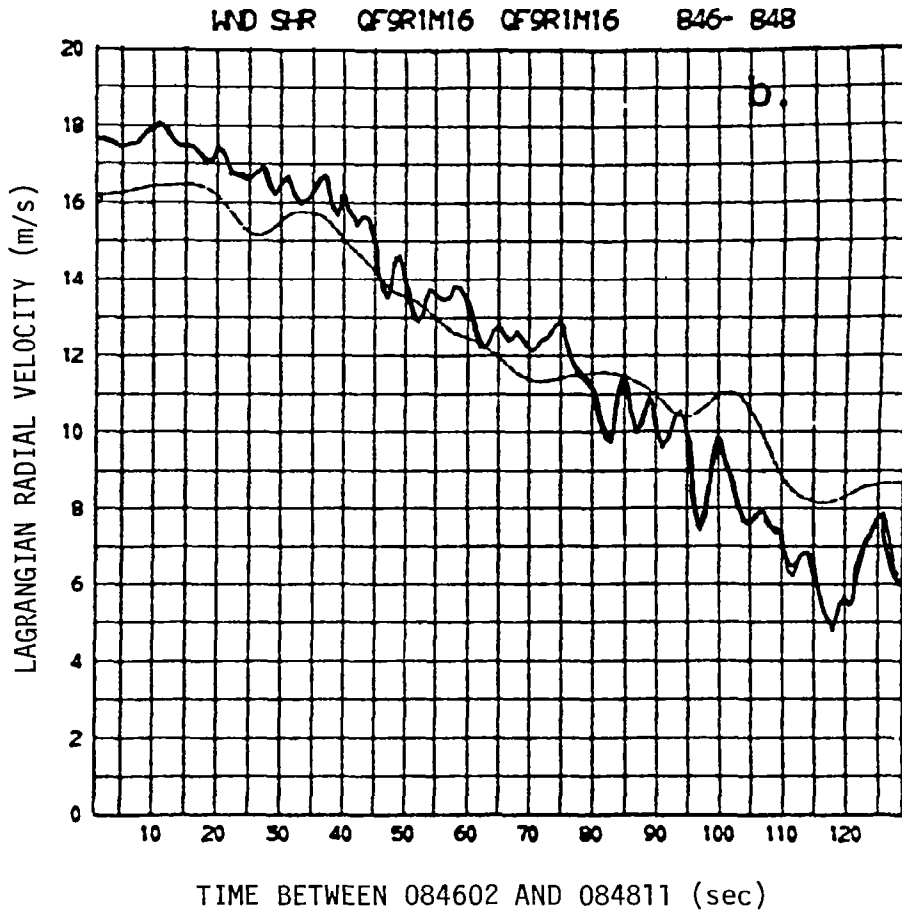


Figure 5.3 Comparison of aircraft (solid line) longitudinal wind and Lagrangian Doppler velocity (dashed line) as a function of time, for May 16, 1979, as part of SESAME 1979 [79].

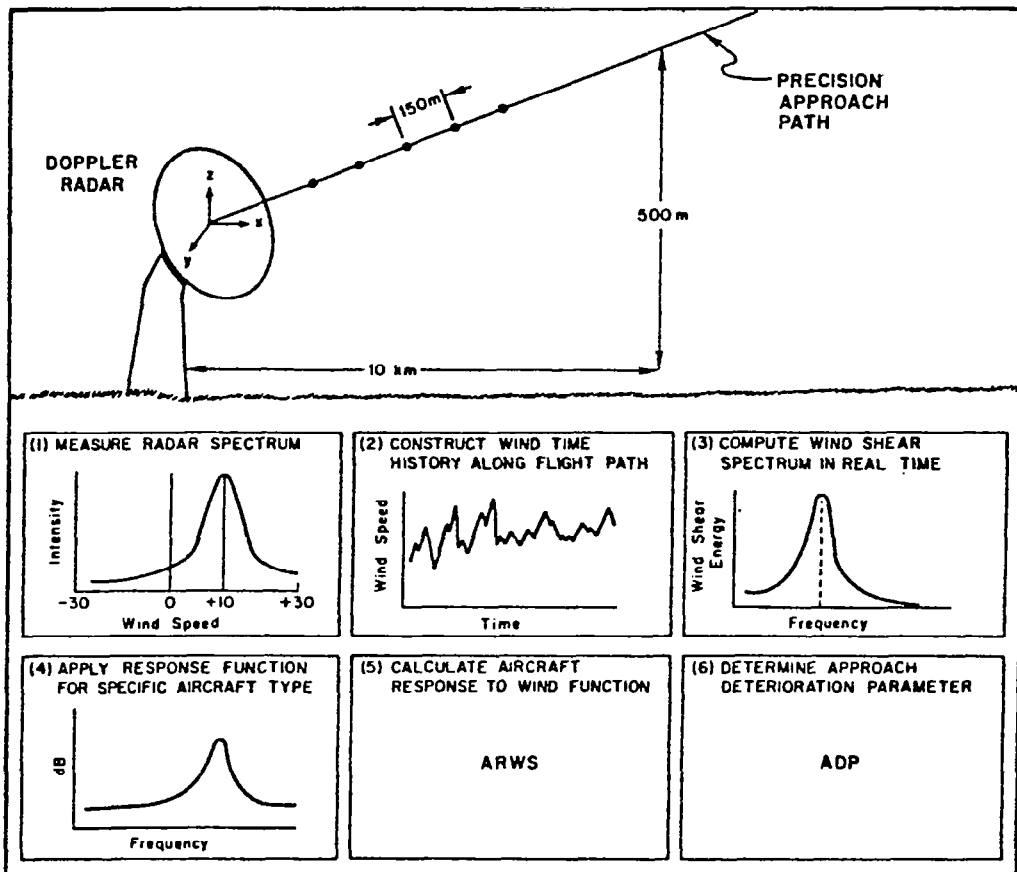


Figure 5.4 Conceptual illustration of the Doppler-based wind shear detection and warning system.

commercial airliners; (6) the system provides capabilities for both ground-based and airborne displays (data uplink); and (7) the system is an all-weather system.

Two advantages of this system were strongly supported by the air traffic control committee at the Third Annual Workshop on Meteorological and Environmental Inputs to Aviation Systems [84]. These are: (1) A ground-based detection system must be able to detect wind shear along the approach to and departure from the runway and at an altitude to support the en route air traffic control system; and (2) wind shear intensity should be reduced to a numerical value which the pilot can use to determine if the intensity of the system is too great for his type of aircraft to penetrate (which currently is operationally undefined).

Some disadvantages of the system include: (1) The system best measures the radial or longitudinal component along the intended approach path, the vertical component or downdraft cannot be measured directly in the current system; and (2) to utilize this system, each airport must be equipped with a Doppler radar, which can be a substantial expense.

5.3 Current Status of Low-Level Wind Shear Detection and Warning Systems

Although all the reported wind shear detection and warning systems have merit, no one system has proven to be fully adequate for fail-safe detection of low-level wind shear. Many of the systems are preliminary solutions which have been partially implemented without a thorough understanding of the nature of the problem.

As noted, the LLWSAS and pressure jump systems do not measure the environment above the surface in which the aircraft may encounter wind shear. Moreover, they probably do not provide protection for the small-scale microburst-type wind shears. A relatively negative consequence of these two ground systems may be that they provide confidence for the pilot and controller in a system that may be less than adequate for certain dangerous situations. Moreover, the designers of the system may well understand the limitations but the users may not.

The various airborne systems are extremely useful but are not fail-safe. Based upon the method of storing kinetic energy to overcome sudden airspeed losses occurs only in the case when enough energy can be banked to accelerate the aircraft faster than the wind is decaying. Obviously, this does not work for takeoff. Moreover, the detailed flight simulation studies of this system may have some inherent disadvantages. The wind shear models utilized in perfecting the MDF/ ΔA , i.e., modified flight director acceleration margin system, are incomplete wind shear models. These models contained neither the lateral variations in wind, the appropriate turbulence intensity and distribution over the aircraft, nor include the very localized intense short-duration microburst which has been clearly identified from radar Doppler measurements. Moreover, the question remains as to how significant is the phugoid oscillation of the aircraft. Aerodynamicists and pilots frequently point out that the phugoid oscillation is of such low frequency that it can easily be controlled. They have not considered the fact that forcing the aircraft with a forcing function, having the frequency of the phugoid, can appreciably augment the difficulty to control the subsequent motion. In turn, many flight simulators do not appropriately model the phugoid oscillations. If these oscillations are not appropriately modeled by the simulator, then the performance of the aircraft will be quite different in a wind shear forcing the aircraft at this frequency than the flight simulator would demonstrate.

Another question associated with the airborne system is: Can the airlines absorb the high cost of implementing the ground-speed and aircraft-speed measuring systems? Moreover, there must be some method for providing in real time the runway threshold winds to the aircraft. Finally, the very important question which must be resolved is whether a warning and detection system, either ground based or airborne, is adequate if only a measurement of the longitudinal wind speed is utilized, i.e., how significant is the vertical wind speed component in creating hazardous flight conditions?

The ground-based pulse microwave Doppler can provide a great deal of help to the wind shear detection and warning requirements. It

provides the high-resolution detail of low-level shear, which can be processed to give predicted aircraft response, for either potential approach to landing and takeoff modes, without the aircraft actually entering the expected hazardous airspace. Its capability, however, has not been fully tested. Studies need to be carried out to determine whether it would ultimately be cost effective to the public to have a dedicated Doppler for the airport environment.

There is also the problem of the basic theoretical concepts of aircraft performance in wind shear conditions. Practically all aircraft analyses are based on steady or zero wind conditions. A better understanding of the ability of various aircraft to survive wind shear is necessary. There is a strong probability that several general aviation aircraft accidents, where flight data records are not available, have occurred due to wind shear and have gone undetected. Wind shear models typically utilized are two-dimensional steady-state models. Most all aircraft analyses have utilized three-degrees-of-freedom systems of equations. The microburst is clearly not a simple two-dimensional model but highly three-dimensional and time-dependent as well. Wind shear data input to numerical simulation models and to flight simulators must therefore be improved. Improvement in such models is particularly important with the airlines moving toward nearly 100 percent reliance on flight simulators for their training and proficiency needs. The flight procedures for pilots when encountering wind shear must be totally developed in manned flight simulators. Severe wind shear would be encountered by most pilots once, if at all, in a lifetime. However, if a wind shear encounter under realistic conditions is mandatory during flight simulator training, the pilot will have a much better concept of wind shear and be less likely to take lightly any wind shear alert warnings he may receive.

6.0 CONCLUSIONS

Based on the review of wind shear hazard studies, the following conclusions have been reached.

1. Current mathematical wind shear models, fast becoming standards, are not three-dimensional and are based on a few highly smoothed data. Turbulence superimposed on the wind shear is artificial and does not simulate the extreme turbulence reported by Bliss during his approach to Kennedy prior to the Eastern 66 accident.

Realistic time-dependent three-dimensional wind shear models based on complete data sets are needed to fully verify airborne warning and detection systems, to develop flight procedures, and to train flight crews. The NASA Gust Gradient and NCAR JAWS programs have provided some data sets, but they remain to be analyzed.

2. Order of magnitude analyses of the aircraft equations of motion show that horizontal wind shear terms generally produce the largest forces disrupting flight. These analyses suggest that values of horizontal wind shear smaller than 8 kts/100 ft, given in AC-20-57A for certification of automatic control systems, can be critical. Values of wind shear should be specified as applied along the line of flight. Currently, vertical variation of wind speed is implied in AC-20-57A.
3. Disagreement exists relative to the optimum flight procedures to employ when caught in wind shear. The argument of trading velocity down to stick-shaker speeds to enhance climb is opposed by the ALPA Airworthiness and Performance Committee who argues best climb performance occurs at minimum drag speed. The committee's premise is that flying at this speed leaves some excess kinetic energy or velocity to flair the aircraft at the last moment if impact is unavoidable. These arguments are primarily based on performance analyses using charts which are valid for 1-g flight conditions at constant indicated airspeeds. Dynamic analyses with realistic wind shear models are required to clearly resolve optimum flight procedure in severe wind shear.
4. Simple mathematical studies of aircraft motion without control laws using linear as contrasted to logarithmic vertical wind speed profiles show conflicting results.

The reason for this is that the initial or trimmed flight conditions remain constant without control input. For the linear wind speed profile, the wind shear term is also constant and the aircraft remains in trim relative to the magnitude of the wind shear. For the logarithmic profile the wind shear term changes continuously along the flight path and the aircraft is thus always out of trim relative to the wind shear.

5. Linear stability analysis clearly indicates that wind shear strongly affects the phugoid stability of the aircraft. This is further verified by nonlinear analysis which shows strong amplification of the phugoid oscillation in typical thunderstorm-type wind shear. Pilot models and automatic control laws can, in general, cope with these oscillations although they may become uncontrollable if the simulated pilot's skills are low or if the control laws lack sophistication.
6. Computer and manned flight simulator studies of aircraft performance in sine and half-sine wave longitudinal winds and $1 - \cos$ ine downdrafts were carried out. The sinusoidal wind profiles were applied along the flight path and represented a hypothetical representation of thunderstorm wind shear. The results of this study show that both the computer models and the manned flight simulators have most difficulty coping with combined longitudinal and downdraft wind shear. The second most difficult wind condition was the $1 - \cos$ ine downdraft used alone. These results suggest that a wind shear warning and detection system must measure the vertical wind component as well as the longitudinal component. Serious implications are inherent in this observation because the vertical wind component is much more difficult to measure than the longitudinal component. The magnitude of the downdraft velocities for the hypothetical wind shear models were chosen somewhat arbitrarily, however, and further study is required using realistic downdraft wind shear models to fully verify this conclusion.
7. Six flight path deterioration parameters, FPDP, defined as a measure of the severity of a given wind shear condition on aircraft performance were tested. Both computer analyses and manned flight simulator studies were carried out which showed general correlation between the magnitude of the FPDP and the quality of the computed and measured flight paths. In general, the FPDP defined as the root mean square difference between actual airspeed and reference approach airspeed showed the best correlation with hazardous conditions for longitudinal wind shear. In turn, the FPDP defined as the difference of the actual flight path height minus the intended glide slope height divided by the aircraft's absolute altitude served as a

better measure of flight deterioration in downdrafts. All studies of the FPDP's were carried out using hypothetical sinusoidal wind shear models of different frequencies and amplitudes. Studies using realistic wind shear models based on measured data are needed to fully determine a realistic FPDP or to define an alternate measure of the severity of the wind shear to the aircraft performance. A quantitative value of the FPDP which can be computed in real time with a microcomputer "slaved" to a Doppler radar measuring the wind speed along the flight path is believed to promise the most effective operational system for warning of wind shear hazards. When the critical value of the FPDP parameter is exceeded, a warning alarm would sound in the control tower and in the TRACON as well, if needed. In general, flight controllers prefer a numerical value of a warning parameter which can be used in the above fashion.

8. Airborne systems developed to date measure only the longitudinal wind speed component and, in general, incorporate the concept of conserving energy for the situation when the wind shears from a head wind to a tail wind. These systems will not work during takeoff where maximum or essentially maximum thrust is already employed. Although the system has the advantage of being carried with the aircraft such that the warning and detection system is available regardless of where the approach or takeoff is made, it has the disadvantage that one must enter the hazardous airspace prior to the system providing any useful information. Additionally, the system requires a highly accurate ground speed measurement which is not generally available on the majority of commercial air carriers. In turn, most of the airborne systems have been developed and verified in manned flight simulators using incomplete wind shear profiles. There is clear evidence that wind shears can be encountered which are so severe that a suitable acceleration margin is unavailable for the aircraft to survive the wind shear encounter.
9. The current ground-based low-level wind shear alert system, LLWSAS, is only a near-term solution to the wind shear hazard. The LLWSAS system does not measure the environment above the surface in which the aircraft may encounter wind shear, and moreover increasing evidence illustrates the many severe wind shears are of sufficiently small scale, i.e., microburst-type wind shear, that they can occur directly over the airport and go undetected by the LLWSAS.
10. The ground-based pulse microwave Doppler promises to provide the most effective wind shear detection and warning capability. The Doppler has been demonstrated to provide

high-resolution details of low-level wind shear which can be processed with a microcomputer to give predicted aircraft performance. Both the approach and takeoff modes can be handled without the aircraft actually entering a hazardous wind shear condition. The Doppler radar directly measures the wind along the glide slope and is not limited to a surface measurement such as the LLWSAS. Obviously, one Doppler radar can only measure the radial or longitudinal component of the wind along the intended approach path. If the vertical or downdraft wind speed component must be measured directly, two radars are required. The implementation of all major airports with one Doppler radar will be expensive but feasible; two radars may be prohibitive. Additional studies to fully develop the flight path deterioration parameter concept and to illustrate that one Doppler radar per airport is sufficient to serve as a warning and detection system, are required.

The hazard of wind shear to aviation operations is far from solved. The LLWSAS system currently installed at 58 airports may give too many false alarms and consequently causes complacency relative to wind shear situation. Airborne systems have not been implemented to any major extent and in turn may provide a sense of capability to cope with wind shear which is not real.

The NCAR JAWS and NASA Gust Gradient field programs have provided the necessary data to make a quantum step forward in solving the wind shear problem. These data must be thoroughly analyzed, however, and appropriately formulated to allow development of effective warning and detection systems to provide mathematical wind shear models for flight crew training and to establish aircraft design criteria. Analysis of these data should proceed as rapidly as possible before further catastrophes occur due to insidious wind shear lurking in the approach and takeoff air corridors of our major airport terminals.

REFERENCES

1. Laynor, W. G., and Roberts, C. A.: A Wind Shear Accident as Evidenced by Information from the Digital Flight Data Recorder, Paper presented at the 1975 SASI International Seminar, October 7-10, 1975, Ottawa, Canada.
2. USAF Wind Shear Conference, May 3-4, 1978, Travis AFB, California.
3. Tinsley, H. G., Coons, F. G., and Wood, L. W.: Possible Near-Term Solutions to the Wind Shear Hazard, Preprints: Air Transportation Meeting, Boston, Mass. Warrendale, Penn.: Society of Automotive Engineers, Inc., 1978.
4. Etkin, B.: Dynamics of Atmospheric Flight. New York: John Wiley and Sons, Inc., 1972.
5. Perkins, C. D., and Hage, R. E.: Airplane Performance Stability and Control. New York: John Wiley and Sons, Inc., 1963.
6. Houghton, E. L., and Brock, A. E.: Aerodynamics for Engineering Students. New York: St. Martin's Press, 1972.
7. Babister, A. W.: Aircraft Dynamic Stability and Response. New York: Pergamon Press, 1980.
8. Roskam, J.: Flight Dynamics of Rigid and Elastic Airplanes, Part I. Printed by the author: Professor of Aerospace Engineering, The University of Kansas, Lawrence, Kansas, 1973.
9. Houbolt, J. C., Steiner, R., and Pratt, K. G.: Dynamic Response of Airplanes to Atmospheric Turbulence Including Flight Data on Input and Response, NASA Lewis Research Center, TR R-199, 1964.
10. Peloubet, R. P., and Haller, R. L.: Application of a Power Spectral Gust Design Procedure to Bomber Aircraft," USAF Wright-Patterson Technical Report AFFDL-TR-66-35, June 1966.
11. Wang, S. T., and Frost, W.: Atmospheric Turbulence Simulation Techniques with Application to Flight Analysis, NASA Marshall Space Flight Center, CR 3309, 1980.
12. Flight in Turbulence, AGARD Conference Proceedings, AGARD-CP-140, 1973.

13. Reeves, P. M., Joppa, R. G., and Ganzer, V. M.: A Non-Gaussian Model of Continuous Atmospheric Turbulence for Use in Aircraft Design, NASA Ames Research Center, CR-2639, 1976.
14. Frost, W., Camp, D. W., and Wang, S. T.: Thunderstorm Wind Shear Modeling for Aircraft Hazard Definition, Paper presented at the WMO Technical Conference on Aviation Meteorology, November 5-9, 1979, Geneva, Switzerland.
15. Goff, C.: Measuring Weather for Aviation Safety in the 1980's, Proceedings: Fourth Annual Workshop on Meteorology and Environmental Inputs to Aviation Systems, NASA CP-2139/FAA-RD-80-67, 1980.
16. Frost, W., Camp, D. W., and Wang, S. T.: Wind Shear Modeling for Aircraft Hazard Definition, FAA Report No. FAA-RD-78-3, U.S. Department of Transportation, Washington, D.C., 1978.
17. Goff, R. C.: Thunderstorm Outflow Kinematics and Dynamics, NOAA Technical Memorandum ERL NSSL-75, December 1975.
18. Federal Aviation Administration, U.S. Department of Transportation, Docket No. 19758, Notice of Proposed Rule Making 79-18, Federal Register, Vol. 44, No. 220, November 13, 1979, Washington, D.C.
19. Foy, W. H.: Airborne Aids for Coping with Low-Level Wind Shear, FAA Report No. FAA-RD-79-117, U.S. Department of Transportation, Washington, D.C., 1979.
20. Fichtl, G. H.: Interagency memorandum entitled Wind Profiles for Aircraft Landing Simulation, from NASA/MSFC, Alabama, to Frank Coons, DOT/FAA, Washington, D.C., December 15, 1975.
21. Fujita, T. T.: Downbursts and Microbursts--An Aviation Hazard, Preprints: 19th Conference on Radar Meteorology. Boston, Mass.: American Meteorological Society, pp. 135-143, 1980.
22. Goff, C., Lee, J. T., and Brandes, E. A.: Gust Front Analytical Study, FAA Report No. FAA-RD-77-19, U.S. Department of Transportation, Washington, D.C., 1977.
23. Frost, W., and Camp, D. W.: Wind Shear Modeling for Aircraft Hazard Definition, FAA Report No. FAA-RD-77-36, U.S. Department of Transportation, Washington, D.C., 1977.
24. Goff, R. C.: Some Observations of Thunderstorm Induced Low-Level Wind Variations, AIAA Paper No. 76-388, AIAA 9th Fluid and Plasma Dynamics Conference, San Diego, Calif., July 14-16, 1976.
25. Fujita, T. T., and Wakimoto, R. M.: Five Scales of Airflow Associated with a Series of Downbursts on 16 July 1980, Mon. Wea. Rev., 109(7), July 1981.

26. Fujita, T. T., and Caracena, F.: An Analysis of Three Weather-Related Aircraft Accidents, SMRP Research Paper 145, The University of Chicago, April 1977.
27. Keenan, M. G.: Personal communications. Stanford Research Institute, Manlo Park, California, October 1977.
28. Fujita, T. T.: Manual of Downburst Identification for Project NIMROD, SMRP Research Paper 156, The University of Chicago, 1978, 104 pp.
29. Alexander, M. B.: An Analysis of Maximum Vertical Gusts Recorded at NASA's 150 m Ground Winds Tower Facility at Kennedy Space Center, Florida, NASA TM 78139, 1977.
30. Sinclair, P.: Personal communications, Colorado State University, December 20, 1977.
31. Williamson, G. G., Lewellen, W. S., and Teske, M. E.: Model Predictions of Wind and Turbine Profiles Associated with an Ensembler of Aircraft Accidents, NASA CR-2884, 1977.
32. Fujita, T., McCarthy, J., and Wilson, J.: Joint Airport Weather Studies Project. Proposal for joint sponsorship by NSF, FAA, NOAA, and NASA submitted by The University of Chicago, December 1980.
33. Steiner, R., and Rhyne, R. H.: Some Measured Characteristics of Severe Storm Turbulence, National Severe Storms Project Report No. 10, NOAA/National Severe Storms Lab., Norman, Oklahoma, July 1962.
34. Houbolt, J. C., Steiner, R., and Pratt, K. G.: Dynamic Response of Airplanes to Atmospheric Turbulence Including Flight Data on Input and Reponse, NASA TR R-199, 1964.
35. Camp, D. W. et al.: NASA's B57B Gust Gradient Program, Paper to be presented at the 21st AIAA Aerospace Sciences Meeting, January 10-13, 1983, Reno, Nevada.
36. Houbolt, J. C.: Rolling Moment Induced by Nonuniform Spanwise Gusts, AIAA Paper No. 81-0296, Proceedings: AIAA 19th Aerospace Science Meeting, January 12-15, 1981, St. Louis, Missouri.
37. Safety Recommendations A-80-115 through -119, National Transportation Safety Board, Washington, D.C., issued November 19, 1980.
38. Pocock, C. L.: Anatomy of an Investigation. Unpublished report by the Air Force Inspection and Safety Center, Norton AFB, Calif., November 1978.

39. Camp, D. W.: NASA Gust Gradient Program, Atmospheric Sciences Division, Space Sciences Laboratory, Marshall Space Flight Center, Ala., 1981.
40. Frost, W., and Crosby, W. A.: Investigations of Simulated Aircraft Flight Through Thunderstorm Outflows, NASA CR 3053, 1978.
41. Beaulieu, G.: The Effects of Wind Shear on Aircraft Flight Path and Methods for Remote Sensing and Reporting of Wind Shear at Airports, UTIAS Technical Note No. 216, September 1977.
42. U.S. Department of Transportation, Federal Aviation Administration, Advisory Circular No. 20-57A, January 12, 1971.
43. Fichtl, G. H., Camp, D. W., and Frost, W.: Sources of Low-Level Wind Shear Around Airports, Journal of Aircraft, 14(1):5-14, 1977.
44. Melvin, W. W.: Effects of Wind Shear on Approach with Associated Faults of Approach Couplers and Flight Directors, Paper presented at AIAA Aircraft Design and Operations Meeting, July 14-16, 1969, Los Angeles, Calif., Paper No. 69-796.
45. Melvin, W. W.: Effects of Wind Shear on Approach. Pilots Safety Exchange Bulletin, 70-103/105, April/June 1970.
46. Melvin, W. W.: Flight Safety Facts and Analysis, Flight Safety Foundation, Inc., Arlington, Virginia, March 1974.
47. Melvin, W. W.: The Bastard Method of Flight Control, Pilot Safety Exchange Bulletin, March/April 1976.
48. U.S. Department of Transportation, Federal Aviation Administration, Advisory Circular No. 00-50, April 1976.
49. Bliss, J. H.: Groundspeed Called Key to Wind Shear Problem, Aviation Convention News, Teterboro, N.J., September 1, 1979, pp. 1-10.
50. Sowa, D. F.: Low Level Wind Shear, Its Effects on Approach and Climbout, D.C. Flight Approach, published by Douglas Aircraft Co., June 1974.
51. Higgins, P. R., and Patterson, D. H.: More About Wind Shear Hazards, Boeing Airliner, p. 3, January, 1979, Boeing Commercial Airplane Company, Seattle, Wash.
52. Steenblik, J. W.: Wind Shear Update, Airline Pilot, August 1981.
53. Bliss, J. H.: Personal communications, Flying Tiger Line, February 5, 1979.
54. Etkin, B.: Effect of Wind Gradient on Glide and Climb, November 1946.

55. Gera, J.: The Influence of Vertical Wind Gradients on the Longitudinal Motion of Airplanes, NASA TN D-6430, 1978.
56. Sherman, W. L.: A Theoretical Analysis of Airplane Longitudinal Stability and Control as Affected by Wind Shear, NASA TN D-8496, 1977.
57. Moorhouse, D. J.: Airspeed Control Under Wind Shear Conditions, Journal of Aircraft, 14(12), 1977.
58. Frost, W., Long, B. H., and Turner, R. E.: Engineering Handbook on the Atmospheric Environmental Guidelines for Use in Wind Turbine Generator Development, NASA TP 1359, 1978.
59. Barr, N. M., Gangsaas, D., Schaeffer, D. R.: Wind Models for Flight Simulator Certification of Landing and Approach Guidance and Control Systems, FAA Report No. FAA-RD-74-206, U.S. Department of Transportation, Federal Aviation Administration, Washington, D.C., 1974.
60. Luers, J. K., and Reeves, J. B.: Effects of Shear on Aircraft Landing, NASA CR-2287, 1973.
61. Frost, W.: Unpublished results, 1975.
62. Frost, W., and Reddy, K. R.: Investigation of Aircraft Landing in Variable Wind Fields, NASA CR 3073, 1978.
63. Denaro, R. P.: The Effects of Wind Shear on Automatic Landing, Technical Report AFFDL-TR-77-14, Wright-Patterson Air Force Base, Ohio, April 1977.
64. Turkel, B. S., and Frost, W.: Pilot-Aircraft System Response to Wind Shear, NASA CR 3342, 1980.
65. Wang, S. T., and Frost, W.: Atmospheric Turbulence Simulation Techniques with Application to Flight Analysis, NASA CR 3309, 1980.
66. McCarthy, J., and Blick, E. F.: Aircraft Response to Boundary Layer Turbulence and Wind Shear Associated with Cold-Air-Outflow from a Severe Thunderstorm, University of Oklahoma, Norman, Oklahoma.
67. McCarthy, J., Blick, E. F., and Bensch, R. R.: Jet Transport Performance in Thunderstorm Wind Shear Conditions, NASA CR 3207, 1979.
68. McCarthy, J., Blick, E. F., and Bensch, R. R.: A Spectral Analysis of Thunderstorm Turbulence and Jet Transport Landing Performance, Preprint: Conference on Atmospheric Environment of Aerospace Systems and Applied Meteorology. Boston, Mass.: American Met. Society, 1978.

69. Fujita, T. T.: Spearhead Echo and Downburst Near the Approach End of a John F. Kennedy Airport Runway, New York City, SMRP Research Paper 137, The University of Chicago, March 1976.
70. Adams, J. J., and Bergeron, H. P.: Measured Variation in the Transfer Function of a Human Pilot in Single Axis Tasks, NASA TN D-1952, 1963.
71. McCarthy, J., Blick, E. F., and Elmore, K. L.: An Airport Wind Shear Detection and Warning System Using Doppler Radar, Subcontract report by MCS, Inc., Boulder, Col., to FWG Associates, Inc., Tullahoma, Tenn., under NASA Contract NAS8-33458 with Marshall Space Flight Center, October 1980.
72. Frost, W., Turkel, B. S., and McCarthy, J.: Simulation of Phugoid Excitation Due to Hazardous Wind Shear, Paper presented at the AIAA 20th Aerospace Sciences Meeting, Orlando, Fla., January 11-14, 1982.
73. McCarthy, J., and Norviel, V.: Numerical and Flight Simulator Test of the Flight Deterioration Concept, Final subcontractor report by MCS, Inc., Boulder, Col., to FWG Associates, Inc., Tullahoma, Tenn., under NASA Contract NAS8-33458 with Marshall Space Flight Center, April 1981.
74. Turkel, B. S., Kessel, P. A., and Frost, W.: Feasibility Study of a Procedure to Detect and Warn of Low Level Wind Shear, NASA CR 3480, 1981.
75. Tiedeman, D. A. et al.: Inertially Augmented Approach Couplers, Report on Contract DOT-FA75WA-3650, U.S. Department of Transportation, Federal Aviation Administration, SRI International, Menlo Park, Calif., and Collins-Rockwell, July 1979.
76. Stein, K. J.: Wind Shear Development Provides Timely Warning, Aviation Week & Space Technology, p. 62, March 2, 1981.
77. Greene, R. A.: The Effects of Low-Level Wind Shear on the Approach and Go-Around Performance of a Landing Jet Aircraft, Paper No. 790568, SAE Technical Paper Series, Society of Automotive Engineers, Inc., Warrendale, Penn., 1979.
78. McCarthy, J., Frost, W., Turkel, B., Doviak, R. J., Camp, D. W., Blick, E. F., and Elmore, K. L.: An Airport Wind Shear Detection and Warning System Using Doppler Radar, Preprints: 19th Conference on Radar Meteorology, Miami Beach, Fla., Am. Met. Soc., Boston, Mass., pp. 135-142, 1980.
79. McCarthy, J., Elmore, K. L., Doviak, R. J., and Zrnic, D. S.: Instrumented Aircraft Verification of Clear-Air Radar Detection of Low-Level Wind Shear, Preprints: 19th Conference on Radar Meteorology, Miami Beach, Fla., Am. Met. Soc., Boston, Mass., pp. 143-149, 1980.

80. Wilson, J., Carbone, R., and Serafin, R.: Detection and Display of Wind Shear and Turbulence, Preprints; 19th Conference on Radar Meteorology, Miami Beach, Fla., Am. Met. Soc., Boston, Mass., pp. 150-156, 1980.
81. Wilson, J., Carbone, R., Baynton, H., and Serafin, R.: Operational Application of Meteorological Doppler Radar, Bull. Am. Meteor. Soc., 61:1154-1168, 1980.
82. Offi, D. L., Lewis, W., and Lee, T.: Wind Shear Detection with an Airport Surveillance Radar, Preprints: 19th Conference on Radar Meteorology, Miami Beach, Fla., Am. Met., Soc., Boston, Mass., pp. 130-134, 1980.
83. Strauch, R. G.: Applications of Meteorological Doppler Radar for Weather Surveillance Near Air Terminals, IEEE Trans. Geoscience Electronics, GE-17:105-112, 1979.
84. Camp, D. W., and Frost, W. (editors): Proceedings: Third Annual Workshop on Meteorological and Environmental Inputs to Aviation Systems, NASA CP-2104/FAA-RD-79-49, 1979.

APPENDICES

APPENDIX A

GENERAL EQUATIONS OF UNSTEADY MOTION

Etkin [4] gives a complete development of the general equations of unsteady motion. However, the variation of wind velocity is not generally incorporated into the equations, i.e., a zero or constant wind is assumed.

In this study, incorporation of the wind vector components into the governing equations is discussed. The set of equations is based on the assumption that the earth is a stationary plane in inertial space. This assumption is well justified for takeoff and landing problems. A coordinate system fixed at the earth thus becomes the inertial frame of reference, designated F_E . The vehicle is assumed to be a rigid body having a plane of symmetry.

In establishing the appropriate reference frame for computing the motion of the aircraft subject to a ground wind, we are particularly interested in an atmosphere-fixed reference frame, F_A , since the aerodynamic forces depend on the velocity of the vehicle relative to the local atmosphere. If the atmosphere is in uniform motion with velocity \vec{W} relative to the earth, then F_A moves relative to F_E with that velocity.

Two other reference frames of interest are the air-trajectory reference frame, F_W (also called the wind-axis reference frame; this "wind" should not be confused with the atmospheric motion), and the body-fixed reference frame, F_B , or body-axis reference frame. The wind-axis reference frame, F_W , has the origin fixed to the vehicle, usually at the mass center, and the axis is directed along the velocity vector of the vehicle relative to the atmosphere, \vec{V} . Thus,

$$\vec{V} = \vec{V}_E - \vec{W} \quad (\text{A.1})$$

where \vec{V}_E is the inertial velocity or the velocity of the vehicle relative to the fixed earth. The axis $0_W z_W$ lies in the plane of symmetry of the vehicle. The frame F_W has angular velocity relative to the inertial

frame, F_E , the components of which are conventionally designated by p_w , q_w , and r_w .

The body axes are in a body-fixed reference frame in a rigid body. Bodies with articulated control surfaces and/or elastic motions for which the body cannot be taken as rigid are not considered in this equation development.

The origin of the body axes is usually the mass center of gravity, C. The plane of symmetry is generally taken as Cxz, with z directed downward. By convention, the components of angular velocity of the body-axis frame of reference, F_B , relative to F_E are designated p, q, and r and the components along the body axis of aircraft velocity relative to the atmosphere frame of reference, F_A , are denoted by u, v, and w.

On these assumptions, the classical six-degrees-of-freedom equations of motion (Equations 5, 8, 1, and 7 of Etkin [4] with the atmospheric wind effects included) become:

Force Equations in Wind Axes, F_W :

$$T_{xw} - D - mg \sin \theta_w = m(\dot{V} + \dot{W}_{xw}) + m(q_w W_{zw} - r_w W_{yw}) \quad (A.2a)$$

$$T_{yw} - C + mg \cos \theta_w \sin \phi_w = m\dot{W}_{yw} + m[r_w(V + W_{xw}) - p_w W_{zw}] \quad (A.2b)$$

$$T_{zw} - L + mg \cos \theta_w \cos \phi_w = m\dot{W}_{zw} + m[p_w W_{yw} - q_w(V + W_{xw})] \quad (A.2c)$$

Force Equations in Body Axes, F_B :

$$X - mg \sin \theta = m(\dot{u} + \dot{W}_x) + m[q(w + W_z) - r(v + W_y)] \quad (A.3a)$$

$$Y + mg \cos \theta \sin \phi = m(\dot{v} + \dot{W}_y) + m[r(u + W_x) - p(w + W_z)] \quad (A.3b)$$

$$Z + mg \cos \theta \cos \phi = m(\dot{w} + \dot{W}_z) + m[p(v + W_y) - q(u + W_x)] \quad (A.3c)$$

The components of the wind velocity vector are most frequently given in the earth frame of reference. The relationships between the earth components and those in the aircraft wind frame of reference, F_W , are given by:

$$W_{xw} = W_{xE} \cos \theta_w \cos \psi_w + W_{yE} \cos \theta_w \sin \psi_w - W_{zE} \sin \theta_w \quad (A.4a)$$

$$\begin{aligned}
W_{yW} &= W_{xE}(\sin \phi_W \sin \theta_W \cos \psi_W - \cos \phi_W \sin \psi_W) \\
&\quad + W_{yE}(\sin \phi_W \sin \theta_W \sin \psi_W + \cos \phi_W \cos \psi_W) \\
&\quad + W_{zE} \sin \phi_W \cos \theta_W
\end{aligned} \tag{A.4b}$$

$$\begin{aligned}
W_{zW} &= W_{xE}(\cos \phi_W \sin \theta_W \cos \psi_W + \sin \phi_W \sin \psi_W) \\
&\quad + W_{yE}(\cos \phi_W \sin \theta_W \sin \psi_W - \sin \phi_W \cos \psi_W) \\
&\quad + W_{zE} \cos \phi_W \cos \theta_W
\end{aligned} \tag{A.4c}$$

The velocity vector components in the body frame of reference are the same with the Euler angles $(\phi_W, \theta_W, \psi_W)$ replaced by (ϕ, θ, ψ) .

The total derivatives of the wind vector components are:

$$\dot{W}_{xE} = \left(\frac{\partial W_x}{\partial x} \right)_E \dot{x}_E + \left(\frac{\partial W_x}{\partial y} \right)_E \dot{y}_E + \left(\frac{\partial W_x}{\partial z} \right)_E \dot{z}_E + \left(\frac{\partial W_x}{\partial t} \right)_E \tag{A.5a}$$

$$\dot{W}_{yE} = \left(\frac{\partial W_y}{\partial x} \right)_E \dot{x}_E + \left(\frac{\partial W_y}{\partial y} \right)_E \dot{y}_E + \left(\frac{\partial W_y}{\partial z} \right)_E \dot{z}_E + \left(\frac{\partial W_y}{\partial t} \right)_E \tag{A.5b}$$

$$\dot{W}_{zE} = \left(\frac{\partial W_z}{\partial x} \right)_E \dot{x}_E + \left(\frac{\partial W_z}{\partial y} \right)_E \dot{y}_E + \left(\frac{\partial W_z}{\partial z} \right)_E \dot{z}_E + \left(\frac{\partial W_z}{\partial t} \right)_E \tag{A.5c}$$

Additional equations are:

Moment Equations in Body Axes:

$$L = I_x \dot{p} - I_{zx}(\dot{r} + pq) - (I_y - I_z)qr \tag{A.6a}$$

$$M = I_y \dot{q} - I_{zx}(r^2 - p^2) - (I_z - I_x)rp \tag{A.6b}$$

$$N = I_z \dot{r} - I_{zx}(\dot{p} - qr) - (I_x - I_y)pq \tag{A.6c}$$

Kinematic Equations in Wind Axes:

$$\dot{\phi}_W = p_W + q_W \sin \phi_W \tan \theta_W + r_W \cos \phi_W \tan \theta_W \tag{A.7a}$$

$$\dot{\theta}_W = q_W \cos \phi_W - r_W \sin \phi_W \tag{A.7b}$$

$$\dot{\psi}_W = (q_W \sin \phi_W + r_W \cos \phi_W) \sec \theta_W \tag{A.7c}$$

Without subscripts, the above equations also apply in body axes.

Additional Kinematic Relationships:

$$\dot{\alpha} = q - q_w \sec \beta - p \cos \alpha \tan \beta - r \sin \alpha \tan \beta \quad (\text{A.8a})$$

$$\dot{\beta} = r_w + p \sin \alpha - r \cos \alpha \quad (\text{A.8b})$$

$$p_w = p \cos \alpha \cos \beta + (q - \dot{\alpha}) \sin \beta + r \sin \alpha \cos \beta \quad (\text{A.8c})$$

The velocity components relative to the earth fixed reference system F_E in terms of V are:

$$\dot{x}_E = V \cos \theta_w \cos \psi_w + W_{xE} \quad (\text{A.9a})$$

$$\dot{y}_E = V \cos \theta_w \sin \psi_w + W_{yE} \quad (\text{A.9b})$$

$$\dot{z}_E = -V \sin \theta_w + W_{zE} \quad (\text{A.9c})$$

For the body frame of reference, we obtain:

$$\begin{aligned} \dot{x}_E &= u \cos \theta \cos \psi + v(\sin \phi \sin \theta \cos \psi - \cos \phi \sin \psi) \\ &\quad + w(\cos \phi \sin \theta \cos \psi + \sin \phi \sin \psi) + W_{xE} \end{aligned} \quad (\text{A.10a})$$

$$\begin{aligned} \dot{y}_E &= u \cos \theta \sin \psi + v(\sin \phi \sin \theta \sin \psi + \cos \phi \cos \psi) \\ &\quad + w(\cos \phi \sin \theta \sin \psi - \sin \phi \cos \psi) + W_{yE} \end{aligned} \quad (\text{A.10b})$$

$$\dot{z}_E = -u \sin \theta + v \sin \psi \cos \theta + w \cos \phi \cos \theta + W_{zE} \quad (\text{A.10c})$$

Finally, the relationship between the velocity in the body frame of reference and that in the wind frame of reference is given by:

$$u = V \cos \alpha \cos \beta \quad (\text{A.11a})$$

$$v = V \sin \beta \quad (\text{A.11b})$$

$$w = V \sin \alpha \cos \beta \quad (\text{A.11c})$$

Small Disturbance Theory with Variable Wind Field

In most of the conventional analyses of aircraft motion, a linearized form of the equations, for small disturbances about a reference

condition of steady rectilinear flight over a flat earth, is employed. (Symmetric flight requires \vec{V} to lie in the plane of symmetry). The linearized equations are developed by conventional methods; however, it will become apparent in the development that the reference conditions in the presence of a wind field are developed by conventional methods; however, it will become apparent in the development that the reference conditions in the presence of a wind field are difficult to define. The frame of reference for the small disturbance model is generally taken as the "stability" frame, with a special set of body axes coinciding with the wind axes F_W in the reference condition, but departing from it and moving with the body during a disturbance.

The steady state values of the variables are denoted by a subscript e, and changes from the steady state values are denoted by the prefix Δ , i.e.,

$$V = V_e + \Delta V$$

$$\phi = \phi_e + \Delta\phi \tag{A.12}$$

etc.

In this reference frame the state variables are normally taken as V_e , α_e , θ_{we} , and ψ_{we} . All other variables are zero in the reference state and for these the prefix Δ is dropped.

The small disturbance equations are now developed following Etkin [4]. The angle of climb θ_w is denoted by γ , a more commonly used symbol. The angle ψ_{we} is set equal to zero since initial heading has no special significance in the flat-earth approximation. This does not preclude the possibility of winds other than head-on wind, however, since the angle of the wind relative to the flight path is determined by the three components of the wind field. The thrust vector, T , is permitted to be at large angles α_T to the direction of motion but is required to rotate rigidly with the vehicle when the vehicle is perturbed. Thus, in body axes:

$$\vec{T}_B = (T + \Delta T) \begin{pmatrix} \cos \alpha_T \\ 0 \\ \sin \alpha_T \end{pmatrix}$$

and in wind axes:

$$T_{xW} = (T + \Delta T)(\cos \alpha_T \cos \alpha \cos \beta + \sin \alpha_T \sin \alpha \cos \beta) \quad (A.13a)$$

$$T_{yW} = (T + \Delta T)(-\cos \alpha_T \cos \alpha \sin \beta - \sin \alpha_T \sin \alpha \sin \beta) \quad (A.13b)$$

$$T_{zW} = (T + \Delta T)(-\cos \alpha_T \sin \alpha + \sin \alpha_T \cos \alpha) \quad (A.13c)$$

In the stability reference frame, $\alpha_e = 0$, hence, $\alpha = \Delta\alpha$. If one makes the approximation $\sin \Delta \approx \Delta$, $\cos \Delta = 1.0$ and neglects the squares and products of the Δ terms, Equation A.2a becomes:

$$\begin{aligned} (T + \Delta T)\cos \alpha_T - \Delta\alpha T_e \sin \alpha_T - D - \Delta D - mg \sin(\gamma_e + \Delta\gamma) \\ = m(\dot{V} + \dot{W}_{xW}) + m(q_W W_{zW} - r_W W_{yW}) \end{aligned} \quad (A.14)$$

where the reference state is defined by:

$$T_e \cos \alpha_T - D - mg \sin \gamma_e = 0 \quad (A.15)$$

Under the assumption of uniform wind, $\dot{W}_{xW} = 0$, the small disturbance approach is justified. On the other hand, for nonuniform wind fields:

$$\dot{W}_{xW} = \left(\frac{\partial W_x}{\partial t} + (V_e + \Delta V) \frac{\partial W_x}{\partial x} \right)_W \quad (A.16)$$

in the wind frame of reference, and

$$\dot{W}_{xB} = \left(\frac{\partial W_x}{\partial t} + \frac{\partial W_x}{\partial x} u + \frac{\partial W_x}{\partial y} v + \frac{\partial W_x}{\partial z} w \right)_B \quad (A.17)$$

in the body frame of reference. Thus, a problem is encountered with the method of small disturbances for the case of a general wind field since a continual departure from the reference state with time occurs.

If the wind is considered time dependent and the reference state is allowed to vary with time, then from Equation A.2 the governing equations of the reference state become:

$$T_e \cos \alpha_T - D - mg \sin \gamma_e - m\dot{w}_{xw} = 0 \quad (\text{A.18a})$$

$$C_e + m\dot{w}_{yw} = 0 \quad (\text{A.18b})$$

$$T_e \sin \alpha_T + L_e + mg \cos \gamma_e + m\dot{w}_{zw} = 0 \quad (\text{A.18c})$$

These equations could be solved for γ_e , C_e , and L_e , given a specified wind field. The small disturbance equations for this time-dependent reference state then become:

$$\begin{aligned} \Delta T \cos \alpha_T - \Delta \alpha T_e \sin \alpha_T - \Delta D - mg \Delta \gamma \cos \gamma_e = m\dot{v} + m(W_{zw}q_w \\ - W_{yw}r_w) \end{aligned} \quad (\text{A.19a})$$

$$-\beta T_e \cos \alpha_T - \Delta C + mg\phi_w \cos \gamma_e = m[r_w(V_e + W_{xw}) - p_w W_{zw}] \quad (\text{A.19b})$$

$$\begin{aligned} \Delta T \sin \alpha_T + \Delta \alpha T_e \cos \alpha_T + \Delta L + mg \Delta \gamma \sin \gamma_e = m[p_w W_{yw} - q_w(V_e \\ + W_{xw})] \end{aligned} \quad (\text{A.19c})$$

It is apparent, however, that the advantage of the small disturbance equations, which is that they are a linear time-invariant system of equations that can be solved by established mathematical transfer function techniques, is lost since the coefficients containing γ_e are functions of time.

A similar result is obtained with Equation A.2, which with the small disturbance approximation, becomes:

$$\Delta x - mg \cos \Delta \gamma \cos \gamma_e = m\dot{u} + m(qW_z - rW_y) \quad (\text{A.20a})$$

$$\Delta y - mg\phi \cos \gamma_e = m\dot{v} + m[r(V_e + W_x) - pW_z] \quad (\text{A.20b})$$

$$\Delta z - mg\Delta \gamma \sin \gamma_e = m\dot{w} + m[pW_y - q(V_e + W_x)] \quad (\text{A.20c})$$

where the reference state is such that:

$$x_e = mg \sin \gamma_e - m\dot{w}_x = 0 \quad (\text{A.21a})$$

$$y_e = m\dot{w}_y = 0 \quad (\text{A.21b})$$

$$z_e + mg \cos \gamma_e - m\dot{w}_z = 0 \quad (\text{A.21c})$$

Linearized Equation of Motion for Uniform Wind

For a uniform wind, $\dot{W}_x = \dot{W}_y = \dot{W}_z = 0$, and Equations A.6 through A.8 become:

$$\Delta L = I_x \dot{p} - I_{zx} \dot{r} \quad (\text{A.22a})$$

$$\Delta M = I_y \dot{q} \quad (\text{A.22b})$$

$$\Delta N = I_z \dot{r} - I_{zx} \dot{p} \quad (\text{A.22c})$$

$$\dot{\phi}_w = p_w + r_w \tan \gamma_e \quad (\text{A.23a})$$

$$\dot{\gamma} = q_w \quad (\text{A.23b})$$

$$\dot{\psi}_w = r_w \sec \gamma_e \quad (\text{A.23c})$$

Without the subscript w, these equations apply in body coordinates.

Also, we have the kinematic relationships:

$$\dot{\alpha} = q - q_w \quad (\text{A.24a})$$

$$\dot{\beta} = r_w - r \quad (\text{A.24b})$$

$$p_w = p - \beta \dot{\alpha} \quad (\text{A.24c})$$

The aircraft velocity in earth coordinates becomes:

$$\dot{x}_E = V_e (\cos \gamma_e - \Delta\gamma \sin \gamma_e) + \Delta V \cos \gamma_e + W_{xE} \quad (\text{A.25a})$$

$$\dot{y}_E = V_e \cos \gamma_e + W_{yE} \quad (\text{A.25b})$$

$$\dot{z}_E = -V \sin \gamma_e - \Delta V \sin \gamma_e - V_e \Delta\gamma \cos \gamma_e + W_{zE} \quad (\text{A.25c})$$

or in body coordinates:

$$\dot{x}_E = V_e \cos \gamma_e + V_e \Delta\gamma \sin \gamma_e + u \cos \gamma_e + w \sin \gamma_e + W_{xE} \quad (\text{A.26a})$$

$$\dot{y}_E = V_e \psi \cos \gamma_e + v + W_{yE} \quad (\text{A.26b})$$

$$\dot{z}_E = -V_e \sin \gamma_e - V_e \Delta\gamma \cos \gamma_e - u \sin \gamma_e + w \cos \gamma_e + W_{zE} \quad (\text{A.26c})$$

Recall that $u_e = V_e$ and $v_e = w_e = 0$ in the reference state. The relationships among the wind components in the earth frame of reference and

the wind frame of reference become:

$$W_{xw} = W_{xE}(\cos \gamma_e - \Delta\gamma \sin \gamma_e) + W_{yE} \psi_w \cos \gamma_e - W_{zE}(\sin \gamma_e + \Delta\gamma \cos \gamma_e) \quad (\text{A.27a})$$

$$W_{yw} = W_{xE}(\phi_w \sin \gamma_e - \psi_w) + W_{yE} + W_{zE} \phi_w \cos \gamma_e \quad (\text{A.27b})$$

$$W_{zw} = W_{xE}(\sin \gamma_e + \Delta\gamma \cos \gamma_e) + W_{yE}(\psi_w \sin \gamma_e - \phi_w) + W_{zE}(\cos \gamma_e - \Delta\gamma \sin \gamma_e) \quad (\text{A.27c})$$

The equations are valid for the body frame of reference without the subscript w.

Conventionally (i.e., without atmospheric motion, $\vec{W} = 0$), Equations A.19a, A.19b, A.21b, A.23b, A.24a, A.25a, and A.25b are taken to be the longitudinal equations since they contain only longitudinal variables (ΔV , $\Delta\alpha$, q , Δr , x_E , z_E) and Equations A.20b, A.21a, A.21c, A.23a, A.23c, and A.26b are taken to be the lateral equations since they contain only lateral variables (v , p , r , ϕ , ψ , y_E). The equations thus decouple and form two independent sets which can be solved separately. However, with a wind, even a uniform wind, the longitudinal equations do not separate because p_w and r_w appear in Equations A.19c and A.19a, respectively. On the other hand, the lateral equations separate in view of the fact that neither

$$r(V_e + W_x) = r(V_e + W_{xE} \cos \gamma_e - W_{zE} \sin \gamma_e) \quad (\text{A.28a})$$

nor

$$pW_z = p(W_{xE} \sin \gamma_e + W_{zE} \cos \gamma_e) \quad (\text{A.28b})$$

contain any of the longitudinal variables.

Finally, the special case of a horizontal wind oriented parallel to the direction of motion, i.e.,

$$\vec{W}_E = \begin{pmatrix} W_{xE} \\ 0 \\ 0 \end{pmatrix} \quad (\text{A.29})$$

results in a form of the equations which permits separation of the longitudinal equations as well. The equation thus has the familiar form:

$$\Delta T \cos \gamma_T - \Delta \alpha T_e \sin \alpha_T - \Delta D - mg \Delta Y \cos \gamma_e = m\dot{V} + mW_{xE}q_w \sin \gamma_e \quad (\text{A.30a})$$

$$\Delta T \sin \alpha_T + \Delta \alpha T_e \cos \alpha_T + \Delta L + mg \sin \gamma_e = -mq_w(V_e + W_{xE} \cos \gamma_e) \quad (\text{A.30b})$$

$$\Delta Y + mg\phi \cos \gamma_e = m\dot{v} + m[r(V_e + W_{xE} \cos \gamma_e) - pW_{xE} \sin \gamma_e] \quad (\text{A.30c})$$

APPENDIX B

NOMENCLATURE

A_{cap}	Acceleration capability
C	Side force
D	Drag force
DA	Acceleration difference
F	Frame of reference
GNS	Ground speed
GS+	Flight deterioration parameter (Table 4.2, 2a)
GS-	Flight deterioration parameter (Table 4.2, 2b)
g	Gravity
H	altitude of airplane CG
HG	Height of the glide slope above the ground
HP	Height of the aircraft above the ground
h_L	Arbitrary reference height scale
I	Moment and/or product of inertia
IAS	Indicated airspeed
L	Lift force
L	Rolling moment
L	Monin-Obukhov stability length scale
\hat{L}	Turbulence length scale
M	Pitching moment
m	Mass

N	Yawing moment
p	Rate of roll
q	Rate of pitch
r	Rate of yaw
T	Thrust
T	Time period
TAS	True airspeed
u	x-component of aircraft velocity relative to the atmosphere
u*	Friction velocity
V+	Flight deterioration parameter (Table 4.2, 4a)
V-	Flight deterioration parameter (Table 4.2, 4b)
\vec{V}	Relative velocity vector (airspeed)
V _{app}	Selected approach speed (kts)
V _a	Airspeed
V _{a₀}	Approach airspeed
V _{a_{stall}}	Stall airspeed
\vec{V}_E	Inertial velocity vector
v	y-component of aircraft velocity relative to the atmosphere
\vec{W}	Wind velocity vector
\bar{W}	Mean wind speed
WD	Difference in wind speed at the runway and at the aircraft
WX _{gnd}	Wind component at the ground
w	z-component of aircraft velocity relative to the atmosphere
X	X-component of aerodynamic force
x	Distance along x-axis
Y	Y-component of aerodynamic force

y	Distance along y -axis
Z	Z -component of aerodynamic force
z	Distance along z -axis
z_0	Surface roughness

Greek Symbols

α	Angle of attack
β	Angle of yaw
γ	Pitch angle
Γ	Wind shear vertical gradient in horizontal wind ($\partial W_x / \partial z$)
ΔA	Acceleration margin
Δx	Deviation from desired touchdown
θ	Euler angle (elevation)
κ	von Karman constant
λ	Wavelength
σ	Wind shear parameter ($V_e (\partial W_x / \partial z) / g$)
$\hat{\sigma}$	Turbulence intensity
ϕ	Euler angle (bank)
ψ	Euler angle (azimuth)
$\psi(z_E/L)$	Stability parameter
ω_{ph}	Phugoid frequency

Subscripts

i	Initial value
e	Reference state
E	Measured in the inertial coordinates
o	Landing speed

S Stall speed
T Direction of thrust
w Measured in the wind coordinates
x Measured in x-direction
y Measured in y-direction
z Measured in z-direction

Superscript

($\dot{\quad}$) Time derivative $d(\quad)/dt$

Prefix

Δ Small perturbation

1. REPORT NO. NASA CR-3678		2. GOVERNMENT ACCESSION NO.		3. RECIPIENT'S CATALOG NO.	
4. TITLE AND SUBTITLE Flight in Low-Level Wind Shear				5. REPORT DATE March 1983	
				6. PERFORMING ORGANIZATION CODE	
7. AUTHOR(S) Walter Frost				8. PERFORMING ORGANIZATION REPORT #	
9. PERFORMING ORGANIZATION NAME AND ADDRESS FWG Associates, Inc. Rural Route #2, Box 271-A Tullahoma, Tennessee 37388				10. WORK UNIT NO. M-407	
				11. CONTRACT OR GRANT NO. NAS8-33458	
12. SPONSORING AGENCY NAME AND ADDRESS National Aeronautics and Space Administration Washington, D.C. 20546				13. TYPE OF REPORT & PERIOD COVERED Contractor Report June 22, 1981 - Aug. 22, 1982	
				14. SPONSORING AGENCY CODE	
15. SUPPLEMENTARY NOTES Prepared for Atmospheric Science Division, Space Science Laboratory, Marshall Space Flight Center, Huntsville, Alabama 35812 MSFC Technical Monitor: Dennis W. Camp					
16. ABSTRACT Results of studies of wind shear hazard to aircraft operation carried out under NASA Marshall Space Flight Center contract for the period 1979 through 1982 are summarized in this report. The results of the study are integrated with other reported information in the literature and with cooperative manned flight simulator studies carried out with NASA Ames Research Center and United Airlines Flight Training Center. The report first reviews existing wind shear profiles currently used in computer and flight simulator studies. The governing equations of motion for an aircraft are then derived incorporating the variable wind effects. Quantitative discussions of the effects of wind shear on aircraft performance are presented. These are followed by a review of mathematical solutions to both the linear and nonlinear forms of the governing equations. Solutions with and without control laws are presented. The application of detailed analysis to develop warning and detection systems based on Doppler radar measuring wind speed along the flight path is given. A number of flight path deterioration parameters are defined and evaluated. Comparison of computer-predicted flight paths with those measured in a manned flight simulator is made. The report ends with a review of some proposed airborne and ground-based wind shear hazard warning and detection systems. The advantages and disadvantages of both types of systems are discussed.					
17. KEY WORDS Wind Shear Turbulence Aviation Safety Low-Level Flow			18. DISTRIBUTION STATEMENT Unclassified - Unlimited Subject Category 47		
19. SECURITY CLASSIF. (of this report) Unclassified		20. SECURITY CLASSIF. (of this page) Unclassified		21. NO. OF PAGES 121	22. PRICE A06